Are early proteomic and metabolic changes induced by long-term sugar-sweetened beverage consumption the key to unlocking the cardio-metabolic pandemic?

by

Janina Benadè

Thesis presented in partial fulfillment of the requirements for the degree of Master of Science (Physiology) in the Faculty of Natural Science at Stellenbosch University.

Supervisor: Prof M. Faadiel Essop

March 2017

Declaration

By submitting this dissertation electronically, I declare that the entirety of the work contained therein is my own, original work, that I am the sole author thereof (save to the extent explicitly otherwise stated), that reproduction and publication thereof by Stellenbosch University will not infringe any third party rights and that I have not previously in its entirety or in part submitted it for obtaining any qualification.

Janina Benadè
March 2017

Abstract

INTRODUCTION: Cardio-metabolic diseases (e.g. type 2 diabetes mellitus) are a major cause of mortality worldwide. The incidence of cardio-metabolic diseases continues to increase, especially in low and middle income countries. This "pandemic" is possibly brought about by a fairly universal shift towards a more "Westernized" diet. High sugar consumption - a hallmark of the "Westernized" diet - may play a key role in the onset of cardio-metabolic diseases. Accordingly, our research focus moved towards sugar-sweetened beverages (SSBs) as it is a major source of added dietary sugars. The current study aimed to elucidate underlying mechanisms leading to the development of cardiometabolic diseases by exploiting a novel rat model of long-term SSB intake, and by focusing on the liver as a major metabolic organ. Here we evaluated well-known systemic markers together with hepatic proteome analysis and downstream consequences.

METHODS: Male Wistar rats (~200 g) were gavaged with 3-5.1 mL SSB daily for three and six months, respectively. The two control groups were gavaged with an iso-volumetric amount of water and iso-caloric amount of butter, respectively. Body weight and systemic blood markers were measured. A proteomic expression analysis was performed on the six-month liver samples. The rest of our experimental work was guided by the proteomic results. Four markers for oxidative stress were evaluated: malondialdehyde, conjugated dienes, reduced:oxidized glutathioneand oxygen radical absorbance capacity. The non-oxidative glucose pathways (NOGPs): polyol pathway, hexosamine biosynthetic pathway, advanced glycation end-products formation and protein kinase C activation; were measured as elevated activity could be indicative of impaired glycolytic flux. The liver histology was investigated with Hematoxylin and Eosin and Masson's Trichrome stains, respectively. Finally, Western blotting techniques were used to evaluate markers of inflammation.

RESULTS: SSB consumption had little effect on systemic markers of cardio-metabolic health. Our proteomic analysis revealed that the expression level of 140 proteins was significantly altered in the SSB group, with a major finding that SSB consumption induces hepatic endoplasmic reticulum (ER) stress. Initially the liver adapted to SSB-mediated nutrient overload by increasing oxidative phosphorylation, suppressing protein transcription, degrading misfolded

proteins and improving protein folding capacity. However, due to prolonged stress liver cells entered an ''alarm phase'' marked by a decrease in mitocholdrial metabolism. The proteomic results further revealed that SSB-induced effects are largely attributed to excess caloric intake versus SSBs *per se*. Surprisingly, oxidative stress did not precede ER stress as there were no significant changes in any of the oxidative stress markers here evaluated. The activity of the NOGPs did not increase significantly thus suggesting that moderate SSB intake did not suppress glucose metabolism and the glycolytic pathway in particular. Conversely, SSB intake increased hepatic lipid storage while limited changes were detected between the groups regarding inflammation and stress signaling.

CONCLUSION: Frequent SSB consumption triggers metabolic changes in the liver, i.e. ER stress despite the lack of obvious manifestation of macroscopic “warning signs”. Thus the current study identifies hepatic ER stress as a relatively early result of long-term SSB consumption and it therefore emerges as a unique therapeutic target.

Opsomming

INLEIDING: Kardiometaboliese siektes (bv. tipe 2 diabetes mellitus) is wêreldwyd ‘n hoofoorsaak van mortaliteit. Die voorkoms van kardiometaboliese siektes neem voordurend toe, veral in lae- en middel-inkomste lande. Hierdie “pandemie” word moontlik gedryf deur ‘n redelike universiële skuif na ‘n meer “Westerse” dieet. Hoë suikerinname, ‘n kerneienskappe van die “Westerse” dieet, speel moontlik ‘n sleutelrol in die ontwikkeling van kardiometaboliese siektes. Daarvolgens fokus ons navorsing op suiker-versoete drankies (SVDs), die hoofbron van ekstra suikers in die dieet. Hierdie studie poog om insig te kry in die onderliggende meganismes wat die ontwikkeling van kardiometaboliese siekes dryf, deur ‘n nuwe rot model vir lang-termyn SVD inname te gebruik en op die lewer as hoof metaboliese orgaan te fokus. Sistemiese merkers, veranderings in die hepatiese proteoom en die nagevolge daarvan is tydens die studie ondersoek.

METODES: Manlike Wistar rotte (~200 g) is daagliks gevoer met 3-5.1 mL SVD deur orale toediening vir drie en ses maande, onderskeidelik. Die kontrole groepe het onderskeidelik ‘n isovolumetriese hoeveelheid water ‘n isokaloriese hoeveelheid botter ontvang. Liggaamsgewig en sistemiese bloedmerkers is gemeet. ‘n Proteomiese uitdrukkinganalise is op die ses maand lewerweefsel uitgevoer. Die res van ons eksperimentele werk is deur die proteomika resultate gerig. Merkers vir oksidatiewe stres is geëvauleer (malonielaldehied, gekonjugeerde diëne, gereduseer tot geoksideerde glutatioonen suurstofradikaal absorbansie kapasiteit). Die nie-oksidatiewe glukosepaaie (poliolweg, heksosamien-biosinteseweg, vorming van gevorderde glukeringseindprodukte en proteïen kinase C aktivering) is geëvalueer aangesien verhoogde aktiwiteit ‘n teken van onderdrukte glikolise kan wees. Die lewerhistologie is ondersoek deur “Hematoksilien en Eosien” en “Massons Trichroom” kleuringstegnieke. Westerse blottegnieke is gebruik om merkers van inflammasie te evalueer.

RESULTATE: Matige SVD inname het min effek op sistemiese merkers vir kardiometaboliese gesondheid gehad. Die proteomikaanalise wys dat die uitdrukking van 140 proteïene beduidend verander het in die SVD groep en dat SVD inname hepatiese endoplasmiese retikulum- (ER) stres veroorsaak. Aanvanklik het die lewer aangepas by die SVD-bemiddelde voedingstofoorlading deur oksidatiewe fosforilasie te verhoog, transkripsie te verlaag en proteïenvouing en afbreking te bevorder. Weens langdurige stres het die lewer selle egter ‘n

“noodfase” betree, gekenmerk deur ‘n afname in mitokondriese metabolisme. Verder dui die resultate dat die effek van SVDs grootliks aan die oormatige kalorieinname te wyte is, eerder as die SVD self. Dit lyk nie asof oksidatiewe stres die voorafgaande “kondisie” is wat ER-stres geïnisiëer het nie aangesien daar geen beduidende veranderings in oksidatiewe stres merkers waargeneem is nie. Die aktiwiteit van die NOGPs het nie beduidend verhoog nie, dus is glukosemetabolisme en die glikolitiese pad in besonder nie onderdruk nie. SVD inname het wel die stoor van lipiede in die lewer verhoog, maar nie inflammasie en stresseinpaaie geïnisiëer nie.

GEVOLGTREKKING: Gereelde inname van SVDs lei tot metaboliese veranderings in die lewer soos ER-stres sonder duidelike manifesasie van klassieke vroeë makroskopiese gevaartekens. Die huidige studie indentifiseer hepatiese ER-stres as ‘n relatiewe vroeë resultaat van langtermyn SVD inname en daarom kom dit na vore as ‘n unieke terapeutiese teiken.

Acknowledgements

I would like to express my sincere gratitude to the following people:

My supervisor, Prof MF Essop - thank you for your patience and guidance over the past three years and with this project in particular. A special thanks for the time and effort that you invested in the editing of this thesis. I have learned a great deal from you.

The Department of Physiology - thank you for creating a friendly and conducive environment where students can excel.

Lydia, I'd like to thank you for making the time to help proofread my thesis. Your contribution is of great value to me. I'd also like to thank you for always ensuring the molecular lab ran smoothly, your open door and all the laughs we had during undergraduate practicals.

The CMRG group - thank you for the friendships, the support and all the brainstorming. We had a great team spirit and I always knew you had my back. I have to make a few special mentions. Danzil, you have been my "go-to" person for any question or problem since my honors – thank you for the open door, kindness and patience, and for helping my proofread this thesis. Gaurang, you are new to the group but you brought so much energy and enthusiasm with you. Thank you for asking difficult questions and for helping me proofread. Tash, thank you for teaching me all your rat-whispering skills, for all the desperate CPUT-coffees we shared, for you sense of humor and of course for always being the designated driver☺. It was an absolute privilege to work on this project with you.

Dr Fanie Rautenbach, Dr Dirk Bester, Reggie Williams, Dr Carol Chase and Dr Maré Vlok. Thank you for technical support and insight regarding data interpretation. You have greatly contributed to the success of this project.

The NFR and Stellenbosch University, thank you for the financial support that enabled me to study this M.Sc.

And ultimately, my family, friends and my partner in crime. God het my so ryklik geseën! Baie dankie vir die eindelose liefde, ondersteuning en gebed. Dankie dat julle daar was deur al die op's en af's en altyd in my bly glo het. Dankie vir al die saamlag, pret en avontuur so tussen die laboratorium en tesis deur – ek het beslis my "sanity" aan julle te danke. Julle maak my lewe die moeite werd.

Table of Contents

List of figures

Chapter 1

Chapter 2

Chapter 3

Chapter 4

List of tables

List of abbreviations

ADP	Adenosine diphosphate
AGE	Advance glycation end products
AGE-R1	AGE-receptor1
ALT	Alanine transaminase
AR	Aldose reductase
ATP	Adenosine triphosphate
BMI	Body mass index
BSA	Bovine serum albumin
CARDIA	Coronary Artery Risk Development in Young adults
CDs	Conjugated dienes
CHD	Coronary heart disease
ChREBP	Carbohydrate-responsive element binding protein
CRP	C-reactive protein
CVD	Cardiovascular diseases
DNA	Deoxyribonucleic acid
eAG	Estimated average glucose
EGIR	European Group for Study of Insulin Resistance
ER	Endoplasmic reticulum
ETC	Electron transport chain
F-1-P	Fructose-1-phosphate
FA	Fatty acid
$FADH_2$	Flavin adenine dinucleotide
FoxO1	Forkhead box protein O1
G-6-P	Glucose-6-phosphate
GAPDH	Glyceraldehyde 3-phosphate dehydrogenase
GlcN-6-P	Glucosamine-6-phosphate
GLUT	Glucose transporter
GSH	Reduced glutathione
GSK-3β	Glycogen synthase kinase 3β
GSSG	Oxidized glutathione
HBP	Hexosamine biosynthetic pathway
HbA1c	Glycated hemoglobin A1c
HDL	High density lipoprotein

HFCS	High fructose corn syrup
HOMA-IR	Homeostasis model assessment–insulin resistance index
HPFS	Health Professionals Follow-up study
IDF	International Diabetes Federation
IFCC	The International Federation for Clinical Chemistry
IL	Interleukin
INTERMAP	International Study of Macro and Micronutrients and Blood Pressure
IRS	Insulin receptor substrates
JNK	c-Jun amino-terminal kinase
LDL	Low-density lipoproteins
MDA	Malondialdehyde
MetS	Metabolic syndrome
MI	Meta-inflammation
NAD^+	Nicotinamide adenine dinucleotide
NADH	Nicotinamide adenine dinucleotide
NADPH	Nicotinamide adenine dinucleotide phosphate
NCEP ATP III	National Cholesterol Education Program Adult Treatment Panel III
NF-κB	Nuclear factor kappa B
NGSP	National Glycohemoglobin Standardization Program
NHANES	National Health and Nutrition Examination Survey
NHS	The Nurses' Health Study
NOGP	Non-oxidative glucose pathways
NOX	NADPH oxidase
O-GlcNAc	O-linked β-N-acetyl glucosamine
ORAC	Oxygen radical absorbance capacity
PARP	Poly(ADP-ribose) polymerase
PCA	Perchloric acid
PDK	3-phosphoinositide-dependent protein kinases
PEPCK	Phosphoenolpyruvate carboxykinase
PGC-1-α	PPAR-γ coactivator 1-α
PI3K	Phosphatidylinositol-4,5-bisphosphate 3-kinase
PIP_2	Phosphatidylinositol-4,5-bisphosphate
PIP_3	Phosphatidylinositol-3,4,5-triphosphate
PKC	Protein kinase C
PREMIER	Clinical Trial of Comprehensive Lifestyle Modification for Blood Pressure Control

RAGE	Receptors for AGEs
RIPA	Radio immune precipitation buffer
ROS	Reactive oxygen species
RR	Relative risk
SD	Standard deviation
SREBP	Steroid regulatory element-binding protein
SSB	Sugar-sweetened beverage
T2DM	Type 2 diabetes mellitus
TAC	Tricarboxylic acid cycle
TBARS	Thiobarbituric acid reactive substances
TBS-T	Tris-buffered saline and Tween 20
TCEP	Triscarboxyethyl phosphine
TG	Triglycerides
TNF	Tumor necrosis factor
US	United States
WHO	World Health Organization

Chapter 1: Literature Review

1.1 Cardio-metabolic diseases

Non-communicable diseases pose a major threat to public health worldwide. During 2011 the United Nations announced that - for the first time – non-communicable diseases are a greater health risk than infectious diseases in both developed and developing countries (Lustig *et al*., 2012). According to the World Health Organization (WHO), non-communicable diseases result in 38 million deaths annually with cardio-metabolic diseases accounting for ~19 million of these (WHO factsheet #355, 2015). The umbrella term "cardio-metabolic diseases" describes both cardiovascular diseases (CVD) and metabolic conditions such as metabolic syndrome (MetS) and Type 2 diabetes mellitus (T2DM). The increased prevalence of cardio-metabolic disorders is strongly associated with behavioral changes like urbanization, the adoption of a more sedentary lifestyle and the increasingly universal uptake of a "Westernized" diet (Caballero, 2005). This section will provide a brief overview of the prevalence of the major cardio-metabolic complications and associated pathophysiology.

1.1.1 Obesity

Obesity is one of the most prevalent metabolic conditions and is characterized by excessive fat accumulation. Obesity leads to increased morbidity and mortality through its association with a range of pathological states including CVD, certain types of cancer and osteoarthritis (WHO Fact sheet #311, 2016). Furthermore, obesity is robustly linked to insulin resistance, a chief underlying cause of MetS and T2DM (Fezeua *et al*., 2007).

The prevalence of obesity is increasing on a global scale - in 2014 the WHO reported its doubling (since 1980) with more than 600 million adults globally burdened with this condition (WHO Fact sheet #311, 2016). Obesity is also becoming more prevalent amongst children. It is estimated that the percentage of pre-school children in the United States (US) suffering from obesity increased from 5% to 9.5% during the period 1970 to 2008 (Garnett *et al*., 2012). Global estimates report that ~41 million children (under the age of 5 years) were classified as overweight or obese in 2014 (WHO Fact sheet #311, 2016). Moreover, obesity which was once considered to be exclusive to high-income countries, is now increasingly emerging as a health issue in low- and middle-income countries. For example the number of obese children in Africa has doubled over the past ~25 years (WHO Fact sheet #311, 2016).

1.1.2 MetS

MetS refers to a cluster of metabolic conditions including obesity, impaired glucose tolerance and dyslipidemia that manifest concurrently in an individual and serves as a prognostic tool for the future development of T2DM and CVD. Individuals with MetS are about 5 times more likely to develop T2DM compared to matched controls, and about twice as likely to develop CVD (Park *et al*., 2003). MetS is also associated with several other complications including non-alcoholic fatty liver disease and polycystic ovary syndrome (reviewed by Baranova *et al*., 2011).

There are currently four definitions for MetS, stipulated by the International Diabetes Federation (IDF), WHO, European Group for Study of Insulin Resistance (EGIR) and the National Cholesterol Education Program Adult Treatment Panel III (NCEP ATP III). The NCEP ATP III definition is very similar to that of the IDF (refer to Table 1.1.1), while impaired glucose tolerance and elevated insulin levels are mandatory conditions for the WHO and EGIR definitions (Parikh & Mohan, 2012). Although the prevalence of MetS varies depending on the diagnostic criteria used, this condition remains a pressing global health issue. Almost ~37% of US adults exhibited MetS according to criteria stipulated by the IDF (Ford, 2005). Furthermore, in most European countries the average prevalence of MetS in adults exceeds 20%, with some countries reaching a staggering 40% (reviewed by Grundy, 2008; Tanner *et al*., 2012). There is a similar tendency in Africa with some populations showing a prevalence of up to ~50% (reviewed by Okafor, 2012). Here it is important to note that none of the available definitions of MetS has been fully optimized for African ethnicity. MetS also has a high prevalence amongst children and adolescents which Grundy (2008) argues to be directly linked to increased obesity levels in younger populations.

Table 1.1.1: IDF Global MetS definition (Alberti *et al*., 2009)

An individual is diagnosed with MetS when any 3 of the following criteria manifest	
Central obesity	Waist circumference (ethnic-specific): *Europids; Sub-Saharan Africans; Middle East; Eastern Mediterranean* ≥ 94 cm (males) ≥ 80 cm (females) *South Asian; Chinese; Japanese; South and Central Americans* ≥ 90 cm (males) ≥ 80 cm (females)
Raised triglycerides (TGs)	≥ 1.7 mmol/L or on treatment for lipid abnormality
Reduced high-density lipoprotein (HDL) cholesterol	< 1 mmol/L (males) <1.3 mmol/L (females)
Increased blood pressure	Systolic ≥ 130 mmHg Diastolic ≥ 85 mmHg Or on treatment for previously diagnosed hypertension
Elevated fasting blood glucose	≥ 5.6 mmol/L or previously diagnosed with T2DM

1.1.3 T2DM

There are two major categories of diabetes mellitus, namely type 1 and type 2. Type 1, which accounts for ~5-10% of cases, is an auto-immune condition characterized by damaged pancreatic β-cells that result in insufficient insulin secretion. On the contrary, poor dietary choices can lead to reduced insulin sensitivy and are thus a major contributing factor to the development of T2DM (90-95% of all diabetic cases) (Marcovecchio *et al*., 2011).

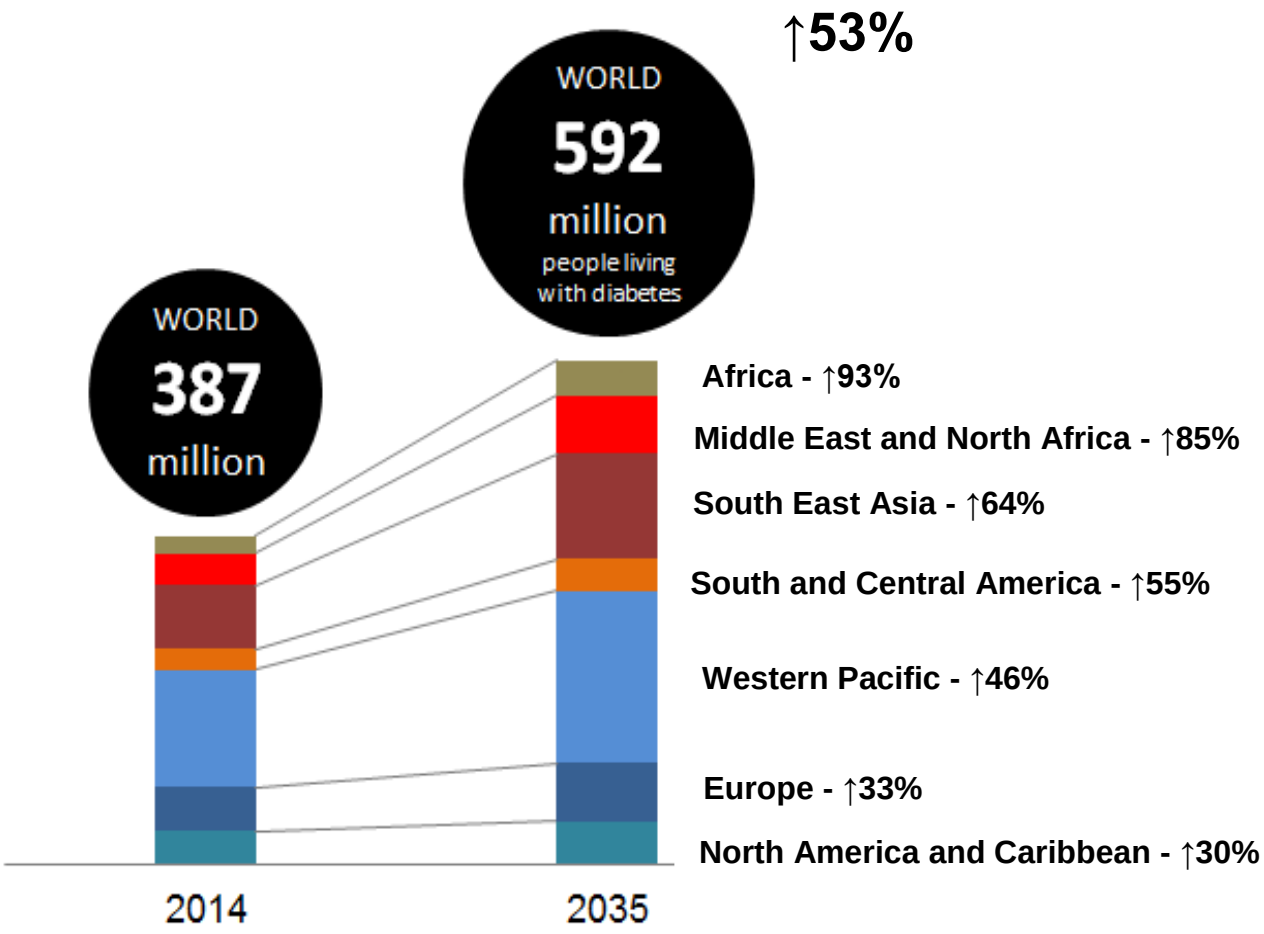

Figure 1.1.1: IDF projections for the global increase of T2DM (2014 and 2035) are 53%. The prevalence of diabetes in Africa, Asia and South America is expected to increase more rapidly than in Europe, North-America and the Caribbean (adapted from IDF Diabetes Atlas, 2014).

A study on the international burden of T2DM (1995 – 2025) projected that the global prevalence of diabetes will rise to ~300 million by 2025 (King *et al*., 1998), but this figure was already exceeded in 2011. It is now estimated that ~422 million people are currently suffering from T2DM globally and it is predicted that the prevalence of T2DM will increase to ~642 million by 2040 (IDF Diabetes atlas, 2015; WHO Global Diabetes Report, 2016). This will elevate diabetes to the seventh leading cause of death worldwide (WHO Fact sheet #312, 2016) with the majority of such mortalities occurring in low- and middle-income countries where the incidence of T2DM is rapidly increasing (IDF Diabetes Atlas, 2014; WHO Fact sheet #312, 2016). South Africa is not unique in this regard – here metabolic disorders already account for ~6% of all mortalities (StatsSA, 2013). The picture remains bleak as the IDF predicts that Africa will suffer the highest increase globally in terms of T2DM incidence (2014 to 2035) with an estimated increase of ~93% versus ~53% expected globally (Figure 1.1.1). Moreover, an increasing number of T2DM cases (together with obesity and MetS) are now also reported for children and adolescents (Vivian, 2006). Together these data raise concerns as to whether this growing prevalence will taper down in the foreseeable future.

In order to determine the T2DM burden of disease it is necessary to also consider conditions that likely result from this condition, e.g. neuropathy, chronic kidney disease, end-stage renal failure, retinopathy and CVD (DeFronzo *et al*., 1992). Such conditions are largely caused by micro- and macro-vascular dysfunction induced by chronic hyperglycemia associated with T2DM and can be equally fatal (Ha *et al*., 2008). The IDF Diabetes Atlas estimated that 40 000 – 100 000 deaths in South Africa during 2011 were attributed to diabetic complications alone (IDF Diabetes Atlas, 2011). Additionally, T2DM is also a primary risk factor for CVD, the number one killer worldwide.

1.1.4 CVDs

CVDs are the leading cause of death worldwide. In 2012 it accounted for ~17.5 million mortalities and it is estimated to increase to ~23.3 million by 2030 (WHO factsheet #317, 2016). As with the other condition, future projections indicate that low- and middle-income countries will be most severely affected by CVD (WHO factsheet #317, 2016). In South Africa CVDs caused 17% of all deaths in 2013 (StatsSA, 2013). Ischemic heart disease accounts for the largest percentage of such mortalities, followed by hypertension-related heart diseases (WHO

Factsheet #317, 2016). Ischemic heart disease is characterized by an insufficient blood supply and nutrients to the heart through the coronary arteries, resulting in myocardial infarction. Hypertensive heart disease refers to a state where chronic hypertension caused pathological cardiac hypertrophy and cardiac inefficiency (Guyton & Hall, 2011).

In summary, the statistics and projections regarding the prevalence of cardio-metabolic diseases serve as motivation for comprehensive research into the underlying molecular mechanisms driving these diseases. Although a variety of detrimental lifestyle choices such as a sedentary behavior, smoking, high intake of salt and processed foods all contribute to the cardio-metabolic pandemic, excess sugar consumption has been identified as one of the most prominent global dietary changes observed during the past few decades and a primary driver of cardio-metabolic diseases (Fagherazzi *et al*., 2013) (Figure 1.1.2). A study conducted in the US over four years (2005 - 2009) established that 74% of the 85, 451 different edible products on the market contained added sugars; these products include mainly cereals, energy bars and beverages (Ng *et al*., 2011). Sugar-sweetened beverages (SSBs) are proposed to be the main culprit with estimates indicating that ~46% of added sugars are consumed through SSBs (US Department of Agriculture & US Department of Health and Human Services, 2010). For this reason, the focus of cardio-metabolic research gradually shifted to SSBs as a leading source of sugar-derived calories. Section 1.2 concentrates on the consumption trends and health risks associated with SSBs.

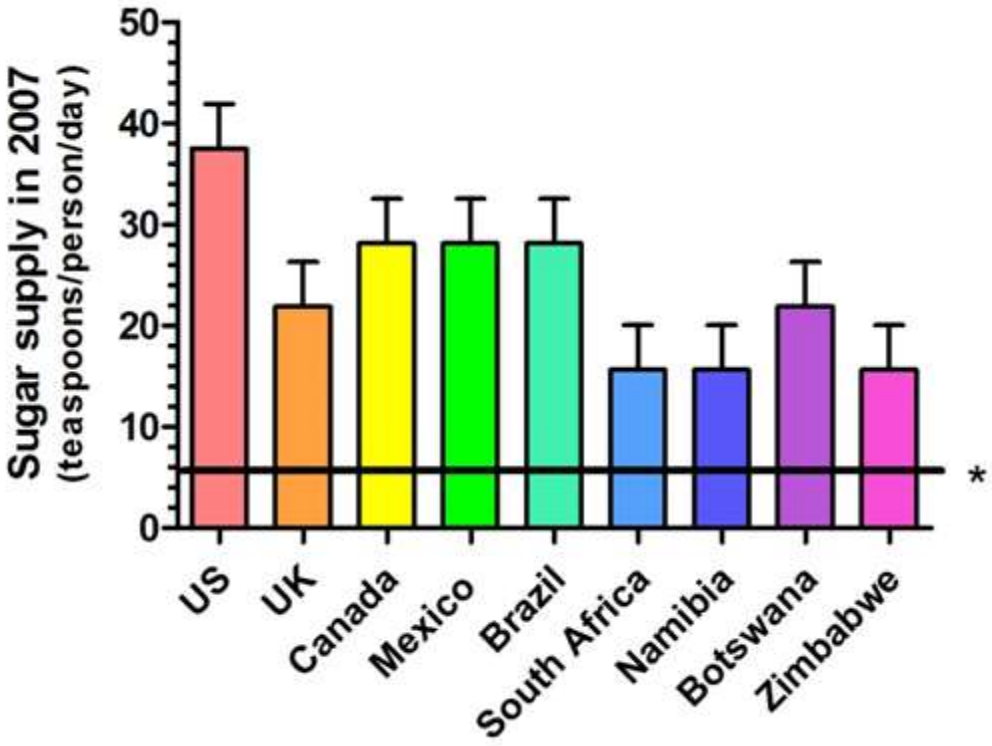

Figure 1.1.2: Global trends in sugar consumption expressed as the amount of teaspoons of sugar consumed per person per day (only selected countries are displayed here). Sugar consumption in low- and middle-income countries globally is on the rise, refer e.g. Mexico and Brazil. This trend is equally prominent in Africa where sugar intake in most southern African countries is above the recommended daily amount put forward by the World Health Organization in 2015 (no more than six teaspoons per day, see * on diagram). (Adapted from Lustig *et al*., 2012; *Guideline: Sugars intake for adults and children*, 2015).

1.2 Sugar-sweetened beverages

The emphasis on SSBs as a source of sugar has increased since the latter has been identified as a key factor in the cardio-metabolic "pandemic". SSB consumption increased drastically in the last 30 years of the twentieth century. The ingestion of SSBs leads to excessive sugar and calorie intake and it is associated with general unhealthy lifestyle choices e.g. frequent fast-food intake (Miller *et al*., 2013). This section explores global trends in SSB consumption, as well as the association between SSB intake and cardio-metabolic disease risk.

1.2.1 SSB consumption

The first SSB was produced and consumed in the 1800s, but only gained popularity during World War II when free Coca Cola™ products were donated to the US army (reviewed by Pendergrast, 2000, Wolf *et al*., 2008). The consumption of all SSBs types including carbonated, sports, fruit drinks and vitamin waters increased significantly between 1970 and 2000, and continued to increase in the 2000s in most parts of the world (reviewed by Basu *et al*., 2013).

Interestingly, there has been a modest decrease in SSB consumption in the US since the turn of the millennium (Hert *et al*., 2014; Welsh *et al*., 2011). Despite the decrease, SSB consumption in the US still exceeds the recommended daily allowance as stated by the WHO. The WHO recently released a bulletin (2015) suggesting that added sugar consumption should be kept below 5% of total caloric intake (~six teaspoons) and not 10% (~12 teaspoons) as stated in the 2003 dietary guideline (*Guideline: Sugars intake for adults and children*, 2015). According to the US National Health and Nutrition Examination Survey (NHANES) (2005-2008) a quarter of the US population consumed at least 1.5 cans of SSB daily (~10% of total recommended calories) and ~5% consume at least 4 cans per day (> 25% of total recommended calories) (Ogden *et al*., 2011). On average SSBs account for ~9.2% of total caloric intake in the US (Miller *et al*., 2013) with the highest being among low-income individuals such as African-Americans and Hispanics who also show an inordinate prevalence of obesity and related diseases (Hu, 2013). SSB-related behavioral patterns are also dependent on age and gender. Data from the US reveal that children and adolescents obtain ~11% of their total daily caloric intake from SSB-derived sugar consumption (Wang *et al*., 2008) and 12% (294 kcal) in the case of male adolescents (Miller *et al*., 2013). Alarmingly, it has also been reported that ~50% of 2-year olds US consume SSBs on a weekly basis (Garnett *et al*., 2012).

Despite the decrease in SSB consumption in the US, research suggests that it is still on the rise globally as reported in a recent study evaluating SSB intake in 75 countries (Basu *et al*., 2013). Additional support comes from country-specific studies, e.g. in the United Kingdom the amount of SSB consumed per capita per week has doubled since 1975 and continues to increase (Ng *et al*., 2012). This also reflects in SSB-derived calories that increased from 113 (1986-1987) to 155 KJ/capita/day (2000-2001) and further to 209 KJ/capita/day by 2008-2009 (Ng *et al*., 2012). Likewise, in South Korea the prevalence in SSB consumption between 2001 and 2009 increased with 7%, 3%, 7% and 18% amongst adolescents, young adults, adults and aged groups, respectively (Han *et al*., 2013). Here the highest prevalence of consumption manifested

in the adult group (70%). Of note, this study included sweetened tea/coffee that are generally not considered to be SSBs. SSB sales are also rapidly increasing in low- and middle-income countries such as China where the trading of Coca Cola™ and PepsiCo™ products increased by 145% and 127%, respectively, between 2000 and 2010 (Kleiman *et al*., 2012). Similarly, SSB sales increased between 1999 and 2012 in Mexico (Stern *et al*., 2014). Here consumption of caloric beverages increased drastically (1999-2006) amongst Mexican children e.g. pre-schoolers derives 27.8% of their daily caloric intake from beverages. However, this is possibly an overestimation as it includes non-sweetened caloric beverages such as milk (Barquera *et al*., 2010). Of particular interest is a South African-based study where 1,233 subjects (rural and urban communities in the Western Cape) completed a 5-year follow up study (Vorster *et al*., 2014). Lifestyle questionnaires revealed that the proportion of participants who consume SSBs increased from 25% to 56% and 33% to 63% in males and females, respectively, over the period of the study. Moreover, the percentage of participants who consumed more than 10% of their daily caloric intake from added sugars increased from 18% to 40% (males) and 29% to 46% (females) (Vorster *et al*., 2014).

1.2.2 The problem with SSB consumption

Why is it so concerning that SSB consumption is increasing on a global scale? Frequent SSB intake may contribute to the onset of cardio-metabolic diseases – one important mechanism is by increasing total calorie intake (Miller *et al*., 2013). In support, a US-based study examining a dietary survey and recall of 488 adults, found that the daily caloric intake of SSB consumers is ~572 kcal higher compared to non-consumers (Ruff *et al*., 2014). Groundbreaking work by Mattes (1996, 2006) and Rolls *et al*. (1990) provide a possible explanation for this increase. Here they found that liquids that are high in energy but have a very low viscosity e.g. SSBs trigger a limited sensation of satiety despite a high caloric count. Thus subsequent food consumption is not reduced to compensate for the SSB-derived calories and hence extra calories are likely to be consumed.

Another explanation is that SSB intake often occurs together with other poor lifestyle choices, e.g. SSB consumers are more likely to consume unhealthy foods (e.g. pizza, hamburgers and savory snacks) compared to non-consumers (Mathias *et al*., 2013). Another study that explored dietary preferences found that SSBs are most often paired with calorie-dense food (Cornwell & McAlister, 2013). These data are supported by a cross-sectional study (9,433 subjects) that found SSB consumption is associated with higher intake of fast foods, savory snacks, iced

puddings and total sugar in an adolescent cohort (Collison *et al*., 2010). These findings also revealed that significantly more vegetables are consumed when meals are accompanied by water instead of SSBs (Cornwell & McAlister, 2013). In agreement, SSB consumers of all ages are more prone to snacking between meals than their counterparts, resulting in a higher calorie intake (Bleich & Wolfson, 2015). Frequent SSB consumption is also associated with other unhealthy lifestyle choices such as smoking and lack of exercise (Kristal *et al*., 2015). Together these studies indicate the SSB consumption is often not an isolated problem, but instead associated with several wide-ranging unhealthy dietary choices that ultimately leads to the onset of cardio-metabolic diseases.

Besides overall calorie consumption and unhealthy lifestyle, the sugar used for sweetening SSBs may also directly induce pathological molecular events. Additionally, the 'type' of sugar could also play a significant role in the consequences of SSB consumption (Aerberli *et al*., 2011). Commercially available SSBs in the US are generally sweetened with sucrose or high fructose corn syrup (HFCS) (Aerberli *et al*., 2011). HFCS is the preferred choice of sweetener since the higher fructose content provides a sweeter taste (Bray *et al*., 2004). Bray *et al*. (2004) found that the consumption of fructose (mainly in the form of HFCS) increased by almost 30% during the last three decades and is considered a major culprit in the onset of metabolic perturbations. There is no set formula for HFCS. Generally HFCS contains 42% or 55% fructose, but Ventura *et al*. (2011) demonstrated that HFCS-sweetened SSBs contain an average of 59% fructose, while some leading US brands contained up to 65% fructose. HFCS has been named and shamed both in popular media and academic circles, yet to date there is not sufficient evidence that HFCS has more severe health consequences compared to sucrose (reviewed by Rippe & Angelopoulos, 2016).

In South Africa SSBs are usually sweetened with sucrose (also known as table sugar) (Vorster *et al*., 2014). Sucrose is a disaccharide consisting of equal amounts of glucose and fructose molecules (Maersk *et al*., 2012) and is sometimes considered to be a "healthier option". However, it is still strongly related to greater weight gain and obesity risk (Ventura *et al*., 2011). The manifestation of chronic SSB consumption is thus determined by both the amount and content of the ingested sweetener (Aerberli *et al*., 2011). Although a theoretical approach provides convincing concerns regarding SSB consumption, it requires support from observed and experimental data. The following section explores epidemiological and clinical data on the link between frequent SSB intake and disease risk.

1.2.3 Metabolic derangements and disease risk

There is considerable observational data linking higher SSB consumption to increased risk for the development of obesity, MetS, T2DM, CVDs (reviewed by Malik *et al*., 2010) non-alcoholic fatty liver disease (Abid *et al*. 2009) and chronic kidney disease (Yuzbashian *et al*., 2015). Yet the question whether sugar consumption actually leads to the onset of cardio-metabolic disease remains controversial (Stanhope, 2015). The subsequent sections will elaborate on the merits and limitations of current epidemiological and (limited) clinical data linking SSB consumption to cardio-metabolic diseases.

1.2.3.1 Weight gain and obesity

Although epidemiological studies are often criticized, there are ample large-scale long-term cohort studies that provide considerable statistical evidence to prove the positive association between SSBs and weight gain and the eventual risk of developing obesity (Malik *et al*., 2010). For example, Shulze *et al*. (2004) followed more than 50, 000 female nurses for 2× four-year periods and established that participants consuming one or more SSB serving per day gained significantly more weight (8 kg) than those consuming less than 1× SSB serving per week (2.8 kg). In agreement, others evaluated the weight gain of more than 40, 000 African American females for six years and found the largest gain in the group where consumption increased to more than one SSB serving per day (Palmer *et al*., 2008). Moreover, the lowest weight gain was observed in the group who reduced their SSB consumption. Similar results were also observed in a cohort of > 43, 000 Singaporean males and females where significant weight gain was observed in participants consuming ≥ 2 SSB servings per week compared to those who rarely consumed SSBs (Odegaard *et al*., 2010). A South African-based study also reported a positive association between SSB consumption and obesity by evaluating waist circumference, body mass index (BMI) and lipid profile (Vorster *et al*., 2010). After a 5-year follow-up period, participants who consume ≥ 10% of daily caloric intake from added sugars (of which SSBs are a significant source) displayed larger waist circumferences, higher BMIs as well as lower levels of HDL-cholesterol (Vorster *et al*., 2010). Observational data further showed that decreasing SSB intake can lead to weight loss. The Clinical Trial of Comprehensive Lifestyle Modification for Blood Pressure Control (PREMIER) study showed that decreasing SSB consumption by one serving daily resulted in weight loss within a 6-month time frame (Chen *et al*., 2009). A similar study was conducted in obese adolescents where the lowering of SSB consumption for one year resulted in significant decreases in weight and BMI (Ebbeling *et al*., 2006; Ebbeling *et al*.,

2012). However, no significant differences were observed between the two groups a year later, proving the complexity of such interventions (particularly within the school system).

Due to the popularity of SSBs amongst children and the increasing prevalence of childhood obesity, cross-sectional and longitudinal epidemiological studies also explored the correlation between SSB intake and weight gain in children (Malik *et al*., 2010). Data gathered from across the globe support the notion that frequent SSB consumption in children leads to significant weight gain. For example, the European Youth Heart Study monitored 358 children for 6 years and concluded that SSB consumption is directly associated with an increased body fat percentage in children and adolescents (Zheng *et al*., 2015). In accordance, Chinese children (n > 6, 900) who regularly consume SSBs exhibited significantly higher BMIs and waist circumferences compared to regular milk consumers and have an increased risk of developing obesity (Shang *et al*., 2012). A cross-sectional study confirmed the positive correlation between SSB intake and the prevalence of obesity amongst Chinese children and adolescents (n = 702) (Jia *et al*., 2012). An earlier study where more than 2, 000 Canadian toddlers (2.5 years of age) were monitored for three years reported that those who frequently consumed SSBs between meals were ~2.4× more likely to be overweight than their counterparts (Dubois *et al*., 2007). Research by DeBoer *et al*. (2013) also found a positive association between SSB consumption and weight gain in children as young as two years old. Although the BMI z-score did not differ significantly between groups at the two year-old age, a prospective analysis showed that frequent consumption in this group resulted in a significant increase in BMI compared to infrequent/non-consumers over the following two years (DeBoer *et al*., 2013). Furthermore, frequent SSB consumption is associated with a high risk of developing obesity in five-year old children (DeBoer *et al*., 2013). A significant association between SSB intake and obesity was also observed in a cohort of Mexican American children (aged 8 – 10) (Beck *et al*., 2014) and Australian children and adolescents (Grimes *et al*., 2013). Here participants consuming more than one SSB serving daily exhibited a 26% increased risk of developing obesity (Relative risk [RR]: 1.26, 95 % CI: 1.03-1.53). Moreover, a Spanish study that used a matched case-control design (comparing 174 obese children/adolescents to 174 healthy body weight controls) found that the obese cohort consumed significantly more SSBs compared to the healthy cohort. The cases and controls were age and gender matched (Martin-Calvo *et al*., 2014). Together these studies demonstrate a robust positive correlation between SSB intake and weight gain in children and adolescents. Additionally, a recent clinical study used functional magnetic resonance imaging to evaluate sugar-induced brain perfusion (Jastreboff *et al*., 2016). The

patterns detected in obese adolescents were markedly different from lean adolescents and may indicate that the obese participants have developed a sugar addiction, thus perpetuating a vicious cycle (Bray, 2016). In light of these studies, it has been recommended that pediatricians and parents should strongly discourage SSB consumption by children (DeBoer *et al*., 2013)

However promising this may be, there are still some studies that produced negative or neutral results. In a cohort of school-aged Saudi Arabian boys (n = 5, 033) and girls (n = 4, 400) SSB intake showed a positive correlation to BMI and waist-circumference in the male, but not the female cohort after the adjustment for potential confounders (Collison *et al*., 2010). Others also found no significant association between SSB consumption and body fat percentage in a cohort of British children (Johnson *et al*., 2007). Of note, the SSBs consumed for this study only accounted for ~3% of the daily calorie intake and may explain this surprising outcome. Despite these studies, the weight of evidence strongly support the notion that frequent SSB consumption leads to an increased risk of weight gain and obesity in young and adult populations. Some of the inconsistency in the data may be due to variation in methodology and study design (Poppitt, 2015). For example, the lack of standardization of measurements used to assess obesity make it difficult to interpret the results of various studies (Poppitt, 2015). While some studies only measured weight gain, others measured BMI, waist-to-hip ratio or skinfold thickness (all markers of obesity). In a cohort of 2, 045 Costa Rican adults, (Rhee *et al*., 2012) found that frequent SSB consumption was associated with a significant increase in BMI and waist-to-hip ratio, but not skinfold thickness, showing variability between various markers. Another concern is that many findings do not take the sex of participants into account although it is evident that this factor may contribute to complexity of the results. A study of a large German cohort (n > 17, 000) found a significant relationship between SSB consumption and obesity in males, but not females after a four-year follow up period (Shulze *et al*., 2002). By contrast, a cross-sectional survey of Chinese males (n = 2, 295) and females (n = 2, 334) found that the frequency of SSB consumption as an independent risk factor for obesity in females, while a sedentary lifestyle, a meat-rich diet and smoking were better predictors of obesity in males (Ko *et al*., 2010). All things considered, epidemiological data strongly suggest that frequent SSB intake is linked to weight gain and obesity. Nonetheless, researchers should take care when selecting study design, parameters and a cohort.

1.2.3.2 MetS and T2DM

High SSB consumption is also considered to be a risk factor for the onset of MetS and T2DM (Malik *et al*., 2010). Dhingra *et al*. (2007) investigated the development of MetS in an adult cohort (n > 6, 000) over a four-year period and concluded that consuming one or more SSB serving daily increased the risk for developing MetS by ~44%. They further elucidated the effects of SSBs on the respective components of MetS. Here subjects consuming ≥ 1 SSB serving/day displayed an increased prevalence of obesity (RR: 1.31; 95 % CI: 1.02–1.68), greater waist circumference (RR: 1.30; 95 % CI: 1.09-1.56), hypertension (RR: 1.18; 95 % CI: 0.96–1.44), elevated fasting glucose (RR: 1.25; 95 % CI: 1.05–1.48), hypertriglyceridemia (RR: 1.25; 95 % CI: 1.04–1.51) and decreased HDL-cholesterol (RR: 1.32; 95 % CI: 1.06–1.64) compared to those who did not consume SSBs on a daily basis (Dhingra *et al*., 2007). In agreement, data from an adult Mexican cohort (n > 5, 200) also demonstrated that frequent SSB consumption leads to increased risk for all the attributes of MetS (Denova-Gutiérrez, *et al*., 2010). Others focused specifically on the effects of SSB consumption on insulin resistance by using the homeostasis model assessment for insulin resistance (HOMA-IR) as an indicator (Kondaki *et al*., 2012). For this cohort (546 European adolescents) they found that the HOMA-index is significantly higher in participants consuming SSBs at least 5-6 times/week compared to those consuming less than one SSB per week (Kondaki *et al*., 2012). Besides the studies described here there are limited epidemiological data available to support the association between SSB consumption and the development of MetS as most of the research focused on T2DM instead.

Murphy *et al*. (2015) investigated the link between SSB consumption and T2DM by collecting data from a diabetic cohort (n = 580). Here 49% of the participants consumed SSBs on a daily basis and ~9% consumed four or more servings per day. These data show that diabetic individuals do not follow health guidelines by abstaining from SSB consumption despite being diagnosed with T2DM. The bigger question is, however, how many SSBs were consumed *prior* to the diagnosis and whether SSB intake actually contributed to T2DM onset? A follow-up study of 8 years found that participants consuming ≥ 1 SSB/day were ~83% more likely to develop T2DM compared to those whose intake were less than one per month (Schulze *et al*., 2004). However, this study did not adjust the data for BMI variations as is the general practice. Similarly, another study found a significant association between SSB intake and T2DM risk in a cohort of > 43, 000 Singaporeans (Odegaard *et al*., 2010). Here the consumption of as little as ≥ 2 SSB servings/week caused a 34% increase in disease risk compared to non- or infrequent

consumers, while consumption of ≥ 2 fruit juice servings per week was also associated with a 24% higher risk (Odegaard *et al*., 2010). Bhupathiraju *et al*. (2013) undertook a long term study with a pooled cohort of over > 110,000 participants and confirmed that frequent SSB intake increased the risk for developing T2DM regardless of whether the SSB is caffeinated or not. Recently, Teshima *et al*., (2015) also found that frequent SSB consumers had more than twice the risk to develop T2DM to non-consuming counterparts Lastly, a number of smaller studies also provide support for the positive association between SSB consumption and the development of T2DM (De Koning *et al*., 2011; Nettleton *et al*., 2009; The InterAct Consortium, 2013).

However, not all of the studies found a positive correlation between SSB intake and T2DM onset. For example, Palmer *et al*. (2008) established that participants who consumed two or more SSBs daily were more prone to developing T2DM than those consuming one or less per month, but the results were not significant after adjustments for BMI. These data therefore indicate that obesity was the biggest contributor to T2DM in this instance. Paynter *et al*. (2006) also rejected the notion that SSB consumption is significantly associated with an increased risk of developing T2DM. In addition, there should also be a consideration for the role of ethnicity. For example, a cohort of more than 2, 037 middle-aged Japanese males (followed for 7 years) displayed no significant association between any of the SSB categories and the development of T2DM, although the consumption of diet soda was positively linked to the onset of T2DM (Sakurai *et al*., 2014).

Most studies discussed used intervals of SSB consumption (lowest: < 1 SSB per month; highest: ≥ 1 SSB per day) but Fagherazzi *et al*. (2013) designed a model to describe the continuous correlation between SSB consumption and T2DM development. In this instance the consumption of SSBs (0 – 1, 000 mL per week) is directly related to a greater T2DM risk (RR: 1.3; 95 % CI: 1.03–1.66). However, when volumes larger than 1, 000 mL is consumed the frequency of consumers and statistical power are too low to make meaningful conclusions. Similarly, an analysis with pooled data attempted to determine the dose-dependent correlation between SSB consumption and T2DM risk. Here it was established that every 330 mL SSB serving (per day) relates to a 20% increase in the risk of developing T2DM, thus clearly indicating a positive relation between disease risk and SSB intake (Greenwood *et al*., 2014) (see Figure 1.2.1).

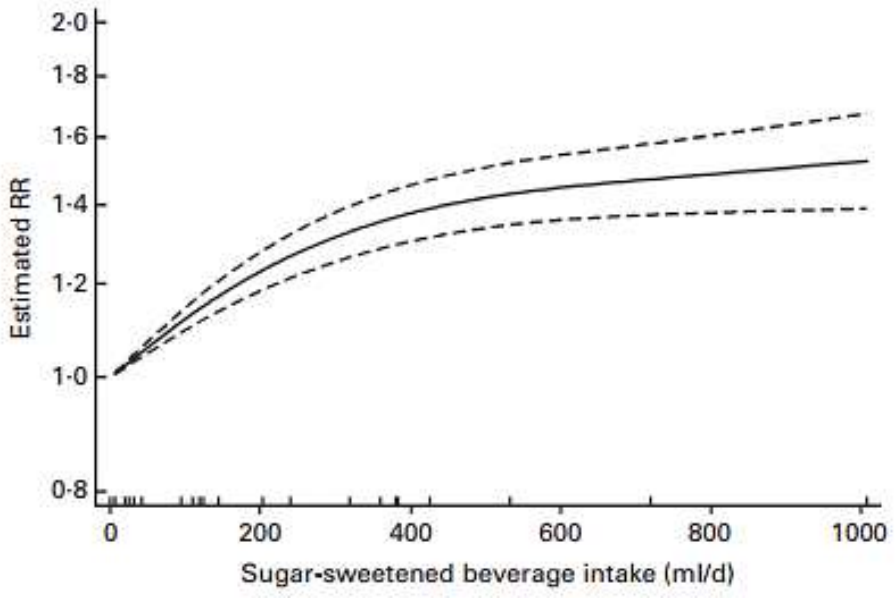

Figure 1.2.1: The association between daily SSB intake and the risk of developing T2DM. Data from five publications were combined and show the risk of developing T2DM increase in a dose-dependent manner – the pooled RR increase by 20% (95 % CI 1·12, 1·29 indicated by the dotted lines) for every 330 mL SSB serving consumed daily (Greenwood *et al*., 2014).

Table 1.2.1 provides a brief summary of the epidemiological studies investigating the association between SSB consumption and T2DM. We conclude that SSBs may play a central role in the onset of MetS and T2DM although some controversy still exists. Clinical data are required to confirm these findings and elucidate possible molecular mechanisms involved.

Table 1.2.1: Studies investigating the link between SSB consumption and T2DM risk (adapted from Greenwood *et al*., 2014 and Wang *et al*., 2015).

Author	Cohort, Location	Participant characteristics (N, Sex, Age)	Average follow-up period (years)	RR (95% CI) for highest vs. lowest intakes	p-value for trend	Confounder Adjustment/ BMI adjustment
Schulze *et al*., 2004	Nurses' Health Study II; US	> 91, 000; F; 24 – 44	8	1.83 (1.42– 2.36), ≥ 1 serving/day vs. <1/month	< 0.01	Yes / No
Odegaard *et al*., 2010	Singapore Chinese Health Study; China	> 43, 000; F ; 45-74	5.7	1.34 (1.17, 1.52), ≥ 2 serving/week vs. rarely	< 0.001	Yes / No
Palmer *et al*., 2008	Black Women's Health Study, US	> 43, 000;	10	1.24 (1.06– 1.45), ≥ 2 serving/day vs. ≤ 1/month	0.0002	Yes / No
Sakurai *et al*., 2014	Japan	> 2, 000; M; 35-55	7	1.34 (0.72– 2.36), ≥ 1 serving/day vs. rare/never	0.424	Yes / Yes
Fagherazzi *et al*., 2013	France	> 66, 000; F; 53 ± 7	14	1.30 (1.02– 1.66), 359 mL/week vs. never	0.0206	Yes / Yes
Teshima *et al*., 2015	Mihama diabetes prevention study; Japan	93; M& F; 40-69 *with impaired glucose tolerance	3.6	3.26 (1.17-9.06), Daily intake vs. never	0.0198	Yes / No
Nettleton *et al*., 2009	Multi-Ethnic Study of Atherosclerosis; US	> 5, 000; M & F; 45 – 84	5	1.38 (1.04–1.82), ≥ 1 serving/day vs. rare/never:	0.01	Yes / No
The InterAct Consortium, 2013	Europe-wide, EPIC-InterAct; Europe	> 15, 000; M; Mean age 55.6	6.9	1.29 (1.02– 1.63), ≥ 1 serving/day vs. <1/month	0.013	Yes / Yes
Bhupathiraju *et al*., 2013	The Health Professionals Follow-up Study; US	> 39, 000; M; 40-75	22	1.37 (1.08– 1.74), ≥ 1 serving/day vs. < 1/month	0.002	Yes / Yes
Bhupathiraju *et al*., 2013	The Nurses' Health Study I; US	> 74,000; M; 30-55	24	1.20 (1.01– 1.42), ≥ 1 serving/day vs. < 1/month	0.05	Yes / Yes
de Koning *et al*., 2011	US	> 40,000; M; 40-75	20	1.24 (1.09– 1.40) 4.5 servings/week to 7.5/day vs. never	< 0.01	Yes / Yes

1.2.3.3 CVDs

SSB intake is considered to be a risk factor for CVD (independent of BMI changes) (reviewed by Richelsen, 2013) and literature suggests that it contributes to such conditions by promoting hypertension, triggering inflammation and altering the lipid profile (Malik *et al*., 2010). As hypertension is a component of MetS and a major risk factor for CVD, an immediate question that arises relates to the link between SSB intake and hypertension. Several studies established a positive correlation between SSB consumption and hypertension (Nettleton *et al*., 2009). For example, the NHANES (2003 – 2006, > 3, 000 adults) found no correlation between overall sugar intake and blood pressure, but the daily consumption of SSBs (≥ 1 to < 3 servings) caused a 43% increase in the risk for developing hypertension (Kim *et al*., 2012). The NHANES also indicated that every additional SSB serving consumed daily (~240 mL) caused a 0.16 mm Hg upsurge in systolic blood pressure (1999 – 2004; n > 6, 5000) (Bremer *et al*., 2009). In agreement, Nguyen *et al*. (2009) used a similar dataset from the NHANES (1999-2004; n > 4, 500) and affirmed a correlation between SSB consumption and increased systolic blood pressure in adolescents. However, the latter conclusion has been criticized because published adult norms were directly applied to an adolescent cohort (White, 2009). A study that used a dataset from the International Study of Macro and Micronutrients and Blood Pressure (INTERMAP) (1996-1999; n > 2, 500) linked daily SSB consumption (≥ 360 mL) to a 1.6 mm Hg increase in systolic blood pressure (Brown *et al*., 2011). Others, however, found the exact opposite, i.e. SSB intake is rather a good indicator of increased diastolic blood pressure (Tayel *et al*., 2013).

Prospective data from the Coronary Artery Risk Development in Young adults (CARDIA) study (n > 2, 500) revealed that frequent SSB consumption causes a marginal increase (6%) in the risk of developing hypertension (Duffey *et al*., 2010). Furthermore, a pooled analysis from three prospective cohorts (The Nurses' Health Study [NHS] I and II as well as the Health Professionals Follow-up study [HPFS]; total n > 220, 000) and found that there is a 13% (RR: 1.13; 95 % CI: 1.09–1.17) higher incidence of hypertension in the population consuming ≥ 1 SSB serving/day compared to non-consumers (Cohen *et al*., 2012). The association between carbonated drinks and hypertension was significantly stronger compared to non-carbonated ones in all three cohorts while the consumption of cola-containing SSBs also indicated a stronger link to hypertension compared to non-cola SSBs (NHS I; HPFS). Increased SSB-derived fructose intake also showed a robust association with the development of hypertension (NHS I; NHS II). Similarly, Winkelmayer *et al*. (2005) used data from the NHS I and II (total n >

230, 000) in a multivariate adjusted model with the follow-up period spanning 18 months to 38 years. Here daily SSB consumption was associated with a 9% and 13% increased risk of developing hypertension in the two cohorts, respectively, and the risk increased linearly with a higher amount of daily servings.

The Framingham Offspring Study generated conflicting results as they established that participants (n > 6000) consuming ≥ 1 SSB serving/day displayed a 18% adjusted risk ratio for developing hypertension compared to infrequent consumers, but this trend was not significant (P = 0.1) (Dhingra *et al*., 2007). Similarly, the outcome of an Australian adolescent cohort (n > 1, 400) was also insignificant after multivariate adjustments were made to the data (Ambrosini *et al*., 2013). Nevertheless they found that increased SSB consumption altered lipid profiles (in boys and girls) and resulted in a greater overall cardio-metabolic risk (girls only) (Ambrosini *et al*., 2013). How does the lowering of SSB intake impact on systolic and diastolic blood pressure? A randomized controlled trial conducted for 18 months (n = 810) found that reducing SSB intake by 310 mL/daily resulted in a decrease of 1.8 mm Hg (95 % CI: 1.2–2.4) and 1.1 mm Hg (95 % CI: 0.7–1.4) in systolic and diastolic blood pressure, respectively, after adjustment for potential confounders (Chen *et al*., 2010). This result is considered to be particularly noteworthy for understanding the association between SSB intake and blood pressure (reviewed by Malik *et al*., 2014). All the relevant studies on the effect of SSB consumption on blood pressure are summarized in Table 1.2.2. However, at present the epidemiological data are not convincing and there is a lack in intervention studies to 'swing the vote'. Further research is required to provide greater insights regarding this intriguing question.

SSB consumption can also contribute to CVD by triggering a pathologic lipid profile (Stanhope, 2015). Data suggest that individuals consuming SSBs on a daily basis are ~22% more likely to suffer from hypertriglyceridemia and have an imbalance between HDL and low-density lipoproteins (LDL) levels compared to non-consumers (Dhingra *et al*, 2007). Moreover, higher SSB consumption was associated with significantly decreased HDL levels in children (n = 4, 880; 3 - 11 years), while total cholesterol, TGs and LDL levels remained unaltered (Kosova *et al*., 2013). Dhingra *et al*. (2007) also investigated the influence of gender and age in this regard, but only observed a positive association between SSB consumption and higher LDL levels in young girls (3-5 years).

Table 1.2.2: Studies investigating the link between SSB consumption and hypertension (adapted from Malik *et al*., 2014).

Author	Cohort, Location	Participants (N, Sex, Age)	Average follow-up period (years)	Outcome as reported (RR [95% CI] / Δ in blood pressure)	p-value for trend	Confounder Adjustment
Bremer *et al*., 2009	NHANES (1999-2004); US	> 6, 000; M & F; 12-19	Cross-sectional	Systolic BP: + 0.16 mm Hg per ~230 mL SSB/day	0.03	Yes
Nguyen *et al*., 2009	NHANES (1999-2004); US	> 4, 000; M & F; 12-18	Cross-sectional	Systolic BP (Δ z-score): 0.18 (0.02-0.34) > 1000mL SSB/day vs. rare/never	0.03	Yes
Kim *et al*., 2012	NHANES (2003-2006); US	> 3, 000; M & F; ≥ 19	Cross-sectional	1.43 (0.93-2.20) 1 to < 3 servings/day vs. < 1/month	0.03	Yes
Brown *et al*., 2011	INTERMAP (1996-1999); United Kingdom & US	> 2, 000; M & F; 40-59	Cross-sectional	Systolic/diastolic BP: +1.1/+0.4 mm Hg per ~355 mL SSB/day	<0.001/ <0.05	Yes
Tayel *et al*., 2013	Egypt	300; M & F; 12-18	Cross-sectional	Associated with prehypertension & hypertension High vs. low SSB consumption	0.005	No
Dhingra *et al*., 2007	Framingham Heart Study; US	> 6, 000; M & F; 42-66	4	1.18 (0.96–1.44) ≥ 1 serving/day vs infrequent consumption	0.1	Yes
Cohen *et al*., 2012	NHS I; NHS II; HPFS; US	> 220, 000; M & F; 25-75 (pooled)	38; 16; 22	1.13 (1.09–1.17) ≥ 1 serving/day vs. < 1 /month	Not stated	Yes
Winkelmayer *et al*., 2005	NHS I; NHS II; US	> 230, 000; F; 25-55	12	1.09 (0.98-1.22) 1 serving/day vs. < 1/day; 1.13 (1.03-1.24) 1 serving/day vs. < 1/day	0.03; <0.001	Yes
Duffey *et al*., 2010	CARDIA cohort; US	> 2, 000; M & F; 18-30	20	1.06 (1.01, 1.12) Consumers vs. non-consumers	0.023	Yes
Ambrosini *et al*., 2013	Offspring from the W. Australian Pregnancy Cohort (Raine) Study; Australia	>1,000; M & F; 14-17	17	Systolic BP: +1.9 mm Hg (girls only) > 1.3 servings/day vs. 0-0.5/day	0.02	Yes

SSB consumption is also a risk factor for the development of coronary heart disease (CHD) (Malik *et al*., 2010). A 22 year follow-up study established a link between SSB consumption and CHD risk (De Koning *et al*., 2012). Here SSB consumption led to an increase of several inflammatory markers such as C-reactive protein (CRP), interleukin-6 (IL-6) and tumor necrosis factor (TNF) receptors 1 and 2, while HDL, lipoprotein A and leptin levels were lower. In support, Kosova *et al*., (2013) found that increased SSB consumption by children is associated with higher CRP levels, irrespective of gender. Others established the incidence of vascular events (stroke, myocardial ischemia) in a US sample group (n > 2, 500) during a 10-year follow up period (Gardener *et al*., 2012). These data revealed that daily SSB consumption is associated with an increased risk for vascular events after controlling for multiple potential confounders (RR = 1.43, 95% CI = 1.06–1.94) compared to regular or ''light'' consumers (Gardener *et al*., 2012). However, this study did not discriminate between genders. Others found that frequent SSB consumption resulted in a worse outcome in females compared to males in a Japanese cohort (n > 39, 000) with a follow-up period of 18 years (Eshak *et al*., 2012). Fung *et al*. (2009) evaluated the effect of SSBs on CHD in the NHS cohort (n > 88, 500) during a 24-year follow-up study with subjects divided into five categories of SSB consumption (with increasing frequency). An increase in risk for CHD was observed for all categories, with the highest (≥ 2 SSB servings/day) displaying a 35% higher risk compared to the lowest category (< 1 SSB serving/month) (HR = 135, 95% CI = 1.07–1.69). A meta-analysis on four of the above-mentioned studies concluded that daily SSB consumption results in a 17% higher risk for developing CHD and that every additional serving per day further increase the risk by 16% (Huang *et al*., 2014). Here they suggest that insulin resistance, inflammation and β-cell dysfunction induced by high glycemic loads may be key mechanisms driving the onset of CHD and metabolic perturbations.

1.2.3.4 Summary of metabolic complications

Epidemiological studies are not sufficient to establish causality between SSB consumption and the development of cardio-metabolic diseases. Thus there is a great need for clinical intervention studies supporting epidemiological findings. Clinical studies could also reveal plausible molecular mechanisms – a necessary step in establishing causality between SSB consumption and cardio-metabolic pathophysiology (Stanhope, 2015). Unfortunately there are limited clinical data available and most of the available studies have some drawbacks. In order to summarize current knowledge, this section will discuss clinical studies from the past decade where SSB intervention groups were compared to SSB naïve groups. In a recent review article Stanhope (2015) explained that SSB consumption could potentially contribute to cardio-metabolic complications though direct or indirect mechanisms. SSBs are energy dense and their consumption is associated with excessive caloric intake (Miller *et al*., 2013) and subsequent weight gain. Indirectly, the increased caloric load and body mass can induce cardio-metabolic perturbations. However, SSB consumption may also have direct metabolic effects independent of body weight and energy balance.

The indirect mechanism, i.e. the effect of SSB intake on body weight and obesity, will be discussed first. De Ruyter *et al*. (2012) conducted a small clinical study (final n = 477) to establish whether SSB consumption *actually* induced weight gain in a clinical setting. Here children of normal weight (4 to 11 years old) were assigned to either experimental or control groups in a double-blinded manner and were expected to consume 250 mL SSB or artificially sweetened beverage, respectively, on a daily basis. After the 18 month intervention period body weight, BMI, waist circumference, waist-to-hip ratio and body fat percentage increased significantly in the SSB group compared to the artificially sweetened group. However, a similar study did not support the link between SSB consumption and weight gain (Maersk *et al*., 2012). This could perhaps be explained by the shorter intervention period (6 months) although the intervention itself was more severe (1 L sucrose-sweetened beverage/day compared to 250 mL/day). Aerberli *et al*. (2011) considered various anthropometric markers of obesity (i.e. body weight, BMI, waist circumference and waist-to-hip) in participants consuming glucose-, fructose- or sucrose-sweetened drinks, respectively (400-800 mL/day for three weeks). A significant increase in body weight and BMI was observed only in the group consuming glucose-sweetened beverages, while sucrose and fructose-sweetened drinks induced changes in waist circumference and waist-to-hip, but body weight and BMI did not increase. Of note, Stanhope *et al*., [2011] and Swarbrick *et al*., [2008] observed a decline in body weight and BMI in fructose-

consuming participants. These findings may provide some insight into the mechanisms in play and possibly explain why the previous study failed to detect changes in body weight. Aerberli *et al*. (2011) explained that increased glucose consumption stimulates an intensified insulin response. Insulin mediates the activity of insulin-dependent lipoprotein lipase that in turn promotes the deposition of subcutaneous fat thereby increasing the BMI. By contrast, fructose (and sucrose to some extent) has a lower glycemic load and does not trigger the release of insulin to the same extent as glucose. Thus the activity of lipoprotein lipase is reduced and the deposition of visceral fat is favored resulting in an increase in waist circumference and waist-to-hip ratio (also concluded by Stanhope *et al*., 2011). Waist circumference and waist-to-hip ratio are markers of abdominal obesity - a key feature of MetS – indicating that SSB consumption has detrimental metabolic consequences even if it does not always reflect in body weight.

This brings us to the direct effect of SSB consumption. Black *et al*. (2006) showed that SSBs can induce cardio-metabolic perturbations in a more direct manner, independent of weight gain. Their experimental groups followed an energy-balanced diet to prevent weight changes, yet they show significant increases in total cholesterol and LDL levels. This outcome is possibly indicative of atherosclerosis risk. In support, another study found that iso-caloric fructose restriction decreased diastolic blood pressure, lactate levels, TGs and LDL-cholesterol. There was also an improvement in glucose tolerance and reduced insulin levels (Lustig *et al.,* 2015). Of note, this study is not included in Table 1.2.3 because the restricted fructose did not come exclusively from SSBs. To elaborate further of the effect of SSBs on lipid profiles, Stanhope *et al*. (2015) observed an increase in LDL levels that were induced by the intake of fructose-sweetened beverages. Glucose- and sucrose-sweetened beverages also lead to elevated LDL levels (sub classes IIb and IIIa) (Aerberli *et al*., 2011). Here it was also observed that sucrose- and fructose sweetened beverages reduced the size of LDL particles – a characteristic in men with borderline hypertension (Kazumi, 2002). Thus the clinical data strongly support the link between SSB consumption and dyslipidemia.

Besides dyslipidemia, hypertension and inflammation are also risk factors for the onset of CVD. Although none of the studies supported the link between SSB consumption and the onset of hypertension (Aerberli *et al*., 2011; Black *et al*., 2006; Maersk *et al*., 2012; Stanhope *et al*., 2011; Swarbrick *et al*., 2008) there is some clinical support for the link between SSB intake and inflammation. For example, Aerberli *et al.* (2011) observed an increase in CRP levels of young men consuming SSB quantities for a 3-week period (here the specific sweetener did not

play a role). The consumption of fructose-sweetened beverages also increased uric acid levels (Stanhope *et al*., 2015), a risk factor for the onset of CVDs (Stanhope, 2015).

Some studies also provide insight into the effect of SSB consumption on glucose handling, e.g. participants consuming glucose- or fructose-sweetened drinks display elevated fasting blood glucose levels after the intervention (Aerberli *et al*., 2011; Stanhope *et al*., 2011; Swarbrick *et al*., 2008). This is an interesting result considering that such beverages have no effect on fasting insulin levels and opposite effects on postprandial insulin secretion. Here glucose consumption spiked an increase in insulin (Stanhope *et al*., 2011) while fructose caused a decrease (Stanhope *et al*., 2011; Swarbrick *et al*., 2008). In the Stanhope *et al*. (2011) study aged overweight males and females consumed either glucose- or fructose-sweetened beverages for 10 weeks (calories of the beverages accounted for ~25% of their total daily calorie intake). The fructose caused a ~17% decrease in insulin sensitivity – explaining the rise in fasting blood glucose levels associated with fructose consumption.

In summary, this section considered the link between SSB consumption and cardio-metabolic diseases. The epidemiological data on this topic is well documented and the bulk of it suggest that frequent SSB intake will increase cardio-metabolic disease risk. At this point there is not sufficient clinical data to confirm this association, fueling the ongoing controversies about the health consequences of SSB intake. However, after carefully dissecting the eight available clinical studies, it is undeniable that SSB consumption does trigger some metabolic response e.g. the participants of some studies displayed increases in various makers of obesity. This supports the data from section 1.2.3.1 concluding that SSB intake is associated with weight gain and obesity. Some of the data also indicate that hepatic glucose handling and insulin sensitivity may be altered which may ultimately lead to SSB-induced onset of MetS and T2DM. There are also signs of dyslipidemia and inflammation (known CVD risk factors) although there is no support for the development of hypertension. Finally, it seems as if glucose and fructose do not necessarily have similar metabolic effects. More well-designed clinical studies would be of great value in the quest to fully understand the metabolic and health consequences of SSB consumption

Table 1.2.3: SSB-induced perturbations in a clinical setting. A: Aerberli *et al*., 2011; B: De Ruyter *et al*., 2012; C: Stanhope *et al*., 2011; D: Swarbrick *et al*., 2008; E: Stanhope *et al*., 2015; F: Maersk *et al*., 2012; G: Black *et al*., 2006. ↑: significant increase; ↓: significant decrease; ▪ measured but no significant change; ND : not determined; s.c.: subclass

	Commercial SSB (Sucrose/HFCS)	Glucose-sweetened	Fructose-sweetened
Weight (kg)	↑ (B) ▪ (A, F, G)	↑ (A)	▪ (A) ↓ (C, D)
BMI (kg/m^2)	↑ (B) ▪ (A)	↑ (A)	▪ (A) ↓ (C, D)
Body fat (%)	↑ (B) ▪ (A, F)	▪ (A)	↑ (A) ▪ (D)
Waist circumference (cm)	↑ (A, B)	▪ (A)	▪ (A)
Waist-to-hip ratio	↑ (A, B)	▪ (A)	↑ (A)
Blood pressure (mmHg)	▪ (A, F, G)	▪ (A)	▪ (A; C, D)
LDL size (nm)	↓ (A)	▪ (A)	↓ (A) ▪ (D)
LDL level (%)	↑ (G) ↓s.c. I (A) ↑ s.c. IIb (A) ↑ s.c. IIIa (A)	↑ s.c. IIb (A)	↑ (E) ▪ (C) ↓s.c. I (A) ↑ s.c. IIb (A) ↑ s.c. IIIa (A)
Free fatty acids (µmol/L)	▪ (A)	▪ (A)	▪ (A)
TGs (mg/dL)	↑ (F) ▪ (G)	ND	↑ (E) ▪ (C, D)
Total cholesterol (mg/dL)	↑ (F, G)	ND	▪ (D)
CRP (ng/mL)	↑ (A,)	↑ (A)	↑ (A)
Leptin (ng/mL)	▪ (A, F)	↑ (A)	▪ (A)
Adiponectin (µg/mL)	▪ (A)	▪ (A)	▪ (A)
Ghrelin (pg/mL)	▪ (A)	▪ (A)	▪ (A)
Fasting glucose (mmol/L)	▪ (A, F, G)	↑ (A; C)	↑ (A; C; D)
Post-prandial glucose (2h) (mmol/L)	▪ (A)	▪ (A) ↑ (C)	▪ (A) ↓ (C, D)
Fasting insulin (µU/mL)	▪ (F, G)	▪ (C)	▪ (C; D)
Post prandial insulin (µU/mL)	ND	↑ (C)	↓ (C; D)
Uric acid (mg/dL)	ND	ND	↑ (E)

1.2.4 Reducing SSB consumption: Strategies and obstacles

Many interventions have been used in an attempt to reduce SSB consumption with varying results. One such strategy that has been making headlines in recent years is sugar/SSB taxation. Some argue that a sugar tax would have a significant effect in terms of overall, daily calorie consumption with the added benefit of securing a generous source of revenue that could be used for public health initiatives (Barry *et al*., 2013). For example, Andreyeva *et al.* (2011) argued that an additional taxation of a penny-per-ounce (~12c / 30 mL) in the US would lead to a ~110 mL decrease in daily SSB consumption per capita. This has led many countries such as France (Sparks, 2011), Mexico (Rodriguez, 2013), the United Kingdom (Gander, 2016) and some cities in the US to introduce sugar/SSB taxation strategies (Nadolny, 2016). In South Africa it was also announced in the 2016 national budget speech that a sugar tax will be levied from 1 April 2017 aiming to significantly curb the incidence of obesity in South Africa (Ismail, 2016). This is supported by research by the University of Witwatersrand (South Africa) that established that a 20% tax would reduce the prevalence of obesity by 2.4% in females and 3.8% in males. Altogether these projections suggest that there could be more than 220, 000 less obese adults in South Africa (Manyema *et al*., 2014).

Despite the potential benefits of sugar/SSB taxation the consequences are not entirely predictable and may have other repercussions. For example, while many countries are considering such a tax, Denmark repealed its long-standing SSB tax in 2014 after deeming it ineffective and detrimental to the economy (Scott-Thomas, 2013). It is also difficult to determine what the net effect of SSB taxation will be on public health as consumers may opt to buy non-taxed alternative beverages like diet sodas, fruit juices and alcoholic beverages that may not necessarily a be healthier option. Consumers may even choose to purchase cheaper and unhealthier food products in order to sustain well-established SSB habits (Edwards, 2011). Early data from Mexico indicated that there was an average decrease of 6% in SSB sales in the first year after a ~10% price increase through taxation. This translates to roughly 12 mL/capita/day (Colchero *et al*, 2016). Although this is a statistically significant decrease and the decline accelerated towards the end of the year, it is difficult to determine the long term clinical relevance. It is projected that a 10% decrease in SSB consumption would result in 189, 300 fewer T2DM and 20, 400 fewer stroke and myocardial infarction incidences over a 10 year period (2013-2022) (Sánchez-Romero *et al*., 2016). Ultimately, 18,900 fewer deaths will occur and the government would spend 983 million international dollars less on healthcare. Although it sounds promising, such projections based on a number of assumptions e.g. it is assumed that

a 10% increase in tax will result in a 10% increase in retail price i.e. that retailers and manufacturers will not absorb the cost of the added tax (Nakhimovsky *et al*., 2016). A second assumption in this particular study is that a 10% increase in tax can achieve and maintain a 10% decrease in SSB intake (Sánchez-Romero *et al*., 2016). Additionally, it is assumed that only 39% of the reduced (SSB-derived) calories will be replaced by the consumption of other foods. Due to the complexity of the matter Colchero *et al*. (2016) could not establish causality between taxation and a decrease in SSB consumption. There have also been attempts by the food industry to counter such taxation initiatives, e.g. by using aggressive marketing strategies (Colchero *et al*, 2016). Furthermore, policies to increase SSB tax generally do not enjoy public support. A survey conducted in a large representative US sample revealed that such taxation was regarded as overwhelmingly negative (Barry *et al*., 2013, Gollust *et al*., 2014). To conclude, Nakhimovsky *et al*. (2016) performed a meta-analysis to determine the effect of sugar/SSB taxation on health outcomes, specifically in middle-income countries (Brazil, Ecuador, India, Mexico, South Africa and Peru). Here they found that at least a 20% tax increase is required in order to halt the growing prevalence of obesity in middle income countries. Additionally they conclude that it is unlikely that sugar/SSB tax alone will have a permanent effect on the overall body weight of the population

Another and perhaps more implementable strategy is to improve public awareness regarding SSB sugar content and the associated health risks (Adams *et al*., 2014). There are several problems with current food labeling procedures, e.g. nutritional labels are often printed in a relatively small font and can easily be overlooked. Food labels also present information in a relatively abstract manner, e.g. grams of sugar/100 mL SSB that makes it hard to relate how much the sugar content *actually* amounts to. However, some found that displaying sugar content in a more "user-friendly" manner (e.g. images displaying sugar content in a sugar cube pyramid) significantly reduced the "attractiveness" of SSBs as well as the intention for consumption (Adams *et al*., 2014). The US Food and Drug Administration recently announced that nutritional labels have to adhere to new requirements within the next two to three years. One of the major amendments is that new labels must disclose the amount of "added sugars" as a percentage of the daily recommended allowance (10% of a 2000 Kcal diet or 12 teaspoons) (Malik *et al*., 2016). This decision was criticized by the food industry based on the argument the all calories are similar despite its source. The FDA also adjusted serving sizes and general issues regarding appearance, visibility and interpretability (Malik *et al*., 2016). An additional limitation of the current food labeling system is that it does not indicate the composition of sugar

content, i.e. the fructose to glucose ratio thus withholding crucial information from the consumer that impacts upon informed decision making (Ventura *et al*., 2011). Adams *et al*. (2014) also found that health messages displayed on SSB cans caused participants to rather choose water. This strategy was recently acknowledged in San Francisco, California (Malik *et al*., 2016). Other possible interventions include restricting SSB quantities (Gollust *et al*., 2014) and regulating availability and sales in schools (Hebden *et al*., 2013).

To conclude this section, there is a lot of epidemiologic data indicating that frequent SSB consumption leads to increased risk of disease onset. At this point, however, the limited clinical studies are not sufficient to make a compelling argument for or against the consumption of SSBs, or to elucidate possible mechanisms involved. Nevertheless, many countries have used strategies to restrict SSB consumption in the hope of curbing the prevalence of obesity and other cardio-metabolic diseases. This has proved to be a complex task, and the best strategy forward is still to be determined. As the focus of this preclinical study is on SSB-mediated metabolic changes in the liver, the emphasis now shifts to liver metabolism

1.3 Summary and Aims

Cardio-metabolic diseases like T2DM are a major global burden of disease due to the rapid increase in prevalence over the past few decades. Projections indicate that low- and middle-income countries will be affected the most by cardio-metabolic diseases in years to come. For example, the IDF estimates that T2DM will increase with 93% in Africa between 2014 and 2035 compared to the average global increase of 53%. The global projections regarding obesity, MetS and CVD are equally calamitous. These projections necessitate research to improve the understanding of the underlying factors driving this “pandemic”

It is argued that the increase in cardio-metabolic disease is caused by a fairly universal shift towards a more “Westernized” diet. The consumption of an excessive amount of added sugars, a hallmark of the “Westernized” diet, is proposed to play a key role in the onset of cardio-metabolic diseases. Subsequently, the role of SSBs in the context of cardio-metabolic diseases has become increasingly relevant. In light of this, the Cardio-Metabolic Research Group (CMRG) initiated a novel preclinical study in 2013 to evaluate metabolic perturbations induced by moderate, chronic SSB consumption in rats. The current study was based on this particular rat model and focused on the liver as a major metabolic organ. Since our previous research focused on the heart, this was an investigative study. We hoped to achieve the following aims and

objectives in order to ultimately gain a greater understanding of molecular mechanisms underlying the onset of cardio-metabolic diseases:

Aims:

1. To evaluate the effects of long-term, moderate SSB intake on systemic cardio-metabolic health markers.

2. To gain insight into changes induced in hepatic structure and function in response to long-term, moderate SSB consumption.

Objectives

1. Collect and characterize sample material from an established rat model of long-term, moderate SSB intake.

2. Perform comprehensive proteomic analysis on liver samples after six months of SSB consumption (Objective 3 and 4 will be based on the findings of Objective 2).

3. Determine the molecular mechanism driving SSB-induced alterations in protein expression.

4. Determine the downstream consequences associated with SSB-induced alterations in protein expression.

1.4 References

Abid, A., Taha, O., Nseir, W., Farah, R., Grosovski, M., & Assy, N. (2009). Soft drink consumption is associated with fatty liver disease independent of metabolic syndrome. *J Hepatol.*, *51*(5), 918–924.

Adams, J., Hart, W., Gilmer, L., Lloyd-Richeardson, E., & Burton, K. (2014). Concrete images of the sugar content in sugar-sweetened beverages reduces attraction to and selection of these beverages. *Appetite*, *83*, 10–18.

Aerberli, I., Gerber, P.A., Hochuli, M., Kohler, S., Haile, S.R., Gouni-Berthold, I., … Bernies, K. (2011). Low to moderate sugar-sweetened beverage consumption impairs glucose and lipid metabolism and promotes inflammation in healthy young men: a randomized controlled trial. *Am J Clin Nutr*, *94*, 479–485.

Alberti, K., Eckel, R., & Grundy, S. (2009). Harmonizing the Metabolic Syndrome. *Circulation*, *120*, 1640–1645.

Ambrosini, G., Oddy, W., Huang, R., Mori, T., Beilin, L., & Jebb, S. (2013). Prospective associations between sugar-sweetened beverage intakes and cardiometabolic risk factors in adolescents. *Am J Clin Nutr*, *98*, 327–334.

Andreyeva, T., Chaloupka, F., & Brownell, K. (2011). Estimating the potential of taxes on sugar-sweetened beverages to reduce consumption and generate revenue. *Prev Med*, *52*, 413–416.

Baranova, A., Tran, T., Birerdinc, A., & Younossi, Z. (2011). Systematic review: association of polycystic ovary syndrome with metabolic syndrome and non-alcoholic fatty liver disease. *Aliment Phamacol Ther*, *33*(7), 801–814.

Barquera, S., Campirano, F., Bonvecchio, A., Hernandez-Barrera, L., Rivera, J., & Popkin, B. (2010). Caloric beverage consumption patterns in Mexican children. *J Nutr*, *9*, 47–56.

Barry, C., Niederdeppe, J., & Gollust, S. (2013). Taxes on Sugar-Sweetened Beverages. Results from a 2011 National Public Opinion Survey. *Am J Prev Med*, *44*(2), 158–163.

Barry, S., Davidson, S., & Townsend, P. (2008). Molecular regulation of cardiac hypertrophy. *Int J Biochem Cell Biol*, *40*, 2023–2039.

Basu, S., McKee, M., Galea, G., & Stuckler, D. (2013). Relationship of soft drink consumption to global overweight, obesity, and diabetes: A cross-national analysis of 75 countries. *American J Public Health*, *103*, 2071–2077.

Beck, A., Tschann, J., Butte, N., Penilla, C., & Greenspan, L. (2014). Association of beverage consumption with obesity in Mexican American children. *Public Health Nutr*, *17*(2), 338--344.

Bhupathiraju, S., Pan, A., & Malik, V. (2013). Caffeinated and caffeine-free beverages and risk of type 2 diabetes. *Am J Clin Nutr*, *97*, 155–156.

Black, R., Spence, M., McMahon, R., Cuskelly, G., Ennis, C., McCance, R., … Hunter, S. (2006). Effect of eucaloric high- and low-sucrose diets with identical macronutrient profile on insulin resistance and vascular risk: a randomized controlled trial. *Diabetes*, *55*, 3566–3572.

Bray, G. (2013). Potential health risks from beverages containing fructose found in sugar or high-fructose corn syrup. *Diabetes Care*, *36*, 11–12.

Bray, G. (2016). Is sugar addictive? *Diabetes*, *65*, 1797–1799.

Bray, G., & Popkin, B. (2004). Consumption of high-fructose corn syrup in beverages may play a role in the epidemic of obesity. *Am J Clin Nutr*, *79*, 537–543.

Bremer, A., Auinger, P., & Byrd, R. (2009). Relationship between insulin resistance-associated metabolic parameters and anthropometric measurements with sugar-sweetened beverage intake and physical activity levels in US adolescents: findings from the 1999-2004 National Health and Nutrition Examination Survey. *Arch Pediat Adolesc Med*, *163*, 328–335.

Brown, I., Stamler, J., Van Horn, L., Robertson, C., Chan, Q., Dyer, A., … Elliot, P. (2011). Sugar-sweetened beverage, sugar intake of individuals, and their blood pressure: International Study of Macro/Micronutrients and Blood Pressure. *Hypertension*, *57*, 695–701.

Caballero, B. (2005). A Nutrition Paradox — Underweight and Obesity in Developing Countries. *N Engl J Med*, *325*, 1514–1516.

Chen, L., Appel, L., Loria, C., Lin, P., Champagne, C., Elmer, P., … Caballero, B. (2009). Reduction in consumption of sugar-sweetened beverages is associated with weight loss: the PREMIER trial. *Am J Clin Nutr*, *89*, 1299–1306.

Chen, L., Caballero, B., Mitchell, D., Loria, C., Champagne, C., Elmer, P., … Batch, B. (2010). Reducing Consumption of Sugar-Sweetened Beverages Is Associated With Reduced Blood Pressure A Prospective Study Among United States Adults. *Circulation*, *121*, 2398–2406.

Cohen, L., Curhan, G., & Forman, J. (2012). Association of Sweetened Beverage Intake with Incident Hypertension. *J Gen Intern Med*, *27*(9), 1127–1134.

Colchero, M., Popkin, B., Rivera, J., & Ng, S. (2016). Beverage purchases from stores in Mexico under the excise tax on sugar sweetened beverages: observational study. *BMJ*, *352*(h6704), 1–9.

Collison, K., Zaidi, M., Subhani, S., Al-Rubeaan, K., Shoukri, M., & Al-Mohanna, F. (2010). Sugar-sweetened carbonated beverage consumption correlates with BMI, waist circumference, and poor dietary choices in school children. *Public Health*, *10*, 234–247.

Cornwell, T., & McAlister, A. (2013). Contingent choice. Exploring the relationship between sweetened beverages and vegetable consumption. *Appetite*, *62*, 203–208.

De Koning, L., Malik, V., & Rimm, E. (2011). Sugar-sweetened and artificially sweetened beverage consumption and risk of type 2 diabetes in men. *Am J Clin Nutr*, *93*, 1321–1327.

De Koning, L., Malik, V.S., Kellogg, M.D., Rimm, E.B., Willett, W.C., & Hu, F.B. (2012). Sweetened beverage consumption, incident coronary heart disease, and biomarkers of risk in men. *Circulation*, *125*, 1735–1741.

De Ruyter, J., Olthof, M., Seidell, J., & Katan, M. (2012). A trial of sugar-free of sugar-sweetened beverages and body weight in children. *N Engl J Med*, *Published online*, 1–10.

DeBoer, M., Scharf, R., & Demmer, R. (2013). Sugar-sweetened beverages and weight gain in 2- to 5-year-old children. *Pediatrics*, *132*(3), 413–420.

DeFronzo, R., Bonadonna, R., & Ferrannini, E. (1992). Pathogenesis of NIDDM. A balanced overview. *Diabetes Care*, *1992*(15), 318–368.

Denova-Gutierrez, E., Talavera, J., Huitron-Bravo, G., Mendez-Hernandez, P., & Salmeron, J. (2010). Sweetened beverage consumption and increased risk of metabolic syndrome in Mexican adults. *Public Health Nutr*, *13*(6), 835–842.

Dhingra, R., Sullivan, L., Jacques, P., Wang, T., Fox, C., Meigs, J., … Vasan, R. (2007). Soft drink consumption and risk of developing cardiometabolic risk factors and the metabolic syndrome in middle-aged adults in the community. *Circulation*, *116*, 480–488.

Dubois, L., Farmer, A., Girard, M., & Peterson, K. (2007). Regular sugar-sweetened beverage consumption between meals increase risk of overweight among preschool-aged children. *J Am Diet Assoc*, *107*, 924–934.

Duffey, K., Gordon-Larsen, P., Steffen, P., Jacobs, D. J., & Popkin, B. (2010). Drinking caloric beverages increases the risk of adverse cardiometabolic outcomes in the Coronary Artery Risk Development in Young Adults (CARDIA) Study. *Am J Clin Nutr*, *92*, 954–959.

Ebbeling, C., Feldman, H., Chomitz, V., Antonelli, T., Gortmaker, S., Osganian, S., & Ludwig, D. (2012). A randomized trial of sugar-sweetened beverages and adolescent body weight. *N Engl J Med*, *367*(15), 1407–1416.

Ebbeling, C., Feldman, H., Osganian, S., Chomitz, V., Ellenbogen, S., & Ludwig, D. (2006). Effects of decreasing sugar-sweetened beverage consumption on body weight in adolescents: a randomized, controlled pilot study. *Pediatrics*, *117*, 673–680.

Edwards, R. (2011). Commentary: Soda taxes, obesity, and the shifty behavior of consumers. *Prev Med*, *52*, 417–418.

Eshak, E., Iso, H., Kokubo, Y., Yamagishi, K., Inoue, M., & Tsugane, S. (2012). Soft drink intake in relation to incident ischemic heart disease, stroke, and stroke subtypes in Japanese men and women: the Japan Public Health Centre–based study cohort I. *Am J Clin Nutr*, *96*(6), 1390–1397

Fagherazzi, G., Vilier, A., Sartorelli, D., Lajous, M., Balkau, B., & Clavel-Chapelon, F. (2013). Consumption of artificially and sugar-sweetened beverages and incident type 2 diabetes in the Etude Epidémiologique auprès des femmes de la Mutuelle Générale de l'Education Nationale–European Prospective Investigation into Cancer and Nutrition cohort. *Am J Clin Nutr*, *97*(3), 517–23.

Fezeua, L., Balkaua, B., Kengnec, A., Sobngwie, E., & Mbanyac, J. (2007). Metabolic syndrome in a sub-Saharan African setting: Central obesity may be the key determinant. *Atherosclerosis*, *193*, 70–76.

Ford, E. (2005). Prevalence of the metabolic syndrome defined by the International Diabetes Federation among adults in the U.S. *Diabetes Care*, *28*, 2745–2749.

Fung, T., Malik, V., Rexrode, K., Manson, J., Willett, W., & Hu, F. (2009). Sweetened beverage consumption and risk of coronary heart disease in women. *Am J Clin Nutr*, *89*(4), 1037–1042

Gander, K. (2016, March 17). Budget 2016: George Osborne announces sugar tax on soft drinks industry. *The Independent*.

Gardener, H., Rundek, T., Markert, M., Wright, C., Elkind, M., & Sacco, R. (2012). Diet Soft Drink Consumption is Associated with an Increased Risk of Vascular Events in the Northern Manhattan Study. *J Gen Intern Med*, *27*(9), 1120–1126.

Garnett, B., Rosenberg, K., & Morris, D. (2012). Consumption of soda and other sugar-sweetened beverages by 2-year-olds: findings from a population based survey. *Public Health Nutr*, *16*(10), 1760–1767.

Gollust, S., Barry, C., & Niederdeppe, J. (2014). Americans' opinions about policies to reduce consumption of sugar-sweetened beverages. *Prev Med*, *63*, 52–57.

Greenwood, D., Threaplton, D., Evans, C., Cleghorn, C., Nykjaer, C., Woodhead, C., & Burley, V. (2014). Association between sugar-sweetened and artificially sweetened soft drinks and type 2 diabetes: systematic review and dose – response meta- analysis of prospective studies. *Br J Nutr*, *112*, 725–734.

Grimes, C., Riddell, L., Campbell, K., & Nowson, C. (2013). Dietary Salt Intake, Sugar-Sweetened Beverage Consumption, and Obesity Risk. *Pediatrics*, *131*, 14–21.

Grundy, S. (2008). Metabolic syndrome pandemic. *Arteroscler Thromb Vasc Biol.*, *27*, 2276–2283.

Guideline: Sugars intake for adults and children. (2015). Geneva: World Health Organization.

Guyton, A., & Hall, J. (2011). *Guyton and Hall textbook of medical physiology* (12th ed.). Philidelphia: PA: Saunders/Elsevier.

Ha, H., Hwang, I., Park, J.H., & Lee, H.B. (2008). Role of reactive oxygen species in the pathogenesis of diabetic nephropathy. *Diabetes Res Clin Pract*, *82 Suppl*, S42–S45.

Han, E., Kim, T., & Powell, L. (2013). Beverage consumption and individual-level associations in South Korea. *Publlic Health*, *13*, 195–204.

Hebden, L., Hector, D., Hardy, L., & King, L. (2013). A fizzy environment: Availability and consumption of sugar-sweetened beverages among school students. *Prev Med*, *56*, 416–418.

Hert, K., Fisk II, P., Rhee, Y., & Brunt, A. (2014). Decreased consumption of sugar-sweetened beverages improved selected biomarkers of chronic disease risk among US adults: 1999 to 2010. *Nutr Res*, *34*, 58–65

Hu, F. (2013). Pro v Con Debate: Role of sugar sweetened beverages in obesity. Resolved: there is sufficient scientific evidence that decreasing sugar-sweetened beverage consumption will reduce the prevalence of obesity and obesity-related diseases. *Obes Rev*, *14*, 606–619.

Huang, C., Huang, J., Tian, Y., Yang, X., & Dongfeng, G. (2014). Sugar sweetened beverages consumption and risk of coronary heart disease: A meta-analysis of prospective studies. *Atherosclerosis*, *234*, 11–16.

IDF Diabetes Atlas: the global burden. International Diabetes Federation [online]. Available: http://www.idf.org/diabetesatlas/5e/the-global-burdan. (2015).

Ismail, A. (2016, February 24). The secret's out - SA to get a sugar tax. *Fin24*. Retrieved from http://www.fin24.com/Budget/the-secrets-out-sa-to-get-a-sugar-tax-20160224

Jastreboff, A., Sinha, R., Arora, J., Giannini, C., Kubat, J., Malik, S., … Caprio, S. (2016). Altered Brain Response to Drinking Glucose and Fructose in Obese Adolescents. *Diabetes*, *65*, 1929–1939.

Jia, M., Wang, C., Zhang, Y., Zheng, Y., Zhang, L., Huang, Y., & Wang, P. (2012). Sugary beverage intakes and obesity prevalence among junior high school students in Beijing – a cross-sectional research on SSBs intake. *Asia Pac J Clin Nutr*, *21*(3), 425–430.

Johnson, L., Mander, A., Jones, L., Emmett, P., & Jebb, S. (2007). Is sugar sweetened beverage consumption associated with increased fatness in children? *Nutrition*, *23*, 557–563.

Kazumi, T., Kawaguchi, A., Sakai, K., Hirano, T., & Yoshino, G. (2002). Young Men With High-Normal Blood Pressure Have Lower Serum Adiponectin, Smaller LDL Size, and Higher Elevated Heart Rate Than Those With Optimal Blood Pressure. *Diabetes Care*, *25*(6), 971–976.

Kim, Y., Abris, G., Sung, M., & Lee, J. (2012). Consumption of Sugar-Sweetened Beverages and Blood Pressure in the United States: The National Health and Nutrition Examination Survey 2003-2006. *Clin Nutr Res*, *1*, 85–93.

King, H., Aubert, R.E., & Herman, W.H. (1998). Global burden of diabetes, 1995-2025. Prevalence, numerical estimates, and projections. *Diabetes Care*, *21*, 1414–143.

Kleiman, S., Ng, S., & Popkin, B. (2012). Drinking to our health: can beverage companies cut calories while maintaining profits? *Obes Rev*, *13*, 258–274.

Ko, G., So, W., Chow, C., Wong, P., Tong, S., Hui, S., … Chan, J. (2010). Risk associations of obesity with sugar-sweetened beverages and lifestyle factors in Chinese: the "Better Health for Better Hong Kong" health promotion campaign. *Eur J Clin Nutr*, *64*, 1386–1392.

Kondaki, K., Grammatikaki, E., Jiménez-Pavon, D., De Henauw, S., Gonzalez-Gross, M., Sjostrom, M., … Manios, Y. (2012). Daily sugar-sweetened beverage consumption and insulin resistance in European adolescents: the HELENA (Healthy Lifestyle in Europe by Nutrition in Adolescence) Study. *Public Health Nutr*, *16*(3), 479–486.

Kosova, E., Auinger, P., & Bremer, A. (2013). The Relationships between Sugar-Sweetened Beverage Intake and Cardiometabolic Markers in Young Children. *J Acad Nutr Diet* , *113*(2), 219–227.

Kristal, R., Blank, A., Wylie-Rosett, J., & Selwyn, P. (2015). Factors Associated With Daily Consumption of Sugar-Sweetened Beverages Among Adult Patients at Four Federally Qualified Health Centers, Bronx, New York, 2013. *Prev Chronic Dis*, *12*(2), 1–16.

Lustig, R., Mulligan, K., Noworolski, S., Tai, V., Wen, M., Erkin-Cakmak, A., … Schwarz, J. (2015). Isocaloric Fructose Restriction and Metabolic Improvement in Children with Obesity and Metabolic Syndrome. *Obesity*, *24*(2), 1–8.

Lustig, R., Schmidt, L., & Brindis, C. (2012). The toxic truth about sugar. *Nature*, *482*, 27–29.

Maersk, M., Belza, A., & Stodkilde-Jorgensen, H. (2012). Sucrose-sweetened beverages increase fat storage in the liver, muscle, and visceral fat depot: a 6-mo randomized intervention study. *Am J Clin Nutr*, *95*, 283–289.

Malik, A., Akram, Y., Shetty, S., Malik, S., & Njike, V. (2014). Impact of Sugar-Sweetened Beverages on Blood Pressure. *Am J Cardiol*, *113*, 1574–1580.

Malik, V., Popkin, B., Bray, G., Despres, J., & Hu, F. (2010). Sugar-sweetened beverages, obesity, type 2 diabetes mellitus, and cardiovascular disease risk. *Circulation*, *212*, 1356–1364.

Malik, V., Willett, W., & Hu, F. (2016). The Revised Nutrition Facts Label. A Step Forward and More Room for Improvement. *JAMA*, *316*(6), 583–584.

Manyema, M., Veerman, L., Chola, L., Tugendhaft, A., Sartorius, B., Labadarios, D., & Hofman, K. (2014). the potential impact of a 20% tax on sugar-sweetened beverages on obesity in South African adults: A mathematical model. *PLoS ONE*, *9*(8), e105287.

Marcovecchio, M.L., Lucantoni, M., & Chiarelli, F. (2011). Role of chronic and acute hyperglycemia in the development of diabetic complications. *Diabetes Technol Ther*, *13*(3), 389–394.

Martin-Calvo, N., Martinez-Gonzoles, M., Bes-Rastrollo, M., Gea, A., Ochoa, M., & Marti, A. (2014). Sugar-sweetened carbonated beverage consumption and childhood/adolescent obesity: a case–control study. *Public Health Nutr*, *17*(10), 2185–2193.

Mathias, K., Slining, M., & Popkin, B. (2013). Foods and Beverages Associated with Higher Intake of Sugar-Sweetened Beverages. *Am J Prev Med*, *44*(4), 351–357.

Mattes, R. (1996). Dietary compensation by humans for supplemental energy provided as ethanol or carbohydrate in fluids. *Physiol Behav*, *59*, 179–187.

Mattes, R. (2006). Fluid calories and energy balance: The good, the bad, and the uncertain. *Physiol Behav*, *89*, 66–70.

Miller, P., McKinnon, R., Krebs-Smith, S., Subar, A., Chriqui, J., Kahle, L., & Reedy, J. (2013). Sugar-Sweetened Beverage Consumption in the U.S. Novel Assessment Methodology. *Am J Prev Med*, *45*(4), 416–421.

Murphy, R., Thornley, S., De Zoysa, J., Stamp, L., Dalbeth, N., & Merriman, T. (2015). Sugar Sweetened Beverage Consumption among Adults with Gout or Type 2 Diabetes. *PLoS ONE*.

Nadolny, T. (2016, June 16). Soda tax passes; Philadelphia is first big city in nation to enact one. *The Philidelphia Enquirer*.

Nakhimovsky, S., Feigl, A., Avila, C., O'Sullivan, G., Macgregor-Skinner, E., & Spranca, M. (2016). Taxes on Sugar-Sweetened Beverages to Reduce Overweight and Obesity in MiddleIncome Countries: A Systematic Review. *PLoS ONE*, *11*(9).

Nettleton, J., Lutsey, P., Wang, Y., Lima, J., Michos, E., & Jacobs, D. J. (2009). Diet soda intake and risk of incident metabolic syndrome and type 2 diabetes in the multi-ethnic study of atherosclerosis (MESA). *Diabetes Care*, *32*, 688–694.

Ng, S., Mhurchu, C., Jebb, S., & Popkin, B. (2011). Use of caloric and noncaloric sweeteners in US consumer packaged foods, 2005–2009. *J Acad Nutr Diet*, *112*, 1828–1834.

Ng, S., Mhurchu, C., Jebb, S., & Popkin, B. (2012). Patterns and trends of beverage consumption among children and adults in Great Britian, 1986 - 2009. *Br J Nutr*, *108*, 536–551.

Nguyen, S., Choi, H., Lustig, R., & Hsu, C. (2009). Sugar-Sweetened Beverages, Serum Uric Acid, and Blood Pressure in Adolescents. *J Pediatr*, *154*, 807–13.

Odegaard, A., Koh, W., Arakawa, K., Yu, M., & Pereira, M. (2010). Soft Drink and Juice Consumption and Risk of Physician-diagnosed Incident Type 2 Diabetes The Singapore Chinese Health Study. *Am J Epidemiol*, *171*(6), 701–708.

Ogden, C., Kit, B., Carroll, M., & Park, S. (2011). Consumption of sugar drinks in the United States, 2005-2008. *NCHS Data Brief*, *11*, 1–8.

Okafor, C. (2012). The metabolic syndrome in Africa: Current trends. *Indian J Endocrinol Metab*, *16*(1), 56–66.

Palmer, J., Boggs, D., Krishnan, S., Hu, F., Singer, M., & Rosenberg, L. (2008). Sugar-sweetened beverages and incidence of type 2 diabetes mellitus in African American women. *Arch Intern Med*, *168*, 1487–1492.

Parikh, R., & Mohan, V. (2012). Changing definitions of metabolic syndrome. *Indian J Endocrinol Metab*, *16*(1), 7–12.

Park, Y., Zhu, S., Palaniappan, L., Heshka, S., Carnethon, M., & Heymsfield, S. (2003). MetS: prevalence and associated risk factor findings in the US population from the Third National Health and Nutrition Examination Survey, 1988–1994. *Arch Intern Med*, *163*, 427–436.

Paynter, N., Yeh, H., Voutilainen, S., Schmidt, M., Heiss, G., Folsom, A., … Kao, W. (2006). Coffee and Sweetened Beverage Consumption and the Risk of Type 2 Diabetes Mellitus. The Atherosclerosis Risk in Communities Study. *Am J Epidemiol*, *164*(11), 1075–1084.

Pendergrast, M. (2000). *For God, country and Coca-Cola: The definitive history of the great American soft drink and the company that makes it.* (2nd ed.). New York: NY: Basic Books.

Poppitt, S. (2015). Beverage Consumption: Are Alcoholic and Sugary Drinks Tipping the Balance towards Overweight and Obesity? *Nutrients*, *7*(8), 6700–6718.

Rhee, J., Mattei, J., & Campos, H. (2012). Association between commercial and traditional sugar sweetened beverages and measures of adiposity in Costa Rica. *Public Health Nutr*, *15*(8), 1347–1354.

Richelsen, B. (2013). Sugar-sweetened beverages and cardio-metabolic disease risk. *Curr Opin Clin Nutr Metab Care*, *16*(4), 478–484.

Rippe, J., & Angelopoulos, T. (2016). Sugars, obesity, and cardiovascular disease: results from recent randomized control trials. *Eur J Nutr*. https://doi.org/10.1007/s00394-016-1257-2 Rodriguez, R. (2013, October 31). Experts applause ten percent on soda tax (in Spanish). *El Universal*.

Rolls, B., Kim, S., & Fedoroff, I. (1990). Effects of drinks sweetened with sucrose or aspartame on hunger, thirst and food intake in men. *Physiol Behav*, *48*, 19–26.

Ruff, R., Akhund, A., Adjoian, T., & Kansagra, S. (2014). Calorie Intake, Sugar-Sweetened Beverage Consumption, and Obesity Among New York City Adults: Findings from a 2013 Population Study Using Dietary Recalls. *J Community Health*, *39*, 1117–1123.

Sakurai, M., Nakamura, K., Miura, K., Takamura, T., Yoshita, K., Nagasawa, S., … Nakagawa, H. (2014). Sugar-sweetened beverage and diet soda consumption and the 7-year risk for type 2 diabetes mellitus in middle-aged Japanese men. *Eur J Nutr*, *53*, 251–258.

Sánchez-Romero, L., Penko, J., Coxson, P., Fernández, A., Mason, A., Moran, A., … Bibbins-Domingo, K. (2016). Projected Impact of Mexico's Sugar-Sweetened Beverage Tax Policy on Diabetes and Cardiovascular Disease: A Modeling Study. *PLoS Med*. Retrieved from http://dx.doi.org/10.1371/journal.pmed.1002158

Schulze, M., Kroke, A., Liese, A., Hoffmann, K., Bergmann, M., & Boeing, H. (2002). Food groups as predictors for short-term weight changes in men and women of the EPIC-Potsdam cohort. *J Nutr*, *132*, 1335–1340.

Schulze, M., Manson, J., Ludwig, D., Colditz, G., Stampfer, M., Willett, W., & Hu, F. (2004). Sugar-sweetened beverages, weight gain, and incidence of type 2 diabetes in young and middle-aged woman. *JAMA*, *292*, 927–934.

Scott-Thomas, C. (2013, April 25). Denmark to scrap decades-old soft drink tax. *Foodnavigator*. Retrieved from http://www.foodnavigator.com/Policy/Denmark-to-scrap-decades-old-soft-drink-tax

Shang, X., Liu, A., Zhang, Q., Hu, X., Du, S., Ma, J., … Ma, G. (2012). Report on Childhood Obesity in China (9): Sugar-sweetened Beverages Consumption and Obesity. *Biomed Environ Sci*, *25*(2), 125–132.

Sparks, I. (2011, October 6). France to impose fat tax on drinks with added sugar such as Coca-Cola and Fanta. *Daily Mail*. London.

Stanhope, K. (2015). Sugar consumption, metabolic disease and obesity: The state of the controversy. *Crit Rev Clin Lab Sci*, *Early online*, 1–16. https://doi.org/10.3109/10408363.2015.1084990

Stanhope, K., Griffen, S., Bremer, A., Vink, R., Schaefer, E., Nakajima, … Havel, P. (2011). Metabolic responses to prolonged consumption of glucose- and fructose-sweetened beverages are not associated with postprandial or 24-h glucose and insulin excursions. *Am J Clin Nutr*, *94*, 112–119.

Stanhope, K., Medici, V., Bremer, A., Lee, V., Lam, H., Nunez, M., … Havel, P. (2015). A dose-response study of consuming high-fructose corn syrup-sweetened beverages on lipid/lipoprotein risk factors for cardiovascular disease in young adults. *Am J Clin Nutr*, *101*(6), 1144–1154.

Statistics South Africa. (2013). Causes of Death 2013. Retrieved from http://www.statssa.gov.za/wp-content/uploads/2015/02/cod_2013.png

Stern, D., Piernas, C., Barquera, S., Rivera, J., & Popkin, B. (2014). Caloric Beverages Were Major Sources of Energy among Children and Adults in Mexico, 1999–2012. *J Nutr*, *144*, 949–956.

Swarbrick, M., Stanhope, K., Elliott, S., Graham, J., Krauss, R., Christiansen, M., … Havel, P. (2008). Consumption of fructose-sweetened beverages for 10 weeks increases postprandial triacylglycerol and apolipoprotein-B concentrations in overweight and obese women. *Br J Nutr*, *100*(5), 947–952.

Tanner, R., Brown, T., & Munter, P. (2012). Epidemiology of Obesity, the Metabolic Syndrome, and Chronic Kidney Disease. *Curr Hypertens Rep*, *14*, 152–159.

Tayel, D., El-Sayed, N., & El-Sayed, N. (2013). Dietary patterns and blood pressure levels of adolescents in Sohag, Egypt. *J Egypt Public Health Assoc*, *88*, 97–103.

Teshima, N., Shimo, M., Miyazawa, K., Konegawa, S., Matsumoto, A., Onishi, Y., … Sumida, Y. (2015). Effects of sugar-sweetened beverage intake on the development of type 2 diabetes mellitus in subjects with impaired glucose tolerance: the Mihama Diabetes Prevention Study. *J Nutr Sci Vitaminol*, *61*, 14–19.

The InterAct consortium. (2013). Consumption of sweet beverages and type 2 diabetes incidence in European adults: results from EPIC-InterAct. *Diabetologia*, *56*, 1520–1530. US Department of Agriculture, & US Department of Health and Human Services. (2010). Dietary Guidelines for Americans. Retrieved from http://www.health.gov/dietaryguidelines/dga2010/DietaryGuidelines2010.pdf

Ventura, E., Davis, J., & Goran, M. (2011). Sugar Content of Popular Sweetened Beverages Based on Objective Laboratory Analysis: Focus on Fructose Content. *Obesity*, *19*(4), 868–874.

Vivian, E. (2006). Type 2 diabetes in children and adolescents - the next epidemic? *Curr Med Res Opin*, *22*(2), 297–306.

Vorster, H., Kruger, A., Wentzel-Viljoen, E., Kruger, H., & Margetts, B. (2014). Added sugar intake in South Africa: findings from the Adult Prospective Urban and Rural Epidemiology cohort study. *Am J Clin Nutr*, *99*, 1479–1486.

Wang, M., Yu, M., Fang, L., & Hu, R. (2015). Association between sugar-sweetened beverages and type 2 diabetes: A meta-analysis. *J Diabetes Invest*, *6*, 360–366.

Wang, Y., Bleich, S., & Gortmaker, S. (2008). Increasing caloric contribution from sugar-sweetened beverages and 100% fruit juices among US children and adolescents, 1988–2004. *Pediatrics*, *121*, e1604–e1612.

Welsh, J., Sharma, A., Grellinger, L., & Vos, M. (2011). Consumption of added sugars is decreasing in the United States. *Am J Clin Nutr*, *94*, 726–734.

White, J. (2009). Sugar-sweetened beverage effect on cardiovascular risk factors lacks significance. Letter to Editor: The J Pediatr.

Winkelmayer, W., Stampfer, M., Willett, W., & Curhan, G. (2005). Habitual caffeine intake and the risk of hypertension in women. *JAMA*, *294*, 2330–2335.

Wolf, A., Bray, G., & Popkin, B. (2008). A short history of beverages and how our bodies treat them. *Obes Rev*, *9*, 151–164.

World Health Organization. (2015). Noncommunicable diseases Fact Sheet 355. Retrieved from http://www.who.int/mediacentre/factsheets/fs355/en/

World Health Organization. (2016) Global Diabetes Report. Retrieved form http://apps.who.int/iris/bitstream/10665/204871/1/9789241565257_eng.pdf

World Health Organization. (2016a). Cardiovascular diseases Fact Sheet 317. Retrieved from http://www.who.int/mediacentre/factsheets/fs317/en/

World Health Organization. (2016b). Diabetes factsheet 312. Retrieved from http://www.who.int/mediacentre/factsheets/fs312/en/

World Health Organization. (2016c). Obesity and overweight Fact Sheet 311. Retrieved from http://www.who.int/mediacentre/factsheets/fs311/en/

Yuzbashian, E., Asghari, G., Mirmiran, P., Zadeh-Vakili, A., & Azizi, F. (2015). Sugar-sweetened beverage consumption and risk of incident chronic kidney disease: Tehran Lipid and Glucose Study. *Nephrology*, *Epub ahead of print*. https://doi.org/10.1111/nep.12646

Zheng, M., Rangan, A., Olsen, N., Anderson, L., Wedderkopp, N., Kristensen, P., … Heitmann, B. (2015). Substituting sugar-sweetened beverages with water or milk is inversely associated with body fatness development from childhood to adolescence. *Nutrition*, *31*, 38–44.

Chapter 2: Model overview

2.1 Introduction

There are various systemic markers that reveal valuable information about the overall cardio-metabolic health of the organism e.g. insulin and uric acid. The current model was established in 2013 by the CMRG and the effect of moderate SSB intake on glucose tolerance, total cholesterol and triglyceride levels has already been determined. This section aims to build on these data to ultimately expand our holistic understanding of SSB-induced perturbations before we zoom in on a specific organ system.

2.2 Materials and methods

2.2.1 Experimental design and procedure

This study was conducted with the permission of the Animal Ethics Committees of Stellenbosch University (South Africa) (Ethics # SU-ACUM13-00012) (Appendix A). All procedures and animal handling were in agreement with the Guide for the Care and Use of Laboratory Animals of the National Academy of Science (NIH publication No. 85-23, revised 1996).

Healthy male Wistar rats weighing ~200 g were randomly divided into three groups i.e. Control, Caloric (cal) control and SSB (n = 12 per group). Each treatment group was further subdivided into a three- and six-month time group (n = 6 per subgroup), respectively. The rats were exposed to a 12 hour day-night cycle and had *ad libitum* access to standard chow and water. They were housed three per cage and familiarized with the environment, handlers and techniques for a week prior to the start of the experimental procedures.

The rats were gavaged on a daily basis with an experimental dosage according to their respective group and current weight. The SSB group received a dosage of Jive® (granadilla flavor) that was equivalent to 100 mL (~54 calories) of soda for an adult weighing 60 kg. Here the body surface area of rats to humans was used to calculate the volume required for various weight categories (Reagan-Shaw *et al*., 2007). Jive® was selected as the SSB of choice since it is locally produced and relatively inexpensive as compared to other brands, making it a popular choice for a large part of the South African population. Additionally, Jive® contains 13 g sugar per 100 mL (~54 calories). The high sugar content allowed us to gavage smaller

volumes to be gavaged. The Cal-control group received an iso-caloric amount of melted butter, while the Control group was gavaged with an iso-volumetric amount of water as stipulated in Table 2.1.1 below. The rats were weighed once a week for the duration of the study (24 weeks) to determine the percentage weight gain.

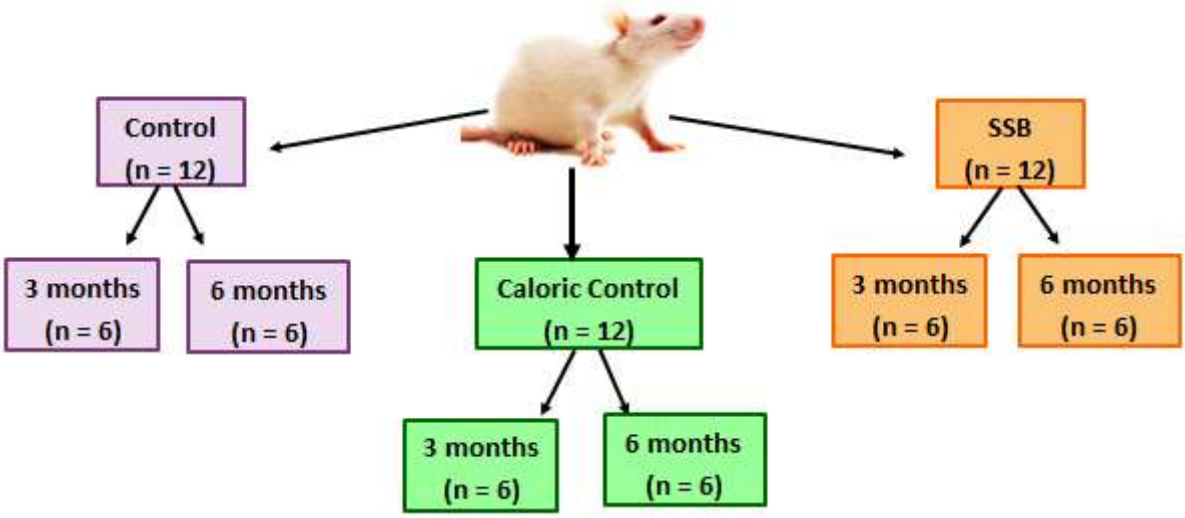

Figure 2.3.1: Experimental design

Table 2.1.1: Treatment volume according to weight classification (mL)

Group	Treatment	250-300 g	300-350 g	350-400 g	400-450 g	>450 g
Control	Water	2.4	2.9	3.4	3.8	4.4
Cal-control	Butter	0.3	0.37	0.43	0.5	0.56
SSB	Jive®	2.4	2.9	3.4	3.8	4.4

2.2.2 Blood and tissue collection

At three and six months, respectively, the rats were fasted overnight and blood glucose levels measured. A prick was made at the tip of the tail to collect a blood droplet on AccuChek® glucostrips (Roche Diagnostics, Risch-Rotkreuz, Switzerland) in the glucometer (Roche Diagnostics, Risch-Rotkreuz, Switzerland). Thereafter, the rats were sedated with 5% isoflurane (Piramal, Bethlehem PA) and pedal reflexes were tested before they were euthanized. Blood

was drawn from the abdominal aorta into serum-separating (gold) and EDTA (lavender) vacutainers (Guangzhou Improve Medical Instruments, Guangzhou, China). Blood samples were stored at -80ºC until it was sent to the National Health Laboratory Service at Tygerberg Hospital (Bellville, South Africa) for analysis - insulin, CRP, uric acid, glycated hemoglobin A1c (HbA1c) and alanine transaminase (ALT) levels were measured. Next the heart, liver, visceral fat pad, kidney, gastrocnemius muscle and pancreas were harvested and weighed. Tissues were either snap-frozen in liquid nitrogen and stored at -80°C or stored in formalin, depending on the nature of further analyses. The entire experimental setup was implemented by the CMRG in our laboratories.

2.2.3 Statistical analysis

Statistica 13.0 (StatSoft Inc., Dell Software, Tulsa OK) was used for statistical analyses. The weight gain data were analyzed with a repeated measures ANOVA test. The rest of the normally distributed data in this section were evaluated with one-way ANOVAs, while Kruskal-Wallis ANOVA and median tests were used in the case of non-parametric data. Outliers and extremes were detected using boxplots with an outlier coefficient of 2.2 and Levene's tests were used to test for homogeneity of variances. A p-value < 0.05 was considered significant. All the data were presented on Graphpad Prism 5.01 (Graphpad Software Inc., San Diego CA) as mean ± standard deviation (SD).

2.3 Results

2.3.1 Body weights

The experimental design entailed weighing the rats on a weekly basis and weight gained by each rat compared to its own baseline weight was expressed as a percentage. Here the Cal-control group gained weight at a faster pace in the first 12 weeks of the study ($P < 0.05$ at week 3 and weeks 5-12). From week 13 onwards there were no significant differences between any of the groups and at the end of the study (six months) all the rats had gained a similar amount of weight regardless of treatment (refer to Figure 2.3.1).

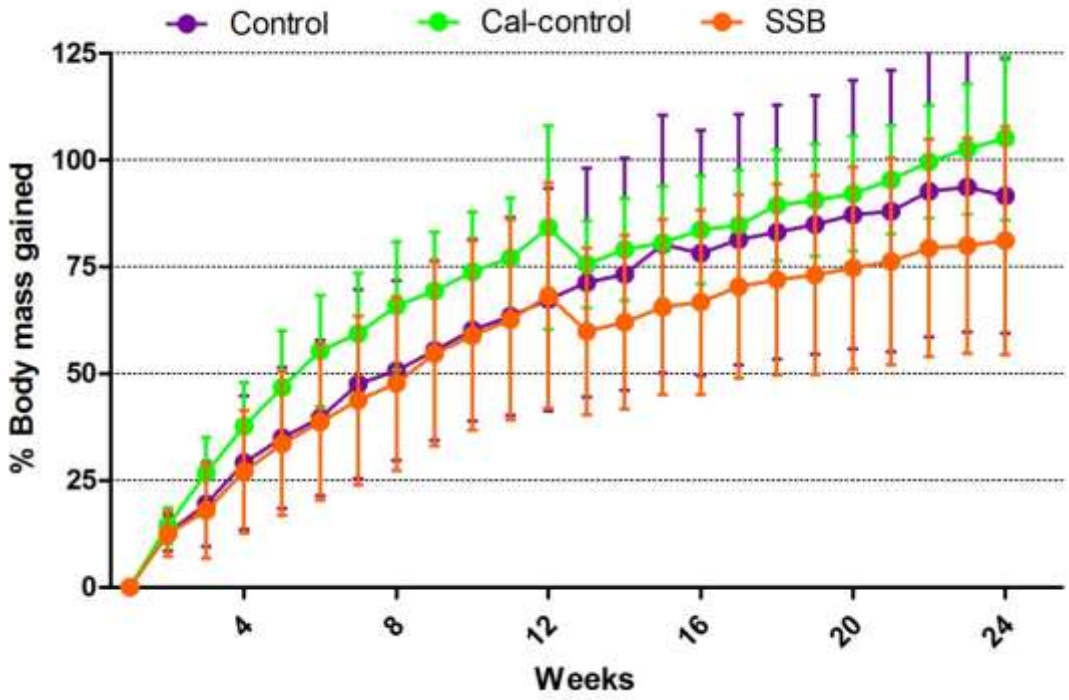

Figure 2.3.2: Percentage weight gain over 24 weeks (6 months). Data are displayed as mean ± SD. For all groups n = 24 (weeks 1-12) and n = 12 (weeks 13-24). Significance is shown as * $P < 0.05$ compared to Control and # $P < 0.05$ compared to SSB.

2.3.2 Organ weights

Tissues samples were blotted dry before weighing. Thereafter the tissues were snap-frozen or stored in formaldehyde. These included the entire liver and heart, the left gastrocnemius muscle, the right kidney and visceral fat pads around the right testicle. A relative increase or decrease in organ weight could be indicative of pathological hypertrophy or atrophy in the respective organ. The weights of various tissues (expressed as a percentage of the final body weight) are portrayed in Table 2.3.1. Here it was observed that liver weights and visceral fat pad mass of the Cal-control group increased ($P < 0.05$) compared to both the control and SSB groups. This is a noteworthy finding although it is not directly relevant for the purpose of this study. The SSB group did not show any significant changes for any of the tissues at three or six months.

Table 2.3.1: Organ weights expressed as a percentage of final body mass.

Organ	Months	Control	Cal-control	SSB
Liver (%)	Three	2.347 ± 0.330	2.754 ± 0.298 * #	2.405 ± 0.264
	Six	2.446 ± 0.206	2.549 ± 0.194	2.439 ±0.22p
Heart (%)	Three	0.261 ±0.041	0.263 ± 0.018	0.240 ± 0.024
	Six	0.233 ± 0.018	0.236 ± 0.021	0.233 ± 0.020
Muscle (%)	Three	0.599 ± 0.070	0.621 ± 0.131	0.602 ± 0.117
	Six	0.462 ± 0.155	0.566 ± 0.043	0.542 ± 0.086
Kidney (%)	Three	0.285 ± 0.044	0.296 ± 0.037	0.270 ± 0.029
	Six	0.249 ± 0.020	0.2642 ± 0.030	0.263 ± 0.021
Visceral fat pads (%)	Three	1.001 ±0.447	1.337 ± 0.321 * #	0.967 ± 0.243
	Six	1.306 ± 0.253	1.546 ± 0.326	1.582 ± 0.500

Data are displayed as mean ± SD
N ≥ 11 for all groups
***** Significantly different compared to Control group ($P < 0.05$)
# Significantly different compared to SSB group ($P < 0.05$)

2.3.3 Biochemical analyses

Blood samples were collected from the tail and abdominal aorta and then analyzed for systemic markers (findings summarized in Table 2.3.2). Uric acid levels increased in the Cal-control group compared to the Control and SSB groups ($P<0.05$). ALT levels were measured as a marker for liver damage and levels were similar amongst all three groups at both time points. Insulin levels and CRP (a marker for systemic inflammation) were also measured but were below detectable levels in all samples.

Different methods were used to determine blood glucose levels. For example, blood collected by tail pricks was used to determine fasting blood glucose levels. However, no significant changes were observed at time points investigated. HbA1c levels were also measured (provides indication of average blood glucose levels over the past 8-12 weeks) and expressed according to three different systems. The National Glycohemoglobin Standardization Program (NGSP) system is the most widely used and results are expressed as a percentage (Little & Sacks, 2009). Here no significant changes were observed after three or six months versus controls. The International Federation for Clinical Chemistry (IFCC) method relies on high performance liquid chromatography to separate glycated and non-glycated peptides. Thereafter mass spectrometry or capillary electrophoresis is used in order to quantify each respective

group. This method generally yield a result 1.5-2% lower than the NGSP and is expressed in mmol/mol (Little & Sacks, 2009). According to the IFCC method, the SSB group displayed elevated HBA1c levels compared to the Control group at both three and six months ($P < 0.05$). Although the increase compared to the Cal-control is not significant, a definite trend is evident at three months ($P = 0.077$). The last set of readings is the estimated average glucose (eAG) that is calculated with a regression equation and measured in mmol/L. Here the SSB group exhibited an increase ($P < 0.05$) compared to the Control group at three months but no other changes were detected. It is important to note, however, that the validity of the eAG method is often contested (Little & Sacks, 2009).

Table 2.3.2: Various blood markers at three and six months.

Marker	Months	Control	Cal-control	SSB
Uric acid (mmol/L)	Three	0.0617 ± 0.012	0.075 ± 0.010	0.062 ± 0.010
	Six	0.075 ± 0.014	0.043 ± 0.008* #	0.080 ± 0.015
ALT (U/L)	Three	61.60 ± 6.768	55.67 ± 6.088	53.50 ± 14.29
	Six	54.17 ± 6.494	46.50 ± 8.118	66.20 ± 17.02
Fasting blood glucose (mmol/L)	Three	4.717 ± 0.500	4.425 ± 0.347	4.400 ± 0.500
	Six	5.525 ± 0.890	5.417 ± 0.388	5.325 ± 0.723
HbA1c [NGSP] (%)	Three	3.233 ± 0.242	3.333 ± 0.225	3.500 ± 0.346
	Six	3.133 ± 0.320	3.317 ± 0.319	3.333 ± 0.207
HbA1c [IFCC] (mmol/mol)	Three	10.20 ± 1.304	11.50 ± 01.643	15.83 ± 2.787*
	Six	10.67 ± 3.143	12.83 ± 3.656	13.00 ± 12.530 *
HbA1c [eAG] (mmol/L)	Three	2.40 ± 0.268	2.70 ± 0.358	3.183 ± 0.407 *
	Six	2.417± 0.504	2.683 ± 0.504	2.70 ± 0.341

Data are displayed as mean ± SD
N ≥ 11 for all groups
***** Significantly different compared to Control group ($P < 0.05$)
# Significantly different compared to SSB group ($P < 0.05$)

2.4 Discussion

The purpose of the initial part of this study was to establish the effects of SSB consumption on systemic markers related to cardio-metabolic disease states. Here we considered weight gain, relative organ weight and various blood markers. These data, together with data previously generated by the CMRG (Driescher, 2014), provides a comprehensive overview of systemic changes induced by moderate SSB intake.

SSB consumption did not have a significant effect on weight gain in our model (Figure 2.3.1). This finding agrees with the majority of similar animal studies that did not report any differences between the SSB and control groups for body weight/weight gained (Diaz-Aguila *et al*., 2015; Figlewicz *et al*., 2009; Lozano *et al*., 2016; Rebollo *et al*., 2014, Sheludiakova *et al*., 2012). Despite relative consensus on this matter, there were a few studies with an opposite finding, e.g. in a study by Mamikutty *et al*. (2014) rats consuming SSBs gained significantly more weight compared to control rats. However, the fact that ~67% of the total calorie intake of this group was SSB-derived may possibly account for the exaggerated reaction. Others found that HFCS led to excessive weight gain (Bocarsley *et al*., 2010). We speculate that this is due to the intrinsic nature of HFCS bearing in mind that Light *et al*. (2009) evaluated the effect of sucrose, glucose, fructose and HFCS intake, respectively, and only observed significant changes in body weight in the HFCS group. Some studies observed an increase in VAT (based on a combined measure of pericardial, peritoneal and gonadal fat pads), despite no significant increase in body weight (Diaz-Aguila *et al*., 2015). For this reason we measured the relative weight of gonadal fat pads as an indicator of VAT, but SSB consumption had no effect here (Table 2.3.1). However, the gonadal fat pad may not be a sensitive enough marker, as Bocarsley *et al*. (2010) found that HFCS significantly increased abdominal fat pad weight but not that of gonadal fat pads. Additionally, none of the other studies measured only the gonadal fat pad as a marker of VAT.

We also measured the relative weight of the heart, liver, muscle and kidney but here SSB consumption had no detectable effects (Table 2.3.1). Jürgens *et al*. (2005) also determined that neither sucrose nor fructose consumption increased the relative weight of the liver. Of note, in our model the Cal-control group gained weight at a slightly increased pace during the first twelve weeks of the study (Figure 2.3.1). The reason behind this is unclear considering that the Cal-control and SSB group consumed a similar amount of total calories (Driescher *et al*., 2014) but it corresponds with the increased relative weight of the liver and visceral fat pads in the Cal-control group at three months. However, in all instances this effect tapers off by six months where body and organ weights of all groups are similar.

In our model SSB consumption did not alter fasting blood glucose levels at three or six months (Table 2.3.2). This result agrees with other studies that used sucrose as sweetener (Diaz-Aguila *et al*., 2015; Sheludiakova *et al*., 2012). Yet, both these studies observed a decrease in insulin sensitivity despite “healthy” blood glucose levels. Unfortunately, the insulin levels in our model were below detectable levels and prevented us from making meaningful conclusions

regarding insulin sensitivity. Lozano *et al*. (2016) observed impaired glucose tolerance without a rise in fasting blood glucose levels after rats consumed 25% fructose water for eight months. Moreover, others found that fructose consumption was linked to elevated fasting blood glucose levels, but again the dosage of the sweetener was disproportionately high and the study was also conducted on female rats (Rebollo *et al*., 2014). The latter is an important consideration as Vilà *et al*. (2011) observed that fructose intake elicited more severe effects on glucose tolerance and insulin signaling in female rats compared to males. For our model, SSB consumption increased HbA1c levels (IFCC and eAG) but this finding is not clinically relevant although it is statistically significant (Table 2.3.2). We also found that ALT levels were similar between all the experimental groups, indicating that liver function is intact (Table 2.3.2). This finding is supported by a short term clinical study (Aerberli *et al*., 2011). By contrast, others found that HFCS and fructose consumption can induce significant elevations in ALT levels (Figlewicz *et al*., 2009). Although this is contradictory to our finding, this study concluded that the increased ALT levels only point to minor tissue injury as the liver histology did not reveal any profound liver damage. SSB consumption had no significant effects on uric acid levels.

To conclude, in agreement to earlier work, our data confirm that moderate SSB consumption resulted in minimal effects on systemic markers for cardio-metabolic health within a six month time frame. With the characterization of the systemic effects completed we next investigated the effects of SSB consumption on the liver.

2.5 References

Aerberli, I., Gerber, P.A., Hochuli, M., Kohler, S., Haile, S.R., Gouni-Berthold, I., … Bernies, K. (2011). Low to moderate sugar-sweetened beverage consumption impairs glucose and lipid metabolism and promotes inflammation in healthy young men: a randomized controlled trial. *Am J Clin Nutr*, *94*, 479–485.

Bocarsly, M., Powell, E., Avena, N., & Hoebel, B. (2010). High-fructose corn syrup causes characteristics of obesity in rats: Increased body weight, body fat and triglyceride levels. *Pharmacol Biochem Behav*, *97*, 101–106.

Díaz-Aguila, Y., Castelán, F., Cuevas, E., Zambrano, E., Martínez-Gómez, M., Muñoz, A., … Nicolás-Toledo, L. (2015). Consumption of sucrose from infancy increases the visceral fat accumulation, concentration of triglycerides, insulin and leptin, and generates abnormalities in the adrenal gland. *Anat Sci Int*. https://doi.org/10.1007/s12565-015-0279-9

Driescher, N. (2014). *Establishing a rodent model of long-term consumption of sugar-sweetened beverages*. Stellenbosch University, Stellenbosch.

Figlewicz, D., Ioannou, G., Bennett Jay, J., Kittleson, S., Savard, C., & Roth, C. (2009). Effect of moderate intake of sweeteners on metabolic health in the rat. *Physiol Behav*, *98*, 618–624.

Jürgens, H., Haass, W., Castañeda, T., Schürmann, A., Koebnick, C., Dombrowski, F., … Tschöp, M. (2005). Consuming fructose-sweetened beverages increases body adiposity in mice. *Obes Res*, *13*(7), 1146–1156.

Light, H., Tsanzi, E., Gigliotti, J., Morgan, K., & Tou, J. (2009). The type of caloric sweetener added to water influences weight gain, fat mass, and reproduction in growing Sprague-Dawley female rats. *Exp Biol Med*, *234*(6), 651–661.

Little, R., & Sacks, D. (2009). HbA1c: how do we measure it and what does it mean? *Curr Opin Endocrinol, Diabetes & Obes*, *16*(2), 113–118

Lozano, I., Van der Werf, R., Bietiger, W., Seyfritz, E., Peronet, C., Pinget, M., … Dal, S. (2016). High-fructose and high-fat diet-induced disorders in rats: impact on diabetes risk, hepatic and vascular complications. *Nutr Metab*, *13*(15). https://doi.org/10.1186/s12986-016-0074-1

Mamikutty, N., Thent, Z., Sapri, S., Sahruddin, N., Mohd Yusof, M., & Haji Suhaimi, F. (2014). The establishment of metabolic syndrome model by induction of fructose drinking water in male Wistar rats. *Biomed Res Int*. http://doi.org/10.1155/2014/263897

Reagen-Shaw, S., Nihal, M., & Ahmad, N. (2008). Dose translation from animal to human studies revisited. *FASEB J*, *22*(3), 659–661

Rebollo, A., Roglans, N., Baena, M., Padrosa, A., Sánchez, R., Merlos, M., … Laguna, J. (2014). Liquid fructose down-regulates liver insulin receptor substrate 2 and gluconeogenic enzymes by modifying nutrient sensing factors in rats. *J Nutr Biochem*, *25*, 250–258.

Sheludiakova, A., Rooney, K., & Boakes, R. (2012). Metabolic and behavioural effects of sucrose and fructose/glucose drinks in the rat. *Eur J Nutr*, *51*(445). https://doi.org/10.1007/s00394-011-0228-x

Vilà, L., Roglans, N., Perna, V., Sánchez, R., Vázquez-Carrera, M., Alegret, M., & Laguna, J. (2011). Liver AMP/ATP ratio and fructokinase expression are related to gender differences in AMPK activity and glucose intolerance in rats ingesting liquid fructose. *J Nutr Biochem*, *22*(8), 741–751

Chapter 3: Liver - Proteomics

3.1 Introduction

The liver is an important metabolic organ involved in the breakdown, synthesis, storage and redistribution of a variety of substrates i.e. carbohydrates, lipids and proteins (Bechmann, 2012). Since SSB-induced effects on liver structure and function are still poorly understood, we decided to begin our study on the liver with protein expression profiling. This entails the characterization of the entire protein complement expressed in the liver. As protein expression is influenced by the cellular environment, SSB-induced alterations in protein expression should provide a more holistic understanding of the effects of long-term SSB intake on hepatocytes (Graves & Haystead, 2002). The field of proteomics is growing rapidly and to our knowledge this is the first study to perform hepatic proteomics in the context of SSB intake - we hope that the data generated here could guide future cardio-metabolic research. In order to better contextualize this part of the study the following sections (3.1.1 – 3.1.4) provide an overview of the basic physiological processes involved in the metabolism of a SSB.

3.1.1 Hepatic glucose metabolism

The liver plays a central role in glucose homeostasis as it has the ability to either add or remove glucose from circulation depending on the overall metabolic state of the organism (Bizeau & Pagliassotti, 2005). This dynamic balance between glucose storage and production allows blood glucose levels to be maintained within a narrow homeostatic range (3.9 - 5.6 mM), despite temporal changes induced by feeding and fasting (Roden & Bernoider, 2003). The liver is responsible for the clearance of ~60-65% of all consumed glucose (Moore *et al*., 2012).

Directly after the consumption of a SSB, i.e. during the absorptive state, blood glucose concentrations are high and serve as the main source of energy. Excess glucose that cannot be immediately utilized is stored in the form of glycogen or TGs (Sherwood, 2010). Due to the absorption of nutrients into the hepatic portal vein, the liver is rapidly exposed to much higher glucose concentrations compared to other organs (Moore *et al*., 2012). When glucose enters the hepatic portal vein there is increased uptake by the liver, while storage of glucose is stimulated (Moore *et al*., 2012). Hepatic glucose uptake is independent of insulin signaling; the high blood glucose concentration in the liver sinusoid allows glucose to enter the hepatocytes directly by virtue of facilitated diffusion through the glucose transporter (GLUT) 2. This

concentration gradient is maintained by rapid phosphorylation of glucose (after entering the hepatocyte) to glucose-6-phosphate (G-6-P) (Roden & Bernoider, 2003). The continuous hepatic uptake of glucose decreases blood glucose levels in order to return it to physiological levels.

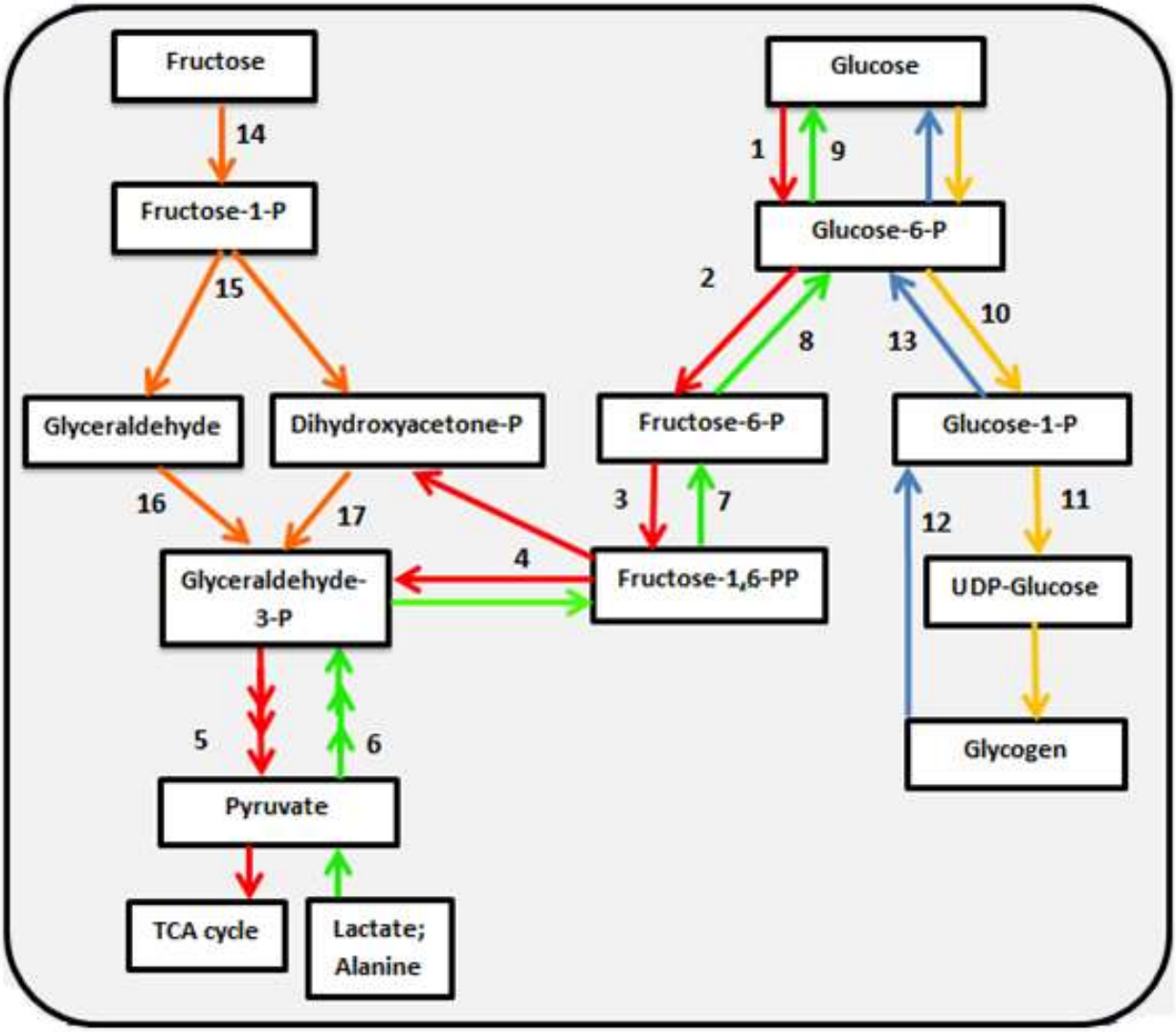

Figure 3.1.1: Hepatic glucose and fructose metabolism.
1 – Glucokinase; 2 – Phosphoglucose isomerase; 3 - Phosphofructokinase; 4- Aldolase; 5 – Pyruvate kinase, 6 – Phosphoenolpyruvate carboxykinase (PEPCK), 7 – Fructose-1,6-biphosphatase; 8 – Phosphoglucose isomerase; 9 – Glucose-6-phosphatase (G-6-Pase); 10- Phosphoglucomutase; 11 - Glycogen synthase; 12 – Glycogen phosphorylase; 13 – Phosphoglucomutase; 14 - Fructokinase; 15 - Frucose-1-phosphoaldose; 16 - Glyceraldehydekinase; 17 - Triose phosphate isomerase

Intrahepatic glucose can either be metabolized through glycolysis or diverted into storage as glycogen molecules depending on the hormonal and the energetic state of the hepatic environment (Roden & Bernoider, 2003). Pancreatic hormones (glucagon and insulin) are secreted directly into the hepatic portal vein to rapidly alter the activity of metabolic enzymes, thereby adapting metabolic processes according nutrient availability. Insulin levels are elevated during the fed (absorptive) state. Although insulin is not required for hepatic glucose uptake, it directs intrahepatic glucose to the glycogenesis pathway – synthesizing glycogen from 20-30% of consumed carbohydrates (Figure 3.1.1 - yellow arrows) (Postic, 2004). Glycogen is also stored in skeletal muscle; thereafter excess glucose can also be directed into a lipogenic pathway to synthesize *de novo* lipids (Postic, 2004). The rate of hepatic glycogen synthesis is regulated by glycogen synthase and here insulin promotes its dephosphorylation by protein phosphatase-1, leading to its activation (Postic, 2004). In parallel, glycogen phosphorylase (GP) is also dephosphorylated resulting in its inhibition (Postic, 2004) and subsequently less glycogen breakdown. Of note, in diabetic patients glycogen synthesis can be faulty thus prohibiting efficient storage and the subsequent lowering of blood glucose levels to within physiologic levels (Postic, 2004).

The post-absorptive state (also known as fasting state) refers to the period roughly four hours after the consumption of the previous meal and is marked by a decrease in blood glucose levels (Sherwood, 2010). Stored nutrients are now catabolized to maintain blood glucose levels within the physiological range where is can fulfill the body's and especially the brain's metabolic demands (Sherwood, 2010). There is therefore a net output of hepatic glucose during the post-absorptive state that occurs as a result of two pathways, i.e. glycogenolysis and gluconeogenesis. The latter is an interesting reaction as it enables both the liver and the kidneys (to a lesser extent) to also produce glucose endogenously (Roden & Bernoider, 2003). Glycogenolysis refers to the breakdown of glycogen stores (Figure 3.1.1 - blue arrows) to form glucose. This pathway generally occurs earlier than gluconeogenesis, roughly 2-6 hours after dietary intake. Glycogenolysis is enhanced by the activation (phosphorylation) of GP and the inhibition of glycogen synthase activity (Postic, 2004). Gluconeogenesis plays a larger role in extended fasting and refers to the *de novo* synthesis of glucose (Figure 3.1.1 - green arrows) from lactate, alanine and other non-carbohydrate precursors (Postic, 2004). Ultimately free glucose is released into the hepatic vein and back into circulation (Roden & Bernoider, 2003).

The post-absorptive state is also marked by a shift in circulating insulin and glucagon levels. Here insulin levels now normalize while glucagon becomes the predominant hormone (Roden &

Bernoider, 2003). Glucagon (together with glucocorticoids) can regulate gluconeogenic enzymes at the transcriptional level e.g. it promotes the expression of PEPCK, a unidirectional and rate-limiting enzyme of the gluconeogenic pathway. In addition, it can increase expression of G-6-Pase that regulates the dephosphorylation of G-6-P to glucose. Glucagon also inhibits the glycolytic enzymes pyruvate kinase and phosphofructo-1-kinase (Roden & Bernoider, 2003). Insulin elicits the opposite effect on these hormones (Postic, 2004). However, in diabetic individuals (both type 1 and type 2) increased hepatic glucose output results in hyperglycemia during both the fed and fasting states (Postic, 2004).

3.1.2 Hepatic fructose metabolism

Fructose has the same chemical formula as glucose, i.e. $C_6H_{12}O_6$ but is structurally distinguishable by the keto-group attached to the second carbon of fructose compared to glucose that has an aldehyde group bound to position 1 of its carbon chain (Tappy & Le, 2010). The ingestion of fructose (e.g. from SSBs) induces a modest increase in insulin levels compared to glucose consumption, together with minor changes in both blood glucose and fructose concentrations. The absorption of fructose, and free fructose in particular, is usually restricted. However, this improves greatly in the presence of glucose (e.g. sucrose or HFCS). Fructose absorption is different from glucose absorption in that it does not require adenosine triphosphate (ATP) and is not coupled to sodium uptake (Tappy & Le, 2010). It is absorbed mainly in the enterocytes of the jejunum (through GLUT5 transporter) and then diffuses into the hepatic portal bloodstream through GLUT2 (Havel, 2005). Although GLUT5 is localized on a variety of tissues, e.g. adipocytes and skeletal muscle, the bulk of fructose is directed towards the liver thus rendering it the primary organ involved in fructose metabolism.

In the liver fructose is rapidly phosphorylated (by fructokinase) to yield fructose-1-phosphate (F-1-P) (Havel, 2005) (Figure 3.1.1 – orange arrows). This is an important step that distinguishes fructose metabolism from glucose metabolism since F-1-P can enter the glycolytic pathway downstream from phosphofructokinase, the rate-limiting step of glycolysis (Havel, 2005). Furthermore, the conversion of fructose to F-1-P takes place independently of insulin levels and is not regulated by the negative feedback mechanisms triggered by citrate and ATP that regulate glucose metabolism (Tappy & Le, 2010). Together this allows fructose to be rapidly metabolized and in a less controlled manner compared to glucose. Fructose metabolism yields triose phosphates (dihydroxyacetone and glyceraldehyde) that can thereafter follow one of three pathways (Havel, 2005). The largest percentage (~50%) of triose phosphates is diverted into

the gluconeogenic pathway to produce glucose. An additional (~14%) is directly diverted into glycogen storage. Another portion is metabolized to pyruvate that can enter the tricarboxylic acid cycle (TAC) together with glucose-derived pyruvate. The last ~15% is utilized to synthesize lactate that is released back into the circulatory system. Of note, the production of glucose and lactate from fructose are interdependent (Tappy & Le, 2010)

3.1.3 Hepatic lipid metabolism

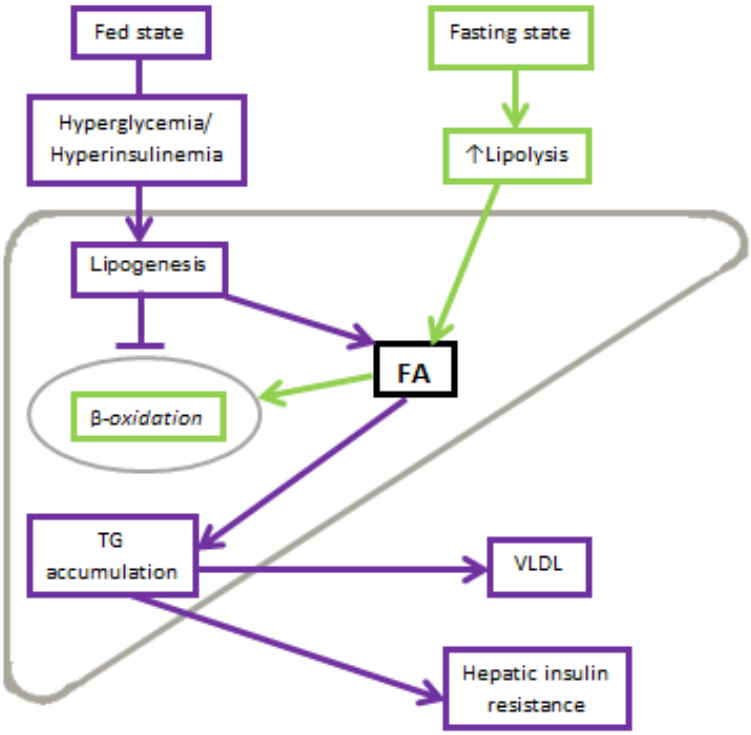

Figure 3.1.2: Hepatic lipid metabolism. Hepatic lipid metabolism during fasting and fed states. Adapted from Fabbrini & Magkos (2015).

Hepatic lipid content depends on the balance between lipid uptake/synthesis versus lipid metabolism and export (Perry *et al*., 2014) (Figure 3.1.2). Since lipid and carbohydrate metabolism are interdependent it is also largely regulated by the same hormones (i.e. insulin, glucagon and epinephrine) and metabolic states (i.e. fed, fasted, starved).

During the fed state, hepatic fatty acids (FAs) are synthesized by endogenous lipogenesis (Bechmann, 2012), a process that is facilitated by insulin (Horton *et al*., 2006). Hepatic *de novo* lipogenesis, a two-phase process, generally occurs during the fed state when glucose is abundant and the liver has reached its capacity for glycogen storage. The initial phase entails the *de novo* synthesis of FAs and here acetyl-CoA and malonyl-CoA can serve as substrates while acetyl-CoA carboxylase and fatty acid synthase catalyze the reaction. The regulation of fatty acid synthase in particular is complex as various ligands and hepatic nuclear receptors are involved. The post-prandial insulin spike promotes intrahepatic FA synthesis by increasing the expression of fatty acid synthase, providing a possible explanation for elevated hepatic lipid deposition observed in the Maersk *et al*. (2012) clinical intervention study..

Besides insulin, carbohydrate-responsive element binding protein (ChREBP) and steroid regulatory element-binding protein (SREBP)-1c also play an important role in the regulation of lipogenesis and linking hepatic glucose and lipid metabolism. Together these two proteins can increase the expression of acetyl-CoA carboxylase and fatty acid synthase, ultimately enhancing FA synthesis (Bechmann, 2012). In particular, the SREBP-1c isoform is linked to perturbations in TG synthesis/storage and insulin resistance (Postic *et al*., 2004). As FAs are also associated with oxidative stress and lipotoxicity, the second phase of *de novo* lipogenesis entails storing FAs as TGs. Here mitochondrial glycerol-3-posphate-aceyltansferase and diacylglycerol-acyltransferase catalyze the esterification of three FA chains to a glycerol backbone to form one TG molecule, thereby reducing the lipotoxic effect of FAs. Intrahepatic TGs will either remain in the liver as lipid droplets or it can enter the circulation packaged as very low-density lipoproteins, a process also facilitated by ChREBP and SREBP-1c (Bechmann, 2012). Insulin promotes intrahepatic lipid accumulation by preventing the breakdown of FAs and TGs (Horton *et al*., 2006).

By contrast, glucagon (together with epinephrine) levels increase during the fasting state (Horton *et al*., 2006) and hepatic FAs are taken up into the liver from free circulating FAs and thereafter catabolized by the β-oxidation pathway (Bechmann, 2012). During the fasting state lipolysis also occurs in adipocytes and results in a large pool of free FAs in circulation. This allows increased FA uptake by hepatocytes (via sarcolemmal FA transport proteins 2 and 5). This process is regulated by altering the transcription of FA transport proteins that is mainly reliant on peroxisome proliferator-activated receptor-α signaling (Bechmann, 2012). Once FAs are taken up by liver cells it can be oxidized to serve as a source of ATP. FA oxidation takes place in mitochondria, peroxisomes or the endoplasmic reticulum (ER), depending on the length

of the FA chain and other environmental factors. Under physiological conditions most FAs are metabolized in the mitochondrion through β-oxidation. Glucagon and epinephrine compensate for the decrease in glucose availability by promoting the transport of activated FAs into mitochondria to serve as an energy source. This is mainly achieved by suppressing the synthesis of malonyl-CoA that usually inhibits carnitne acyltransferase I – the latter catalyzes the association between fatty acyl-CoA and carnitine, a necessary step to allow FAs into mitochondria (Horton *et al*., 2006). When the liver is insulin resistant and there is an excessive amount of FAs present; subsequently long- and very-long chain FAs will be oxidized in the ER and peroxisomes. This will in turn induce oxidative stress, inflammation and apoptosis (Bechmann, 2012).

The important question is, however, how does SSB consumption impact on metabolic pathways here discussed? Based on the clinical data earlier discussed, it emerges that frequent SSB intake can lead to perturbations in hepatic lipid metabolism. This includes excessive hepatic, muscle and visceral lipid deposition (Maersk *et al*., 2012) together with elevated total cholesterol, LDL and plasma TG levels (Black *et al*., 2006; Maersk *et al*., 2012; Stanhope *et al*., 2015). Such perturbations contribute to the development of cardio-metabolic diseases, e.g. there is a strong association between intrahepatic lipid levels and hepatic insulin resistance (Perry *et al*., 2014). The literature suggests that fructose in particular is involved in altering lipid metabolism (Dekker *et al*., 2010). Despite uncertainty regarding the exact mechanisms involved it is important to understand hepatic lipid metabolism under physiological and pathophysiologic conditions in order to better identify the role(s) of SSB consumption in this context

3.1.4 Insulin signaling

During the fed state glucagon levels are relatively low and insulin secretion is increased (Guyton and Hall, 2010). Although hepatic glucose uptake takes place independently of insulin, it is important for priming the liver for sudden changes in carbohydrate and lipid homeostasis. Insulin acts to lower blood glucose levels by promoting glucose utilization and storage and thereby preventing the ‘’toxic’’ effects of hyperglycemia. This is mainly brought about by changes in the expression of genes encoding glycolytic and lipogenic genes (Michael *et al*., 2000). The insulin signaling pathway and its impact on target genes will now be discussed in greater detail.

Pancreatic β-cells secrete insulin directly into circulation to allow it to bind to insulin receptors that are situated on the surface of hepatocytes, adipocytes and myocytes. Insulin receptors are part of a family of receptors named receptor tyrosine kinases that trigger an intracellular signaling cascade in the presence of insulin (Guyton & Hall, 2011). Insulin receptors consist of two extracellular α-subunits and two β-subunits that penetrate the cell membrane. Insulin binds to extracellular α-subunits that initiate auto-phosphorylation by intracellular β-subunits. Insulin signaling is a dynamic process regulated by numerous phosphorylation and dephosphorylating reactions (Choi & Kim, 2010). The phosphorylation of the tyrosine residues on the insulin receptor substrates (i.e. insulin receptor substrate (IRS) 1 – 6, src homology 2, casitas B-lineage lymphoma and GRB-associated binder-1) follows (Meshkani & Adeli, 2009). Phosphatidylinositol-4,5-bisphosphate 3-kinase (PI3K) further relays the signal and consists of two subunits, regulatory (p85) and catalytic (p110), respectively. In the absence of insulin the p85 subunit inhibits the p110 subunit. However, when insulin signaling is initiated the activated IRS acts as a docking station for PI3K. This results in the inhibition of p85 that allows for the enzymatic activation of the p110 subunit (Cuevas *et al*., 2001). PI3K phosphorylates phosphatidylinositol-4,5-bisphosphate (PIP_2) to phosphatidylinositol-3,4,5-triphosphate (PIP_3) which in turn phosphorylates the 3-phosphoinositide-dependent protein kinases (PDK-1; PDK-2) to ultimately activate Akt (Figure 3.1.3) (Choi & Kim, 2010). Akt activation can be inhibited when PIP_3 is converted back to PIP_2 by phosphatase and tensin homologue deleted on chromosome 10. Akt is a central signaling enzyme and altered activity is involved in the pathophysiology of several diseases. Literature show a downregulation of Akt in T2DM (Manning & Cantley, 2007). The following section explores the downstream targets of AKT in more detail.

Insulin action is mainly accomplished via the effects of Akt on downstream targets. Akt is involved in the regulation of cellular processes such as metabolism, cell survival, growth and proliferation (Manning & Cantley, 2007). However, for this component of the thesis the focus will be placed on Akt-mediated regulation of metabolism. Akt facilitates the effects of insulin when there is a rise in blood glucose levels, i.e. to promote glucose uptake, metabolism and storage while inhibiting hepatic glucose production as summarized in Figure 3.1.3 (Manning & Cantley, 2007).

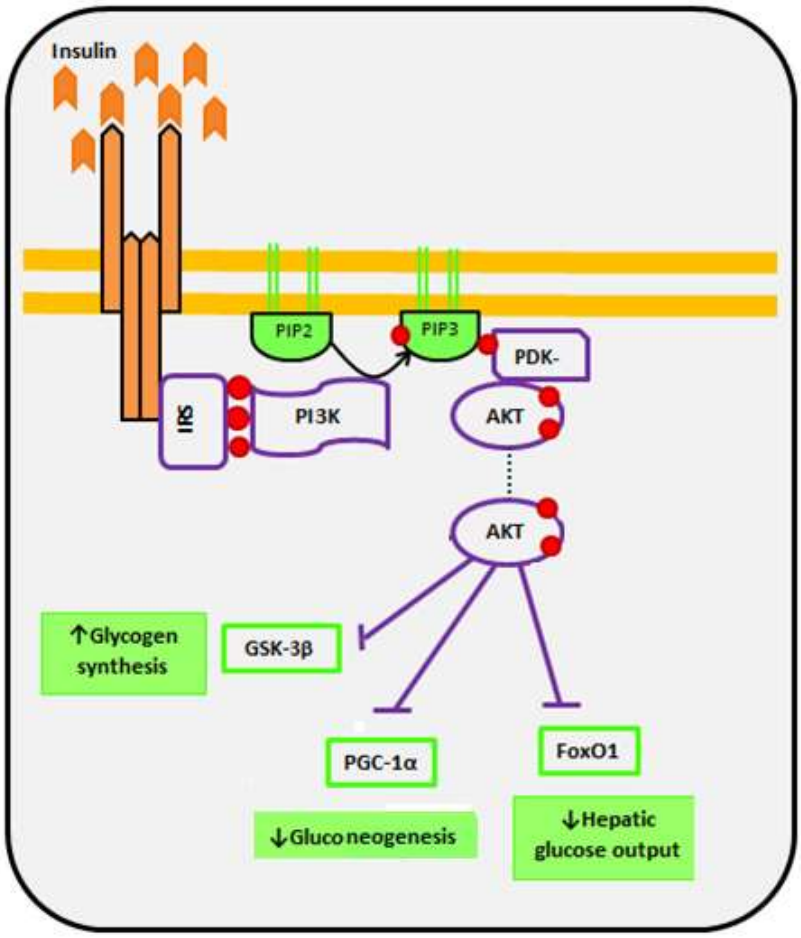

Figure 3.1.3: Hepatic insulin signaling pathway and its effect on glucose handling (with the focus on Akt as signaling molecule). Figure adapted from Benadè (2014).

- Phosphate groups.

Akt directly promotes glucose uptake in a variety of tissues but not in the liver specifically, e.g. it enhances insulin-dependent glucose uptake into skeletal muscle cells by regulating the translocation of GLUT4 to the sarcolemma via the activation of 160 kDa substrate (Choi & Kim, 2010; Manning & Cantley, 2007). Although Akt signaling does not directly mediate nutrient uptake in the liver, it is involved in the regulation of nutrient metabolism and storage (Manning & Cantley, 2007). Akt can accelerate the first step of glucose metabolism (glucose to G-6-P) by enhancing the association between mitochondria and hexokinase (Manning & Cantley, 2007). Akt activity also determines whether G-6-P will be catabolized via the glycolytic pathway or whether it will follow an anabolic pathway and be stored as glycogen. Here glycolysis is favored when Akt phosphorylates hypoxia inducible factor-α to ultimately increase the transcription of glycolytic enzymes. Alternatively, the storage of G-6-P can be promoted by phosphorylation-

mediated inhibition of glycogen synthase kinase 3β (GSK-3β) – which usually inhibits glycogen synthase. However, this is now countered and glycogen can be readily synthesized. Akt also reduces hepatic glucose output by phosphorylating peroxisome proliferator-activated receptor-γ coactivator 1-α (PGC-1-α) to attenuate the subsequent expression of gluconeogenic enzymes (PEPCK and G-6-Pase), and inhibiting the gluconeogenic transcription factor forkhead box protein O1 (FoxO1) (Kitamura, 2013; Postic, 2004). Akt phosphorylates FoxO1 causing it to translocate from the nucleus (site of action) to the cytoplasm (Kitamura, 2013). FoxO1 is involved in the regulation of numerous cellular processes including metabolism, e.g. it can increase hepatic glucose output by upregulating the expression of glucogenic enzymes (Manning & Cantley, 2007). Thus higher FoxO1 activity is a hallmark of T2DM pathogenesis.

The inhibition of FoxO1 is pivotal to maintain glycemic homeostasis since it a central modulator of hepatic lipid and glucose metabolism (Kitamura, 2013). Zhang *et al*. (2006) used a transgenic mouse model to establish that constitutively active hepatic FoxO1 is associated with increased fasting blood glucose levels regardless of insulin levels, reduced insulin sensitivity and impaired glucose tolerance. The transgenic mice also expressed higher levels of PEPCK, G-6-Pase and insulin growth factor binding protein-1, all related to hepatic glucose production. In parallel, there was increased transcription of aquaporin 7 and 9. Aquaporin 7 allows for the release of glycerol from adipocytes, while aquaporin 9 promotes its uptake into the liver – a necessary substrate for glucose production. FoxO1 is also responsible for the release of amino acids (as substrates for gluconeogenesis) through proteasomal degradation, by altering tyrosine transferase and atrogin-1 expression. Furthermore, FoxO1 prevents glycogenesis - important step in decreasing blood glucose levels - by suppressing the transcription of glucokinase. Amino acids are also released to serve as substrates for gluconeogenesis (Zhang *et al*., 2006). Lastly, FoxO1 has been linked to pancreatic β-cell failure that is central in the pathophysiology of T2DM (Guo, 2014).

3.2 Materials and Methods

A detailed protocol is provided in Appendix B. In brief, 100 µg liver tissues (after 6 months of treatment) were homogenized (Polytron PT2100, Kinematica, Luzern, Switserland) in 0.5 mL extraction buffer. The lysates were centrifuged for 10 min at 12000 x g (Spectrafuge™ 24D, Labnet, Edison NJ) and cooled acetone at -20^{o}C was added to the supernatant in a 1:4 ratio. Proteins were allowed to precipitate overnight at -20^{o}C. On the second day the protein pellets were separated and transported to the Central Analytical Facility (Faculty of Medicine and

Health Sciences, Stellenbosch University) where the rest of the experimental work was completed by Dr. Mare Vlok (Laboratory Manager). Here the protein pellets were 'cleaned' and the protein concentration determined spectrophotometrically at 280 nm (NanoDrop spectrophotometer, Thermo Scientific, Waltham MA) (refer Appendix B for details). Next the proteins were digested in a trypsin solution, dried and resuspended. Residual digest reagents were removed and samples were prepared for liquid chromatography and mass spectrometry analysis. Dionex nano-RSLC Liquid chromatography was performed on a Thermo Scientific Ultimate 3000 RSLC and Mass spectrometry was performed using a Thermo Scientific Fusion mass spectrometer Data were acquired and analyzed.

3.3 Results

Proteomic analysis was performed on the six month Control, Cal-control and SSB groups (n = 6 each) and each sample was analyzed in duplicate. A total of 3, 379 proteins were detected in the samples and 3, 156 had similar expression levels between groups at a false discovery rate of 0.5%. The outstanding 222 proteins were uniquely regulated in one or two of the groups compared to the remaining group(s). Here we considered both the effect of the consumption of excessive sugar-derived calories (changes in SSB group only) and the consumption of excess calories in general (the combined effect of the SSB and Cal-control group). Of the 34 proteins affected in the SSB group, 28 displayed >95% probability reading while 95 of the 106 that changed in the SSB/Cal-control combination. These proteins were further examined - summarized in Figure 3.3.1 below. Tables 3.3.1-3.3.4 provide a brief overview of the function and subcellular location of each of the proteins included in the study, together with its full name and accession number.

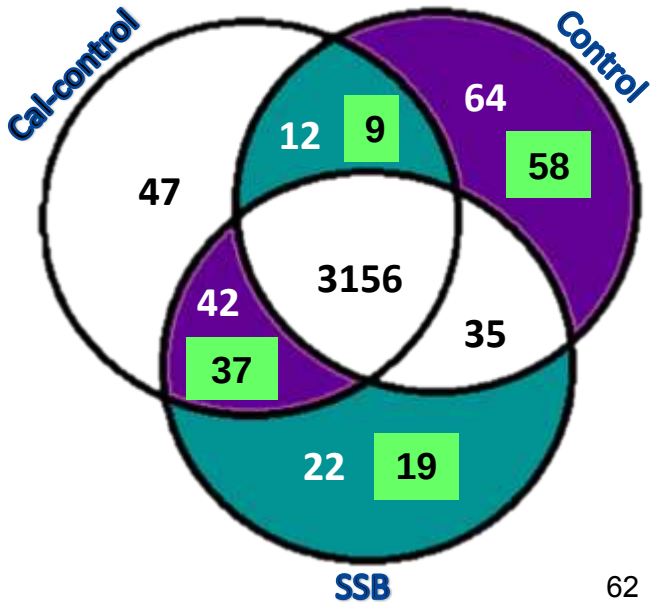

Figure 3.3.1: Proteomic analysis. The Venn diagram indicates the number of proteins per group/combination that increased versus the remaining group(s).
- Sugar-induced up/downregulation of protein expression.
- Calorie-induced up/downregulation of protein expression.
- Number of proteins per group that was included for further analysis.

Table 3.3.1: Proteins exhibiting a sugar-induced decrease in expression (listed from highest to lowest). Some of the important proteins to take note of are those involved in protein folding and transport (marked blue in the last column) e.g. tetratricopeptide repeat protein 36. The color code in the final column will be explained in detail in section 3.4.

Name (accession number)	Function; location	Percentage decrease (%)			
		SSB vs. Control	SSB vs. Cal-control	Average	
Cluster of biliverdin reductase B Flavin reductase (NADPH) (B5DF65)	Reduces biliverdin to bilirubin with the concomitant oxidation of a nicotinamide adenine dinucleotide (NADH) or nicotinamide adenine dinucleotide phosphate (NADPH) cofactor; cytoplasm (UniProtKB) Significance: decrease in SSB group leads to improved recycling of glutathione.	80% ↓	70% ↓	75% ↓	
Cluster of nipsnap1 protein (Q5EBA4)	Involved in pain sensation, cell surface and mitochondrial inner membrane (ScaffoldQ+).	80% ↓	70% ↓	75% ↓	
Cluster of tetratricopeptide repeat protein 36 (TTC36)	Possibly involved in protein folding, also known as HSP70-binding protein 21 (UniProtKB). Subcellular location unknown.	70% ↓	70% ↓	70% ↓	
Cluster of sorbin and SH3 domain-containing protein 2 (tr|F1LPM3|F1LPM3)	Involved in the formation of stress fibers and cell adhesion (Nakatani, 2011; ScaffoldQ+). Associated with obesity, T2DM (Lin, 2001), diabetic complications (Nakatani, 2011) and heart infarcts (Kakimoto, 2013); perinuclear region of cytoplasm (ScaffoldQ+). A decrease could possibly be a protective response.	60% ↓	70% ↓	65% ↓	
Cluster of 1,2-dihydroxy-3-keto-5-methylthiopentene dioxygenase (MTND)	Step 5 of methionine salvage pathway (UniProtKB); cytosol (Reactome).	70% ↓	60% ↓	65% ↓	
Cluster of uncharacterized protein (F1LRJ9)	Intragolgi protein transport (ScaffoldQ+, STRING); nucleus, cytosol, golgi membrane (UniProtKB).	60% ↓	60% ↓	60% ↓	
Cluster of clathrin light chain A (sp|P08081|CLCA)	Intracellular protein transport (clathrin-mediated endocytosis); membrane of clathrin-coated endocytic vesicles and trans-Golgi network (ScaffoldQ+).	40% ↓	80% ↓	60% ↓	

Cluster of tubulin-specific chaperone A (TBCA)	Post-chaperonin tubulin folding pathway (ScaffoldQ+); cytoskeleton (UniProtKB).	60% ↓	60% ↓	60% ↓	
Cluster of enoyl-CoA delta isomerase 2, mitochondrial (ECI2)	Peroxisomal lipid metabolism (Reactome); peroxisomal matrix (ScaffoldQ+).	0% ↓	40% ↓	20% ↓	

Table 3.3.2: Proteins exhibiting a sugar-induced increase in expression (listed from highest to lowest). Here the expression of ECT proteins was significantly upregulated (marked by orange) The color code in the final column will be explained in detail in section 3.4.

Name (accession number)	Function; location	Percentage increase (%)			
		SSB vs. Control	SSB vs. Cal-control	Average	
Death-associated protein 1 (DAP1)	Negatively regulates autophagy; nucleus and cytoplasm (UniProtKB).	470% ↑	150% ↑	310% ↑	
Nicotinamide nucleotide transhydrogenase (Q5BJZ3)	NADPH regeneration and proton transport; mitochondrial inner membrane (ScaffoldQ+).	390% ↑	90% ↑	240% ↑	
Prefoldin 1 (D3ZX38)	Binds specifically to cytosolic chaperonin to promote protein folding; ER (Prefoldin complex) (ScaffoldQ+).	280% ↑	180% ↑	230% ↑	
Transgelin (TAGL)	Form cross-links with actin and possible marker for liver damage; cytoplasm (UniProtKB).	20% ↑	270% ↑	145% ↑	
Cluster of protein Snrpd2 (B5DES0)	Regulation mRNA splicing and snRNP assembly (Reactome); nucleus (UniProtKB).	180% ↑	80% ↑	130% ↑	
Cluster of heterogeneous nuclear ribonucleoprotein (HNRPF)	Regulation of RNA splicing and mRNA processing; nucleoplasm and cytoplasm (ScaffoldQ+).	120% ↑	50% ↑	85% ↑	
Histidine-rich glycoprotein (HRG)	Platelet activation and negative regulation of cell growth (ScaffoldQ+); secreted (UniProtKB).	70% ↑	90% ↑	80% ↑	
Acidic leucine-rich nuclear	Cell-cycle regulation; nucleus (Reactome).	120% ↑	30% ↑	75% ↑	

phosphoprotein 32 family member B (AN32B)					
Cluster of multiple coagulation factor deficiency 2 (Q6GQY2)	Vesicle mediated protein transport (Reactome; ScaffoldQ+); golgi apparatus and ER (ScaffoldQ+).	70% ↑	30% ↑	50% ↑	
Protein mut (D3ZKG1)	Propionyl-CoA catabolism to succinyl-CoA (intermediate of citric acid cycle); mitochondrial matrix (ScaffoldQ+).	30% ↑	50% ↑	40% ↑	
Beta-2-microglobulin (B2MG)	Positive regulation of T cell-mediated cytotoxicity (stress signaling); golgi apparatus (ScaffoldQ+).	30% ↑	50% ↑	40% ↑	
Thymosin β4 (TYB4)	Regulation of cell migration and actin filament organization for tissue repair; cytoskeleton (ScaffoldQ+).	40% ↑	40% ↑	40% ↑	
Cluster of lamina-associated polypeptide 2, isoform β (LAP2)	Regulation of transcription; ER membrane (ScaffoldQ+).	40% ↑	40% ↑	40% ↑	
Cluster of Hnrpa1 protein (Q6P6G9)	Deoxyribonucleic acid (DNA) strand renaturation and mRNA transport; nucleoplasm and cytoplasm (ScaffoldQ+).	40% ↑	40% ↑	40% ↑	
Succinate dehydrogenase [ubiquinone] iron-sulfur subunit (SDHB)	Subunit of Complex II → transfer electrons from succinate to ubiquinone; mitochondrial inner membrane (UniProtKB).	20% ↑	50% ↑	35% ↑	
Calcium-regulated heat stable protein 1 (CHSP1)	Inhibit gluconeogenic gene expression; cytoplasm (UniProtKB).	20% ↑	50% ↑	35% ↑	
ATP synthase subunit d (sp|P31399|ATP5H)	Maintenance of ATP synthase structure during ATP synthesis; mitochondrial inner membrane (UniProtKB).	20% ↑	40% ↑	30% ↑	
NADH dehydrogenase [ubiquinone] iron-sulfur protein 4 (sp|Q5XIF3|NDUS4)	Subunit of Complex I - transfer electrons from NADH to the electron transport chain (ETC); mitochondrial inner membrane (UniProtKB).	30% ↑	30% ↑	30% ↑	
Cluster of 40S ribosomal protein S4, X isoform (RS4X)	Gene translation; cytosolic small ribosomal subunit (ScaffoldQ+).	30% ↑	20% ↑	25% ↑	

Table 3.3.3: Proteins exhibiting a calorie-induced decrease in expression (listed from highest to lowest). Excess calorie consumption decreased the expression of a wide range of proteins involved in various cellular processes. The expression of translocon-associate protein subunit β, a protein involved in ER calcium regulation, was completely suppressed The color code in the final column will be explained in detail in section 3.4.

Name (accession number)	Function; location	Percentage decrease (%)			
		Cal-control vs. Control	SSB vs. Control	Average	
Translocon-associated protein subunit β (B5DEQ0)	Involved in ER calcium homeostasis (STRING); ER membrane (ScaffoldQ+).	100% ↓	100% ↓	100% ↓	
3-hydroxyisobutyryl-CoA hydrolase [mitochondrial] (HIBCH)	Partakes in valine, leucine and isoleucine degradation catabolism; mitochondria (Horton *et al*., 2006; ScaffoldQ+). ER stress downregulates branched-chain amino acid catabolism (Burrill *et al*., 2015).	100% ↓	100% ↓	100% ↓	
Protein Cmc1 (D3ZTN2)	Involved in the assembly and function of cytochrome C oxidase (COX); mitochondria (Complex IV) (ScaffoldQ+).	92% ↓	100% ↓	96% ↓	
Protein Tjp3 (D3Z8G7)	Structural component of tight junctions; between cells (UniProtKB) ER stress has been linked to the degradation of tight junctions (Zhou *et al*., 2016).	92% ↓	100% ↓	96% ↓	
Deubiquitinating protein VCIP135 (VCIP1)	Deubiquitination of proteins to prevent protein degradation; ER and golgi stacks (UniProtKB).	96% ↓	95% ↓	95.5% ↓	
Bile acid-CoA:amino acid N-acyltransferase (BAAT)	Important enzyme in step in the bile acid biosynthetic process before bile is released into canaliculi; cytosol and peroxisomes (ScaffoldQ+). Could regulate intracellular levels of fatty acids through its effects on acyl-CoA (UniProtKB).	90% ↓	100% ↓	95% ↓	
Cluster of LUC7-like (G3V9R0)	Involved in RNA splicing; nucleus (ScaffoldQ+).	90% ↓	100% ↓	95% ↓	
ATPase inhibitor,	Protects cell against ATP-depletion when mitochondrial membrane	90% ↓	98% ↓	94% ↓	

mitochondrial (ATIF1)	potential drops below a critical threshold; mitochondrial proton-transporting ATP synthase complex (ScaffoldQ+; UniProtKB).				
Enthoprotin (Q6DGF2)	Initiates the assembly of clathrin for clathrin-coated endocytosis vesicles; golgi apparatus (UniProtKB).	90% ↓	98% ↓	94% ↓	
Lymphocyte specific 1 isoform CRA_a (Q4QQV6)	Involved in signal transduction and chemotaxis; extracellular exosome and cell membrane (ScaffoldQ+).	92% ↓	91% ↓	91.5% ↓	
Acyl-protein thioesterase 1 (LYPA1)	Involved in fatty acid metabolism and protein depalmitoylation; cytoplasm (ScaffoldQ+, UniProtKB).	100% ↓	80% ↓	90% ↓	
Cluster of isoform 2 of myelin basic protein (sp|P02688-2|MBP)	Possibly involved in the formation of transcriptional complexes; nucleus (UniProtKB).	80% ↓	90% ↓	85% ↓	
Cluster of clathrin light chain B (sp|P08082|CLCB)	Intracellular protein transport; membrane of clathrin-coated endocytic vesicles and trans-Golgi network (ScaffoldQ+).	80% ↓	80% ↓	80% ↓	
Cluster of protein RGD1565183 (D3ZJD3)	Translation - structural component of large ribosomal subunit (ScaffoldQ+); nucleolus (UniProtKB).	80% ↓	80% ↓	80% ↓	
Heat shock protein β8 (HSPB8)	Chaperone activity (response to temperature stress); golgi apparatus, cytoplasm, nucleoplasm (UniProtKB).	60% ↓	100% ↓	80% ↓	
Cluster of annexin A3 (ANXA3)	Promotes angiogenesis and involved in immune responses; cytoplams, cell membrane, extracellular exomes (ScaffoldQ+; UniProtKB).	80% ↓	70% ↓	75% ↓	
Calponin-3 (CNN3)	Involved in epithelial cell differentiation and smooth muscle contractions; cytoplasm and cytoskeleton (ScaffoldQ+, UniProtKB).	70% ↓	80% ↓	75% ↓	
Phosphohistidine phosphatase 1 isoform CRA_a (D3ZP47)	Dephosphorylates proteins and inhibit calcium channels; cytosol and extracellular exosome (ScaffoldQ+).	70% ↓	80% ↓	75% ↓	
Cluster of Pdhx protein (Q5BJX2)	Important structural protein of pyruvate dehydrogenase complex; mitochondria (Gray *et al*., 2014; ScaffoldQ+). Perturbations in pyruvate metabolism are associated with CVD, obesity and T2DM (Gray *et al*., 2014).	80% ↓	70% ↓	75% ↓	
Ddx17 protein	Involved in the regulation of transcription; nucleus (Fuller-Pace & Ali,	80% ↓	70% ↓	75% ↓	

(Q568Z8)	2008).				
Nicotinate-nucleotide pyrophosphorylase [carboxylating] (NADC)	Involved in quinolinate catabolism and nicotinamide adenine dinucleotide (NAD^+) synthesis (ScaffoldQ+). NAD^+ plays a role in cellular metabolism and mitochondrial health (Canto *et al*., 2015).	80% ↓	60% ↓	70% ↓	
Cluster of dimethylglycine dehydrogenase (tr|Q5RKL4|Q5RKL4)	Catabolizes dimethylglycine to glycine; mitochondrial matrix (Magnusson, 2015; UniProtKB). Dimethylglycine is involved in the regulation of glucose metabolism. A decline in dimethylglycine levels correlates with the development of T2DM (Magnusson *et al*., 2015).	60% ↓	70% ↓	65% ↓	
Cluster of ubiquitin-60S ribosomal protein L40 (RL40)	Translation - structural constituent of ribosome; cytoplasm and nucleus (ScaffoldQ+)	70% ↓	50% ↓	60% ↓	
Cluster of 60S ribosomal protein L7 (B0K031)	Translation - structural constituent large ribosome; cytosol (ScaffoldQ+).	60% ↓	60% ↓	60% ↓	
3-mercaptopyruvate sulfurtransferase (THTM)	Involved in the production of the antioxidant hydrogen sulfide (H_2S). Changes in enzyme activity and H_2S is indicative of the development of T2DM and hyperglycemia-induced epithelial cell damage; cytoplasm and mitochondria (Coletta, 2015; UniProtKB).	70% ↓	40% ↓	55% ↓	
Cluster of GM2 ganglioside activator (Q6IN37)	Regulates the degradation of GM2 gangliosides (UniProtKB); mitochondrion (ScaffoldQ+).	40% ↓	70% ↓	55% ↓	
Cluster of isoamyl acetate-hydrolyzing esterase 1 homolog (sp|Q711G3|IAH1)	Lipid catabolism (lipase) and hydrolase activity; extracellular exosome (UniProtKB).	70% ↓	40% ↓	55% ↓	
Cluster of aflatoxin B1 aldehyde reductase member 2 (sp|Q8CG45|ARK72)	Aldehyde reductase activity (requires NADPH) and toxin degradation; Golgi apparatus and cytoplasm (UniProtKB).	60% ↓	50% ↓	55% ↓	
Cluster of NADH	Involved in electron transport from NADH to the ETC; mitochondrial	60% ↓	50% ↓	55% ↓	

dehydrogenase [ubiquinone] 1-α subcomplex subunit 6 (tr|D4A3V2|D4A3V2)	subunit of complex I of ETC (UniProtKB).				
Cluster of LOC689593 (B2RYA8)	ER-associated protein catabolism; cytosol and nucleus (ScaffoldQ+; UniProtKB).	40% ↓	60% ↓	50% ↓	
Cluster of peroxiredoxin-5 [mitochondrial] (D3ZEN5)	Anti-oxidant properties; mitochondria (STRING).	50% ↓	40% ↓	45% ↓	
Cluster of histone H3 (D3ZJ08)	Inhibits transcription from RNA polymerase II promoter and involved in nucleosome assembly; nucleus (ScaffoldQ+; UniProtKB).	50% ↓	40% ↓	45% ↓	
Cluster of 60S ribosomal protein L26 (tr|G3V6I9|G3V6I9)	Translation - structural component of large cytosolic ribosomes (ScaffoldQ+).	40% ↓	50% ↓	45% ↓	
Cluster of sulfotransferase family cytosolic 1B member 1 (sp|P52847|ST1B1)	Involved in the differentiation of epithelial cells; cytoplasm (UniProtKB).	50% ↓	30% ↓	40% ↓	
Alpha-1-antiproteinase (A1AT)	Associated with the acute-phase response and inhibits proteases activity; secreted into intracellular space (ScaffoldQ+; UniProtKB).	50% ↓	30% ↓	40% ↓	
Cluster of uncharacterized protein (D4ADL2)	Involved in translation - peptidyl-serine phosphorylation, nucleus (ScaffoldQ+).	50% ↓	30% ↓	40% ↓	
Cluster of ubiquinone biosynthesis protein COQ9 [mitochondrial] (COQ9)	Partakes in the biosynthesis of coenzyme Q/ubiquinone; mitochondrial inner membrane (UniProtKB).	50% ↓	30% ↓	40% ↓	
Cluster of ATP synthase subunit delta. mitochondrial (G3V7Y3)	Proton-transporting ATPase activity, rotational mechanism, mitochondrial inner membrane (UniProtKB).	40% ↓	30% ↓	35% ↓	

Cluster of phosphoglycerate mutase 1 (sp|P25113|PGAM1)	Catalyzes step 8 of glycolytic pathway (Horton *et al*., 2006), cytosol (ScaffoldQ+).	40% ↓	30% ↓	35% ↓	
Cluster of D-β-hydroxybutyrate dehydrogenase [mitochondrial] (sp|P29147|BDH)	Synthesis of ketone bodies; mitochondrial matrix (Horton *et al*., 2006; ScaffoldQ+).	40% ↓	30% ↓	35% ↓	
Cluster of 40S ribosomal protein SA (RSSA)	Involved in small ribosomal subunit assembly and maintenance; plasma membrane (ScaffoldQ+).	40% ↓	30% ↓	35% ↓	
Cluster of 40S ribosomal protein S8 (tr|M0R7Q5|M0R7Q5)	Translation - small ribosomal subunit; cytosol and cell membrane (ScaffoldQ+; UniProtKB).	30% ↓	40% ↓	35% ↓	
Cluster of protein Taf15 (D3ZSS1)	Involved in binding of nucleotides and the regulation of transcription, nucleoplasm (ScaffoldQ+).	30% ↓	40% ↓	35% ↓	
Cluster of N-acetylneuraminic acid synthase (B1WC26)	Carbohydrate biosynthetic process, cytosol (ScaffoldQ+).	30% ↓	40% ↓	35% ↓	
Cluster of glutathione S-transferase-α1 (GSTA1)	Protects against oxidative stress and products of lipid peroxidation through glutathione peroxidase activity, cytosol and extracellular exome (NCBI; UniProtKB).	20% ↓	50% ↓	35% ↓	
Cluster of Glutathione S-transferase-α3 (GSTA3)	Anti-oxidant properties and involved in the biosynthesis of steroid hormones; cytosol and extracellular exome (UniProtKB).	30% ↓	30% ↓	30% ↓	
Cluster of protein LOC100912599 (tr|D3ZCZ9|D3ZCZ9)	Transports electrons from NADH to ubiquinone; mitochondrial ETC complex I (ScaffoldQ+).	40% ↓	20% ↓	30% ↓	
Cluster of Protein LOC680161 (D4A6B9)	Ribosome biogenesis and RNA binding, cytosolic large ribosomal subunit (ScaffoldQ+; UniProtKB).	20% ↓	40% ↓	30% ↓	
Cluster of GTPase	Nucleotide binding, cytoplasm (UniProtKB).	40% ↓	20% ↓	30% ↓	

activating protein (SH3 domain) binding protein 2 (tr|Q6AY21|Q6AY21)					
Cluster of 3-α-hydroxysteroid dehydrogenase (sp|P23457|DIDH)	Synthesis of bile acids and bile salts; cytoplasm (Reactome; ScaffoldQ+).	30% ↓	20% ↓	25% ↓	
Regucalcin (RGN)	Cellular calcium ion homeostasis, cytoplasm and nucleoplasm (ScaffoldQ+).	30% ↓	20% ↓	25% ↓	
Coiled-coil-helix-coiled-coil-helix domain containing 3 isoform CRA_a (D3ZUX5)	Involved in maintenance of inner mitochondrial membrane and suppress transcription from RNA polymerase II promoter, mitochondria and nucleus (UniProtKB).	30% ↓	20% ↓	25% ↓	
Glutathione S-transferase A6 (GSTA6)	Anti-oxidant properties (glutathione transferase activity); cytoplasm (UniProtKB).	20% ↓	30% ↓	25% ↓	
Cluster of histone H1.4 (H14)	Inhibits transcription from RNA polymerase II promoter and involved in nucleosome assembly, nucleus (ScaffoldQ+; UniProtKB).	30% ↓	10% ↓	20% ↓	
D-dopachrome decarboxylase (DOPD)	Cytoplasm.	20% ↓	20% ↓	20% ↓	
Omega-amidase (NIT2)	Converts potentially toxic metabolic intermediates to beneficial metabolic substrates; cytoplasm (UniProtKB).	20% ↓	20% ↓	20% ↓	
Cluster of 40S ribosomal protein S18 (RS18)	Translation and ribosome biogenesis; cytoplasm (ScaffoldQ+, UniProtKB).	20% ↓	20% ↓	20% ↓	
Cluster of Fumarylacetoacetase (FAAA)	Amino acid catabolism; cytosol (UniProtKB).	20% ↓	10% ↓	15% ↓	

Table 3.3.4: Proteins exhibiting a calorie-induced increase in expression (listed from highest to lowest). DnaJ (Hsp40) homolog subfamily B member 1 isoform CRA_a is the most important protein to consider here. It serves as a marker for ER stress and was not expressed in the Control group at all, but was detected in the SSB and Cal-control groups. The color code in the final column will be explained in detail in section 3.4.

Name (accession number)	Function; location	Percentage increase (%)			
		Cal-control vs. Control	SSB vs. Control	Average	
Cluster of heterogeneous nuclear ribonucleoprotein H2 (HNRH2)	Involved in pre-mRNAs processing; nucleoplasm (Reactome; STRING).	Inf	Inf	Inf (Absent in Control group)	
RGD1307526 protein (Q568Z5)	Function and location unknown.	Inf	Inf	Inf (Absent in Control group)	
Cluster of DnaJ (Hsp40) homolog subfamily B member 1 (predicted) isoform CRA_a (D3ZUU5)	Chaperone cofactor-dependent protein folding; cytosol, extracellular vesicular exosome and nucleus (ScaffoldQ+). Marker for ER stress (Tang *et al*., 2010).	Inf	Inf	Inf (Absent in Control group)	
Cluster of EH domain-containing protein 1 (sp|Q641Z6|EHD1)	Regulates cholesterol homeostasis and lipid droplet storage (Naslavsky *et al*., 2007). Also involved in endocytosis; cytoplasm and endocytic vesicles (ScaffoldQ+).	1800% ↑	1000% ↑	1400% ↑	
Crk-like protein (CRKL)	Mediates intracellular signal transduction; cytosol, endosome and extracellular vesicular exosome (ScaffoldQ+; UniProtKB). CRKL plays a role in the tyrosine kinase signaling pathways, e.g. it binds to IRS of the insulin signaling pathway (Cevik, 2016; Hanke & Mann, 2009).	880% ↑	530% ↑	705% ↑	
Cluster of thioredoxin domain-containing protein 12	Involved in redox homeostasis and inhibits ER stress-induced apoptosis; lumen of ER (UniProtKB). Deng *et al*. (2010) found it downregulated in the liver of a diabetic rat model. Thus upregulation could possibly be an early	790% ↑	460% ↑	625% ↑	

(sp|Q498E0|TXD12)	protective mechanism that fails after prolonged exposure to high calorie diet.				
UPF0449 protein C19orf25 homolog (CS025)	Function and location unknown.	240% ↑	350% ↑	295% ↑	
Cluster of eukaryotic translation initiation factor 3 subunit D (EIF3D)	Part of eukaryotic translation initiation factor 3 (eIF-3) complex that interacts with 40S ribosomes; cytosol (UniProtKB).	230% ↑	210% ↑	220% ↑	
Cluster of mitochondrial import inner membrane translocase subunit TIM44 (TIM44)	Involved in importing proteins from the mitochondrial inner membrane to the mitochondrial matrix (ATP-dependent), chaperone binding; mitochondrial inner membrane and matrix (ScaffoldQ+; UniProtKB).	230% ↑	160% ↑	195% ↑	
Ubiquitin fusion degradation protein 1 homolog (UFD1)	Partakes in the degradation ER-associated degradation (ERAD) and ubiquitin fusion degradation of misfolded proteins and the activation of certain transcription factors; cytosol and nucleus (UniProtKB).	160% ↑	140% ↑	150% ↑	
Cluster of Aa1018 (Q7TQ11)	Structural protein that is involved in receptor-mediated endocytosis and immune response; extracellular vesicular exosome (ScaffoldQ+; UniProtKB).	130% ↑	150% ↑	140% ↑	
Rat apolipoprotein E protein (Q65ZS7)	Facilitates the binding and uptake of lipoprotein particles (LDLs in particular) to clear it out of the plasma (UniProtKB).	140% ↑	100% ↑	120% ↑	
Cluster of nucleophosmin (sp|P13084|NPM)	Involved in various cellular processes including protein chaperoning; cytoplasm and nucleus (UniProtKB).	90% ↑	80% ↑	85% ↑	
Fetuin-B (FETUB)	Secreted by hepatocytes and elevated in diabetic mice; extracellular region. Associated with impaired glucose and steatosis (Meex *et al.*, 2015; Uniport).	60% ↑	100% ↑	80% ↑	
Cluster of bifunctional ATP-dependent dihydroxyacetone	Involved in fructose metabolism; cytosol (Horton, 2006; Reactome). Alternative name: Triose kinase (UniProtKB).	70% ↑	80% ↑	75% ↑	

kinase/FAD-AMP lyase (cyclizing) (DHAK)					
Cluster of 40S ribosomal protein S26 (RS26)	Translation – structural protein of small ribosomal subunit; cytosol and nucleus (ScaffoldQ+; UniProtKB).	70% ↑	80% ↑	75% ↑	
Cluster of protein Ybx2 (D4A3P0)	Binding of nucleic acids; nucleus, nucleolus and cytoplasm (Uniport).	60% ↑	70% ↑	65% ↑	
Protein Snrnp70 (B2RZ74)	Involved in mRNA splicing and gene expression; nucleoplasm and cytoplasm. (Reactome; UniProtKB).	50% ↑	80% ↑	65% ↑	
Cluster of translationally-controlled tumor protein (TCTP)	Involved in cellular calcium homeostasis and inhibits apoptotic process signaling; cytoplasm and extracellular exosome (UniProtKB).	70% ↑	40% ↑	55% ↑	
UBX domain-containing protein 1 (UBXN1)	Negative regulator of protein degradation and nuclear factor kappa B (NF-κB) signaling; nucleus, cytoplasm and ER (UniProtKB; Wang *et al*., 2015).	70% ↑	40% ↑	55% ↑	
Hydroxymethylglutaryl-CoA synthase. cytoplasmic (HMCS1)	Involved in the initial phase of cholesterol biosynthesis; cytoplasm, nucleoplasm and plasma membrane (Horton, 2006; UniProtKB).	70% ↑	40% ↑	55% ↑	
Endoplasmin (sp|Q66HD0|ENPL)	Involved in protein chaperoning and ERAD; ER lumen (UniProtKB).	60% ↑	40% ↑	50% ↑	
Cluster of plasminogen activator inhibitor 1 RNA-binding protein (sp|Q6AXS5|PAIRB)	Partakes in the moduation of mRNA stability; cytoplasm and nucleus (UniProtKB).	40% ↑	60% ↑	50% ↑	
Thioredoxin. mitochondrial (THIOM)	Involved in cellular redox homeostasis and mitochondrial membrane potential. Mitochondrial thioredoxin is also involved in inhibiting apoptosis; mitochondria (UniProtKB).	50% ↑	50% ↑	50% ↑	
Cluster of	Involved in mRNA splicing and nucleotide binding; nucleus, nucleoplasm	50% ↑	50% ↑	50% ↑	

heterogeneous nuclear ribonucleoprotein C (C1/C2) (tr|G3V9R8|G3V9R8)	and extracellular exosome (ScaffoldQ+; UniProtKB).				
Protein G3bp1 (D3ZYS7)	Involved in the assembly of stress granules. Stress granules that form in response to ER stress partake in adjusting protein translation by degrading of silencing RNA transcripts (NCBI; STRING; Wolozin, 2012).	40% ↑	50% ↑	45% ↑	
Cluster of alcohol dehydrogenase 1 (ADH1)	Reduces alcohol molecules to produce NADH; Cytoplasm (UniProtKB).	40% ↑	40% ↑	40% ↑	
SP120 (Q63555)	DNA and RNA binding; nucleus (STRING; UniProtKB).	50% ↑	30% ↑	40% ↑	
Cluster of elongation factor 1-α (tr|M0R757|M0R757)	Translation – assists the binding of aminoacyl-tRNA to the A-site of ribosomes; cytoplasm (UniProtKB).	30% ↑	50% ↑	40% ↑	
Cluster of Antisecretory factor (O88321)	Involved in ubiquitin-dependent protein degradation process; cytosol and nucleoplasm (ScaffoldQ+).	50% ↑	30% ↑	40% ↑	
Cluster of Protein LOC100912618 (tr|D3ZFY8|D3ZFY8)	Catalyzes the attachment of ubiquitin protein to proteins. Also involved in various steps of DNA replication; cytoplasm and nucleus (ScaffoldQ+).	30% ↑	50% ↑	40% ↑	
Cluster of DnaJ homolog subfamily A member 1 (sp|P63036|DNJA1)	Involved in protein transfer into mitochondria whereby it suppresses ER-associated apoptosis by inhibiting the translocation of Bax into mitochondria. Also inhibits c-Jun amino-terminal kinase (JNK) activity; ER and mitochondria (ScaffoldQ+; UniProtKB).	40% ↑	30% ↑	35% ↑	
Cluster of 60S ribosomal protein L12 (RL12)	Translation - assembly and maintenance large ribosomal subunit; cytosol (ScaffoldQ+; UniProtKB).	40% ↑	30% ↑	35% ↑	
Cluster of NADH dehydrogenase [ubiquinone] flavoprotein 2 mitochondrial	Mitochondrial electron transport, NADH to ubiquinone; mitochondrial ETC complex I (ScaffoldQ+).	40% ↑	30% ↑	35% ↑	

(sp|P19234|NDUV2)					
Cluster of 60S ribosomal protein L17 (RL17)	Translation – structural component of large ribosomal subunit; cytosol and nucleus (ScaffoldQ+; UniProtKB).	20% ↑	20% ↑	20% ↑	
Cluster of Phosphatidylethanolamine-binding protein 1 (PEBP1)	Involved in the dephosphorylation of proteins and serine protease inhibition; cytoplasm, nucleus and extracellular exosome (ScaffoldQ+; UniProtKB).	10% ↑	30% ↑	20% ↑	
Cluster of non-specific lipid-transfer protein (sp|P11915|NLTP)	Regulates intracellular cholesterol transport; peroxisome (ScaffoldQ+).	20% ↑	10% ↑	15% ↑	

3.4 Discussion

Figure: 3.4.1: Schematic depiction of main proteomic findings. We theorize that SSB consumption leads to hepatic ER stress through three possible mechanisms. Here ER stress first induces a cellular adaptation, followed by an alarm phase that will eventually result in apoptosis. In addition, such stress may also alter substrate metabolism. The color blocks below each 'event' provide the accession number of the proteins supporting our model and corresponds to the last column of Tables 3.3.1-3.3.4.

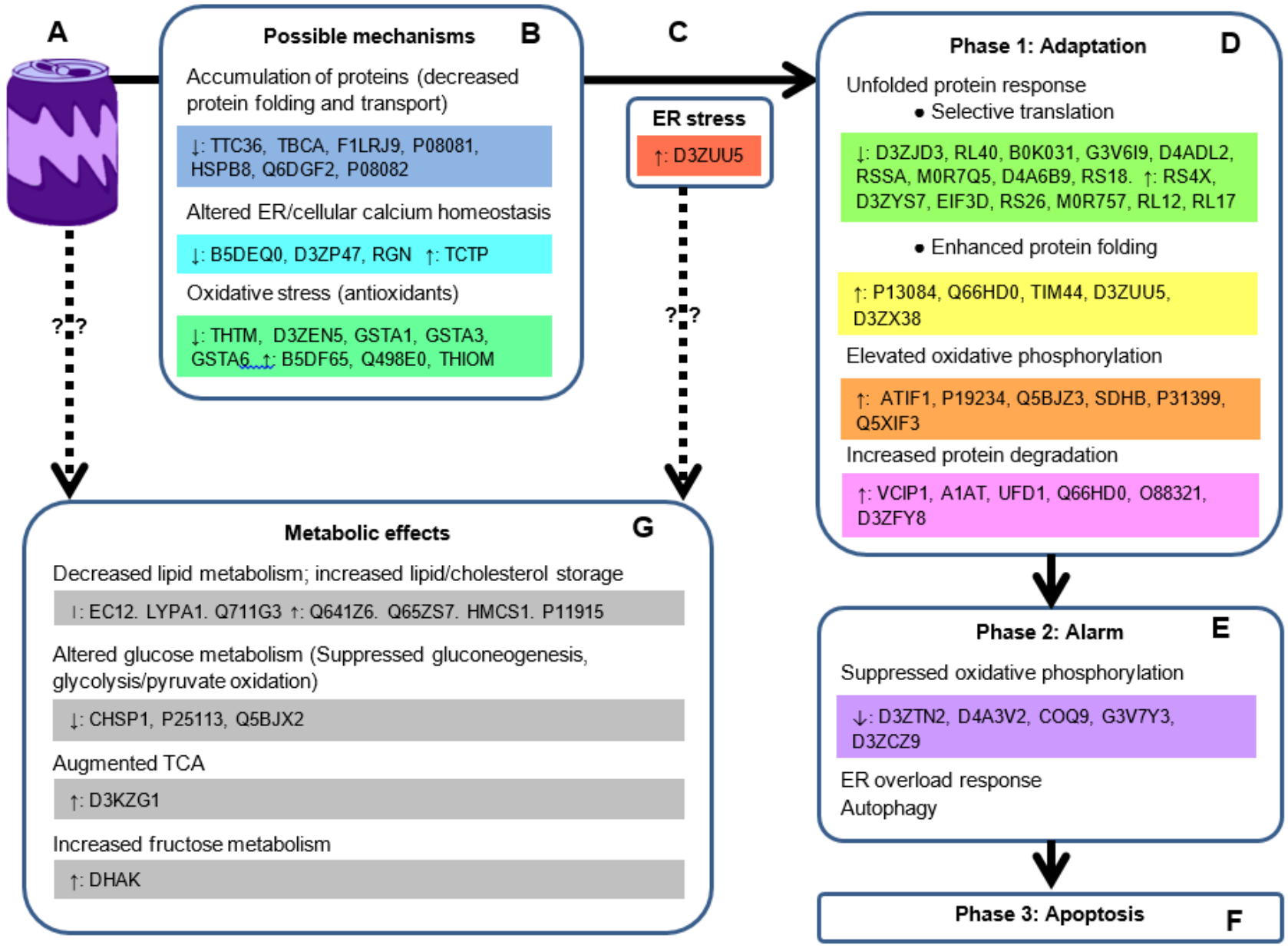

As we had relatively limited insight into the effects of SSB consumption on the liver, we decided to perform a proteomic analysis. Each protein with a unique expression profile in the SSB or SSB and Cal-control groups was identified and its function and subcellular location was determined (Table 3.3.1-3.3.4) in order to detect any meaningful patterns. As Stanhope (2015) explained, SSB consumption could induce metabolic perturbations through direct or indirect (calorie-related) mechanisms. For this reason we tabulated sugar- and calorie induced changes separately. Although the calories triggered more significant effects on protein expression compared to the sugar *per se*, we pooled the data in this section since SSB consumption would lead to a combined (sugar- and calorie-induced) effect. Evidence emerged that moderate but frequent SSB consumption can lead to ER stress. ER stress can be triggered by a variety of cellular stressors e.g. disproportionate levels of reactive oxygen species (ROS), imbalance in calcium homeostasis or the accumulation of misfolded proteins (Senft & Ronai, 2015; Tang *et al*., 2010). Here we detected altered expression of proteins with antioxidant capacity e.g. peroxiredoxin-5, thioredoxin and glutathione S-transferase isoforms, as well as proteins that alter the availability of NADPH and consequently influence glutathione levels (Figure 3.4.1 B). There was also a decrease in several proteins involved in protein folding and transport together with proteins regulating ER and cellular calcium handling, respectively (Figure 3.4.1 B).

ER stress triggers a series of events in order to restore cellular homeostasis and salvage the cell. These events can roughly be divided into three phases (i.e. adaptation, alarm and apoptosis) based on their order and purpose (Xu *et al*, 2005). The main 'event' during the adaptation phase is the induction of the unfolded protein response (UPR). The UPR has two main functions, i.e. to enhance protein folding and to suppress the synthesis of new proteins (note: although the mass of protein synthesis decrease, the synthesis of proteins involved in the stress response are upregulated, hence we refer to this as selective translation) (Tang *et al*., 2010). Here we found that at least five proteins involved in protein folding are upregulated. With regards to protein translation, the expression of a multitude of ribosomal proteins and proteins involved in ribosomal biogenesis or the initiation of translation were significantly altered (Figure 3.4.1 D). Another adaptation associated with ER stress is increased protein degradation through the ubiquitin proteasome pathway, also known as ER associated degradation (ERAD) (Bravo *et al*., 2012; Doroudgar *et al*., 2015; Xu, 2005). Several proteins involved in protein degradation through ERAD were upregulated (Figure 3.4.1 D). The final adaptive mechanism is enhancing mitochondrial function and oxidative phosphorylation. The ER and mitochondria are connected - both physically and functionally (Malhotra & Kaufman, 2011). During this early

response to ER stress mitochondrial bioenergetics are augmented to increase subsequent ATP production and relieve ER stress (Bravo *et al*., 2012). Our proteomic analysis revealed the upregulation of proteins that form part of the ETC e.g. succinate dehydrogenase (ubiquinone iron-sulfur subunit) that is responsible for electron transport at complex II. The promotion of mitochondrial metabolism in response to transient ER stress was also observed in mammalian adrenal glands and gonads (Prasad *et al*., 2016).

If ER stress persists, the cell enters the alarm phase. In contrast to the adaptation phase, mitochondrial metabolism fails during the alarm phase (Bravo *et al*., 2012) and we found a significant decrease in several proteins involved in oxidative phosphorylation (Figure 3.4.1 E). This may indicate that even moderate SSB consumption is sufficient to induce the alarm phase in the liver. Another important 'event' during the alarm phase is the activation of stress-related signaling pathways e.g. NF-κB and JNK (known as the ER overload response) (Xu *et al*., 2005), however, there is no clear evidence of stress signaling in our model. DnaJ homolog subfamily A member 1, a known inhibitor of JNK, was significantly upregulated. A downstream consequence of the stress-signaling is the activation of autophagy (Senft & Ronai, 2015; Xu *et al*., 2005). We did not detect an increase of proteins involved in autophagy. On the contrary, the expression of death-associated protein 1 (negative regulator of autophagy) was significantly upregulated. Perhaps this suggests that the ER overload response and autophagy are initiated late in the alarm phase. Prolonged ER stress will eventually trigger apoptosis in the final stage (Tang *et al*., 2010). As far as we can ascertain, phase 3 has not yet manifested in our model.

The proteomics data also revealed that glucose, fructose and lipid metabolism are potentially altered due to SSB consumption (Figure 3.4.1 G). For example, phosphoglycerate mutase 1 (an enzyme of the glycolytic pathway) and Pdhx protein (structural protein of the pyruvate dehydrogenase complex) are significantly downregulated, perhaps indicating that glucose metabolism is suppressed. The most significant changes were observed in proteins involved in lipid metabolism. On the whole it seems as if proteins involved in lipid/fatty acid catabolism are decreased while lipid/cholesterol synthesis and storage is promoted. It is unclear whether the variation of metabolic proteins is induced by the SSB *per se* or whether it is also a downstream consequence of ER stress, or a combination of both Although ER stress can trigger metabolic changes these are not yet clearly understood. For example, there is evidence that ER stress can both enhance and suppress gluconeogenesis (reviewed by Bravo *et al*., 2013). Similarly, there is an undeniable link between ER stress and lipid metabolism, but the exact mechanisms and consequences of this interaction remain unclear.

To our knowledge no other study has performed a proteomic analysis in the liver in response to long-term SSB consumption. There is, however, an investigation of hepatic protein expression in hamsters consuming a high fructose diet (Zhang *et al*., 2008). In contrast to our study, they observed an upregulation in the expression peroxiredoxin- and glutathione S-transferase isoforms and deemed it a protective mechanism. This inconsistency is perhaps due to unique properties of fructose compared to sucrose or due to the fact that the fructose was consumed in solid form and not liquid as in our model. In another study, hepatocytes cultured in high glucose medium displayed increased expression of proteins responsible for protein folding (e.g. heat-shock proteins) (Chen *et al*., 2013). The authors speculated that this may be a response to unfolded proteins in the ER (and thus ER stress). The expression of proteins involved in redox control was also altered. These glucose-induced effects reflect the findings of our study. There are also a few studies that performed proteomic analysis in the context of insulin resistance/diabetes. For example, Morand *et al*. (2005) studied the expression of ER-related proteins in insulin resistant hamsters on a high fructose diet and found the expression of chaperone proteins and other proteins involved in protein folding were altered. Similar to our results the expression of some of these proteins were downregulated (a possible cause of ER stress) while others were upregulated (as you would expect during the adaptation phase). This finding suggests that although ER stress triggers a sequence of cellular responses, these are much more fluid than depicted in Figure 3.4.1. This may explain our observation that proteins involved in various “phases” are implicated. They also observed a significant increase in apolipoprotein E levels (Morand *et al*., 2005). Another study corroborates the positive association between insulin resistance and ER stress. Here the expression of a variety of ER stress markers were measured (i.e. GRP-78, PERK, IRE1a, XBP1, and CHOP) (Balakumar *et al*., 2016). Additionally, they observed that the change elicited by a high fructose and a high fat diet, respectively, were similar both in nature and intensity. This supports our finding that SSB-induced perturbations can be mainly attributed to the excess calories and not the sugar *per se*. Others found that the onset of diabetes in Goto-Kakizaki rats triggered an increase in the expression of mitochondrial proteins, particularly those involved in oxidative phosphorylation, while antioxidants were suppressed (Deng *et al*., 2010). These data are very similar to our observations (Figure 3.4.1 D). In contrast to our model, the Goto-Kakizaki rats also expressed elevated levels of proteins involved in glycolysis and β-oxidation. The similarity between our data and that of insulin resistant/diabetic models may indicate that moderate but frequent SSB consumption induced early diabetic characteristics in our model despite the fact that it is not yet reflected in the fasting blood glucose levels. Furthermore, these studies support the idea that

ER stress and mitochondrial metabolism may be implicated in the onset of early hepatic pathophysiology.

In summary, our data indicate that moderate long-term SSB consumption may induce hepatic ER stress with subsequent effects on the mitochondria, protein synthesis and metabolism. There is some evidence that this is weighted more towards a calorie-induced effect versus a sugar-induced one since most of the proteins that were altered in the SSB group were also altered in the Cal-control group. The next chapter investigates possible causes and consequences of ER stress based on the above mentioned theoretical framework.

3.5 References

Balakumar, M., Raji, L., Prabhu, D., Sathishkumar, C., Prabu, P., Mohan, V., & Balasubramanyam, M. (2016). High-fructose diet is as detrimental as high-fat diet in the induction of insulin resistance and diabetes mediated by hepatic/pancreatic endoplasmic reticulum (ER) stress. *Mol Cell Biochem*, *423*, 93–104

Bechmann, L., Hannivoort, R., Gerken, G., Hotamisligil, G., Trauner, M., & Canbay, A. (2012). The interaction of hepatic lipid and glucose metabolism in liver diseases. *J Hepatol*, *56*, 952–964.

Benadè, J. (2014). *Cardio-metabolic complications induced by long-term sugar-sweetened beverage consumption*. Stellenbosch University, Stellenbosch, South Africa.

Bizeau, M., & Pagliassotti, M. (2005). Hepatic adaptations to sucrose and fructose. *Metabolism*, *54*(9), 1189–1201.

Black, R., Spence, M., McMahon, R., Cuskelly, G., Ennis, C., McCance, R., … Hunter, S. (2006). Effect of eucaloric high- and low-sucrose diets with identical macronutrient profile on insulin resistance and vascular risk: a randomized controlled trial. *Diabetes*, *55*, 3566–3572.

Bravo, R., Parra, V., Gatica, D., Rodriguez, A., Torrealba, N., Paredes, F., … Lavandero, S. (2013). Endoplasmic Reticulum and the Unfolded Protein Response: Dynamics and Metabolic Integration. *Int Rev Cell Mol Biol*, *301*, 215–290.

Burrill, J., Long, E., Reilly, B., Deng, Y., Armitage, I., Scherer, P., & Bernlohr, D. (2015). Inflammation and ER Stress Regulate Branched-Chain Amino Acid Uptake and Metabolism in Adipocytes. *Mol Endocrinol*, *29*, 411–420.

Canto, C., Menzies, K., & Auwerx, J. (2015). NAD+ Metabolism and the Control of Energy Homeostasis: A Balancing Act between Mitochondria and the Nucleus. *Cell Metab*, *22*, 31–53.

Cevik, O., Baykal, A., & Sener, A. (2015). Platelets Proteomic Profiles of Acute Ischemic Stroke Patients. *PLoS ONE*, *11*(6), e0158287.

Chen, J., Chou, H., Chen, Y., & Chan, H. (2013). High glucose-induced proteome alterations in hepatocytes and its possible relevance to diabetic liver disease. *Journal of Nutritional Biochemistry*, *24*, 1889–1910.

Choi, K., & Kim, Y. (2010). Molecular Mechanism of Insulin Resistance in Obesity and Type 2 Diabetes. *Korean J Intern Med*, *25*.

Coletta, C., Módis, K., Szczesny, B., Brunyánszki, A., Oláh, G., Rios, E., … Szabo, C. (2015). Regulation of Vascular Tone, Angiogenesis and cellular Bioenergetics by the 3-Mercaptopyruvate Sulfurtransferase/H2S Pathway: Functional Impairment by Hyperglycemia and Restoration by DL-α-Lipoic Acid. *Molecular Medicine*, *21*, 1–14.

Croft, D., Mundo, A., Haw, R., Milacic, M., Weiser, J., Wu, G., … D'Eustachio, P. (2014). The Reactome pathway knowledgebase. *Nucleic Acids Res*, *42*(Database issue), D472–D477.

Cuevas, B.D., Lu, Y., Mao, M., Zhang, J., LaPushin, R., Siminovitch, K., & Mills, G.B. (2001). Tyrosine phosphorylation of p85 relieves its inhibitory activity on phosphatidylinositol 3-kinase. *J Biol Chem*, *276(29), 27455-27461*.

Dekker, M., Su, Q., Baker, C., Ruthledge, A., & Adeli, K. (2010). Fructose: a highly lipogenic nutrient implicated in insulin resistance, hepatic steatosis, and the metabolic syndrome. *Am J Physiol Endocrinol Metab*, *299*, E685–E694.

Deng, W., Nie, S., Dai, J., Wu, J., & Zeng, R. (2009). Proteome, Phosphoproteome, and Hydroxyproteome of Liver Mitochondria in Diabetic Rats at Early Pathogenic Stages. *Mol Cell Proteomics*, *9*(1), 100–116.

Deng, W., Nie, S., Dai, J., Wu, J., & Zeng, R. (2010). Proteome, Phosphoproteome, and Hydroxyproteome of Liver Mitochondria in Diabetic Rats at Early Pathogenic Stages. *Mol Cell Proteomics*, *9*(1), 100–116.

Doroudgar, S., Völkers, M., Thuerauf, D., Mohsin, S., Respress, J., Wang, W., … Glembotski, C. (2015). Hrd1 and ER-Associated Protein Degradation, ERAD, are Critical Elements of the Adaptive ER Stress Response in Cardiac Myocytes. *Circ Res*, *117*(6), 536–546.

Fabbrini, E., & Magkos, F. (2015). Hepatic Steatosis as a Marker of Metabolic Dysfunction. *Nutrients*, *7*(6), 4995–5019.

Fabregat, A., Sidiropoulos, K., Garapati, P., Gillespie, M., Hausmann, K., Haw, R., … D'Eustachio, P. (2016). The Reactome pathway Knowledgebase. *Nucleic Acids Res*, *44*(D1), D481–D487.

Fuller-Pace, F., & Ali, S. (2008). The DEAD box R NA helicases p68 (Ddx5) and p72 (Ddx17): novel transcriptional co-regulators. *Biochem. Soc. Trans.*, *36*, 609–612.

Graves, P., & Haystead, T. (2002). Molecular Biologist's Guide to Proteomics. *Microbiol Mol Biol Rev*, *66*(1), 39–63.

Gray, L., Tompkins, S., & Taylor, E. (2014). Regulation of pyruvate metabolism and human disease. *Cell. Mol Life Sci.*, *71*, 2577–2604.

Guo, S. (2014). Insulin signaling, resistance, and metabolic syndrome: insights from mouse models into disease mechanisms. *J Endocrinol*, *220*(2), T1–T23.

Guyton, A., & Hall, J. (2011). *Guyton and Hall textbook of medical physiology* (12th ed.). Philidelphia: PA: Saunders/Elsevier.

Hanke, S., & Mann, M. (2009). The Phosphotyrosine Interactome of the Insulin Receptor Family and Its Substrates IRS-1 and IRS-2. *Mol Cell Proteomics*, *8*(3), 519–534.

Havel, P. (2005). Dietary Fructose: Implications for Dysregulation of Energy Homeostasis and Lipid/Carbohydrate Metabolism. *Nutr Rev*, *63*(5), 133–157.

Horton, H., Moran, L., Scrimgeour, K., Perry, M., & Rawn, D. (2006). *Principles of Biochemistry* (4th ed.). United States of America: Pearson Education

Kakimoto, Y., Ito, S., Abiru, H., Kotani, H., Ozeki, M., Tamaki, K., & Tsuruyama, T. (2013). Sorbin and SH3 Domain-Containing Protein 2 Is Released From Infarcted Heart in the Very Early Phase: Proteomic Analysis of Cardiac Tissues From Patients. *J Am Heart Assoc*.

Kitamura, T. (2013). The role of FOXO1 in β-cell failure and type 2 diabetes mellitus. *Nat Rev Endocrinol*, *9*, 615–623.

Lin, W., Chiu, K., Chang, H., Lee, K., Tai, T., & Chuang, L. (2001). Molecular scanning of the human sorbin and SH3-domain-containing-1 (SORBS1) gene: positive association of the T228A polymorphism with obesity and type 2 diabetes. *Hum Mol Gen*, *10*(17), 1753–1760.

Maersk, M., Belza, A., & Stodkilde-Jorgensen, H. (2012). Sucrose-sweetened beverages increase fat storage in the liver, muscle, and visceral fat depot: a 6-mo randomized intervention study. *Am J Clin Nutr*, *95*, 283–289

Magnusson, M., Wang, T., Clish, C., Engstrom, G., Nilsson, P., Gerszten, R., & Melander, O. (2015). Dimethylglycine Deficiency and the Development of Diabetes. *Diabetes*, *64*, 3010–3016.

Malhotra, J., & Kaufman, R. (2011). ER stress and its functional link to mitochondria: role in cell survival and death. *Cold Springs Harb Perspect Biol*, *3*(9), a004424.

Manning, B.D., & Cantley, L.C. (2007). AKT/PKB Signaling: Navigating Downstream. *Cell*, *129*, 1261–1274

Meex, R., Hoy, A., Morris, A., Brown, R., Lo, J., Burke, M., … Watt, M. (2015). Fetuin B Is a Secreted Hepatocyte Factor Linking Steatosis to Impaired Glucose Metabolism. *Cell Metab*, *22*(6), 1078–1089.

Meshkani, R., & Adeli, K. (2009). Hepatic insulin resistance, metabolic syndrome and cardiovascular disease. *CLB*, *42*, 1331–1346.

Michael, M., Kulkarni, R., Postic, C., Previs, S., Shulman, G., Magnuson, M., & Kahn, C. (2000). Loss of insulin signaling in hepatocytes leads to severe insulin resistance and progressive hepatic dysfunction. *Mol Cell*, *6*(1), 87–97.

Moore, M., Coate, K., Winnick, J., & Cherrington, A. (2012). Regulation of Hepatic Glucose Uptake and Storage In Vivo. *Adv. Nutr.*, *3*, 284–294.

Morand, J., Macri, J., & Adeli, K. (2005). Proteomic Profiling of Hepatic Endoplasmic Reticulum-associated Proteins in an Animal Model of Insulin Resistance and Metabolic Dyslipidemia. *J Biol Chem*, *280*(18), 17626–17633

Nakatani, S., Kakehashi, A., Ishimura, E., Yamano, S., Mori, K., Wei, M., … Wanibuchi, H. (2011). Targeted Proteomics of Isolated Glomeruli from the Kidneys of Diabetic Rats: Sorbin and SH3 Domain Containing 2 Is a Novel Protein Associated with Diabetic Nephropathy. *Exp Diabetes Res*. https://doi.org/10.1155/2011/979354

Naslavsky, N., Rahajeng, J., Rapaport, D., Horowits, M., & Caplan, S. (2007). EHD1 regulates cholesterol homeostasis and lipid droplet storage. *Biochem Biophys Res Commun*, *357*(3), 792–799.

O'Leary, N., Wright, M., Brister, J., Ciufo, S., Haddad, D., McVeigh, R., … Pruitt, K. (2016). Reference sequence (RefSeq) database at NCBI: current status, taxonomic expansion, and functional annotation. *Nucleic Acids Res*, *44*(D1), D733–D745.

Perry, R., Samuel, V., Petersen, K., & Shulman, G. (2014). The role of hepatic lipids in hepatic insulin resistance and type 2 diabetes. *Nature*, *510*, 83–90

Postic, C., Dentin, R., & Girard, J. (2004). Role of the liver in the control of carbohydrate and lipid homeostasis. *Diabetes Metab*, *30*, 398–408

Prasad, M., Walker, A., Kaur, J., Thomas, J., Powell, S., Pandey, A., … Bose, H. (2016). Endoplasmic Reticulum Stress Enhances Mitochondrial Metabolic Activity in Mammalian Adrenals and Gonads. *Mol Cell Biol*, *36*, 3058–3074.

Roden, M., & Bernroider, E. (2003). Hepatic glucose metabolism in humans—its role in health and disease. *Best Pract Res Clin Endocrinol Metab*, *17*(3), 365–383

Senft, D., & Ronai, Z. (2015). UPR, autophagy, and mitochondria crosstalk underlies the ER stress response. *Trends in Biochemical Sciences*, *40*(3), 141–148.

Sherwood, L. (2007). *Human Physiology: From Cells to Systems* (7th ed.). Canada: Brooks/Cole.

Stanhope, K. (2015). Sugar consumption, metabolic disease and obesity: The state of the controversy. *Crit Rev Clin Lab Sci*, *Early online*, 1–16. https://doi.org/10.3109/10408363.2015.1084990

Szklarczyk, D., Franceshini, A., Wyder, S., Forslund, K., Heller, D., Huerta-Cepas, J., … Von Meiring, C. (2015). STRING v10: protein-protein interaction networks, integrated over the tree of life. *Nucleic Acids Res*, *43*(Database issue), D447–D452.

Tang, Y., Xiang, W., Terry, L., Kretzschmar, H., & Windl, O. (2010). Transcriptional Analysis Implicates Endoplasmic Reticulum Stress in Bovine Spongiform Encephalopathy. *PloS ONE*, *5*(12), e14207.

Tappy, L., & Le, K. (2010). Metabolic Effects of Fructose and the Worldwide Increase in Obesity. *Physiol Rev*, *90*, 23–46

The UniProt Consortium. (2014). UniProt: a hub for protein information. *Nucleic Acids Res*, *43*(D1), D204–D212.

Wang, Y., Tan, B., Mu, R., Chang, Y., Wu, M., Tu, H., … Li, H. (2015). Ubiquitin-associated domain-containing ubiquitin regulatory X (UBX) protein UBXN1 is a negative regulator of nuclear factor κB (NF-κB) signaling. *J Biol Chem*, *290*(16), 10395–103405.

Wolozin, B. (2012). Regulated protein aggregation: stress granules and neurodegeneration. *Mol Neurodegener*, *7*(56).

Xu, C., Baily-Maitre, B., & Reed, J. (2005). Endoplasmic reticulum stress: cell life and death decisions. *J Clin Invest*, *115*(10), 2656–2664.

Zhang, L., Perdomo, G., Kim, D., Qu, S., Ringquist, S., Trucco, M., & Dong, H. (2008). Proteomic Analysis of Fructose-Induced Fatty Liver in Hamsters. *Metabolism*, *57*(8), 1115–1124.

Zhang, W., Patil, S., Chauhan, B., Guo, S., Powell, D., Le Angelos Klotsas, J., … Montminy, M. (2006). FoxO1 regulates multiple metabolic pathways in the liver: effects on gluconeogenic, glycolytic and lipogenic gene expression. *J Biol Chem*, *281*(15), 10105–10117

Zhou, Y., Zhang, H., Zheng, B., Ye, L., Zhu, S., Johnson, N., … Xiao, J. (2016). Retinoic Acid Induced-Autophagic Flux Inhibits ER-Stress Dependent Apoptosis and Prevents Disruption of Blood-Spinal Cord Barrier after Spinal. *Int J Biol Sci, 12(1),* 87-99

Chapter 4: Understanding ER stress

4.1 Introduction

The purpose of this chapter is to build on the data generated in the proteomic analysis. Here we investigated oxidative stress as a possible underlying cause of ER stress. Additionally, we investigated perturbations of glucose and lipid metabolism since it is poorly understood in the context of ER stress. Lastly we hoped to determine whether the ER overload response is triggered in our model since the proteomic data in were inconclusive in the regard. Section 4.1.1-4.1.4 provides a theoretical background for the experimental work that follows.

4.1.1 Oxidative stress

Over-nutrition is closely linked with oxidative stress, a parameter that plays an important role in cardio-metabolic disease onset (Matsuda, 2013). Oxidative stress refers to a state where excess ROS molecules induce physiological dysfunction by reacting with, and damaging, proteins, DNA and lipids (Araki & Nishikawa, 2010). While relatively small amounts of ROS are essential for proper functioning of the cell, the presence of excessive amounts is detrimental (Styskal *et al*., 2012). It is widely assumed that hyperglycemia aggravates ROS, yet clinical studies exploring the association between acute glycemic load and oxidative stress produced inconsistent and inconclusive results (reviewed by Choi *et al*., 2008). Others confirmed a positive association between chronic hyperglycemia (diagnosed diabetes or based on HbA1c measurements) and oxidative stress (Aouacheri *et al*., 2015; Araki & Nishikawa, 2010).

Theoretically, hyperglycemia should have significant effects on mitochondrial ROS production (Rolo & Palmeira, 2006). Here the glucose is metabolized to form ETC donors, NADH and flavin adenine dinucleotide ($FADH_2$), thereby enabling the production of ATP. Under physiological conditions NADH and $FADH_2$ donate electrons to protein complex I and protein complex II, respectively. These electrons are then transferred through the ETC (Figure 4.1.1) until it reaches complex IV. Here the electrons leave the ETC to reduce oxygen to water. In parallel, complexes I, III and IV also pump protons across the inner membrane of mitochondria to generate a trans-membrane voltage gradient that drives ATP generation through ATP synthase. Frequent SSB consumption may, result in an excess availability of NADH and $FADH_2$. Electrons now enter the ETC at a faster pace causing a shift in ATP/adenosine diphosphate (ADP) ratio and hyperpolarization of the mitochondrial inner membrane (Rolo &

Palmeira, 2006). Subsequently, complex III can become partially congested resulting in electron accumulation and leakage at coenzyme Q that can bind to molecular oxygen to yield superoxide (Rolo & Palmeira, 2006).

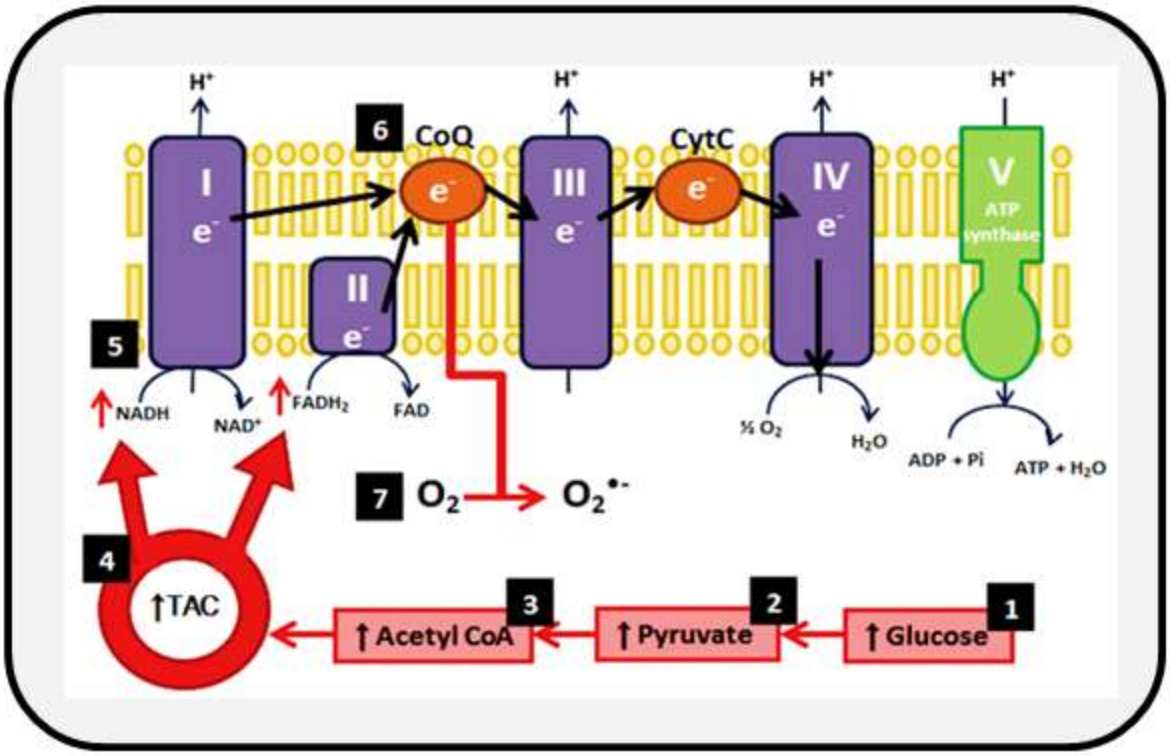

Figure 4.1.1: Mitochondrial superoxide production induced by hyperglycemia. Glucose metabolism ultimately leads to the production of NADH and $FADH_2$ (steps 1-4). NADH and $FADH_2$ donate electrons to the complex I and complex II of the electron transfer chain ETC, respectively. Hyperglycemia results in an excess availability of NADH and $FADH_2$ (5) which cause congestion and untimely electron leakage. Each of these electrons bind to an oxygen molecule to generate superoxide (6-7). Diagram from Benadè (2014).

Although mitochondria are considered the main source of intracellular ROS, there are other processes and enzymes that also contribute to oxidative stress e.g. NADPH oxidase (NOX), xanthine oxidase , endothelial nitric oxide synthase and angiotensin II (reviewed by Giacco & Brownlee, 2010; Johnson *et al*., 2009, Panigrahy, 2016). Xanthine oxidase activity is linked to CVD as it generates superoxide that reacts with nitric oxide, thereby interfering with the relaxation of vascular smooth muscle and promoting the aggregation of platelets. Additionally, it promotes the generation of peroxynitrite anions that can deactivate several signaling enzymes (Bocci *et al*., 2011). However, data suggest that besides mitochondrial ROS, NOX likely plays

the most noteworthy role in the context of SSB consumption and the onset of cardio-metabolic diseases, e.g. NOX are overexpressed in Zucker fatty rats that are often used as models for obesity and T2DM (Shen, 2010). NOX is a family of enzymes located in the membranes of organelles. NOX interacts with other transmembrane proteins to capture NADPH from within the organel and convert it to superoxide that is released back into the cytosol. In addition, NOX further exacerbates oxidative stress by weakening the antioxidant capacity of the cell, i.e. by depleting NADPH that is required in the regeneration of the antioxidant reduced glutathione (Johnson *et al*., 2009). How does this relate to SSB consumption? Frequent SSB intake is associated with increased body fat e.g. fructose consumption can trigger visceral fat deposition (Aeberli *et al*., 2011). Here the release of adipokines from adipocytes can dysregulate NOX activity (Matsuda & Shimomura, 2013). Another mechanism by which SSB consumption, or fructose consumption in particular, can enhance NOX activity is via uric acid (Johnson *et al*., 2009). The notion that fructose intake leads to oxidative stress is supported by animal studies although the precise underlying mechanisms remain unclear (Chandramohan & Pari, 2014).

In the literature one of the primary links between oxidative stress and cardio-metabolic diseases is the increase in NOGP activity. The NOGPs are alternative pathways for glucose metabolism, but inappropriate activation of the NOGPs may have detrimental cardio-metabolic consequences (reviewed by Poornima *et al*., 2006). Oxidative stress induces DNA strand breakage (Matsuda & Shimomura, 2013) that activates poly(ADP-ribose) polymerase (PARP). The latter is located within the nucleus and plays a central role in DNA repair by inducing the accumulation of ADP-ribose polymers. DNA damage also triggers the translocation of the glycolytic enzyme glyceraldehyde 3-phosphate dehydrogenase (GAPDH) from the cytosol to the nucleus to facilitate the DNA repair. In the nucleus ADP-ribose polymers modify the structure of GAPDH thereby inhibiting subsequent glycolytic activity (Du *et al*., 2003). The glycolytic intermediates upstream of GAPDH accumulate and divert into the NOGPs, which will be discussed in the following section (Ceriello & Testa, 2009).

Although this is the most documented example of how oxidative stress can contribute to cardio-metabolic complications, there are also other mechanisms that may play a role (refer Figure 4.1.2). For example, as discussed in Chapter 3, redox imbalance may induce ER stress and subsequent detrimental consequences (Senft & Ronai, 2015). Oxidative stress can also contribute to the development of T2DM in a more direct manner, e.g. by interfering with insulin secretion by inhibiting the activity of the insulin gene promoter and insulin mRNA expression (Panigrahy, 2016, Tangvarasittichai, 2015). ROS can also halt insulin signaling, induce

pancreatic β-cell apoptosis and suppress the expression of the insulin gene through NF-κB and JNK signaling, respectively (Lazo-de-la-Vega-Monroy & Fernández-Mejía, 2013). In severe cases, oxidative stress can also suppress hepatic glucose uptake by decreasing the availability of sarcolemmal GLUT2 in hepatocytes thereby causing chronic hyperglycemia. Oxidative stress can induce apoptosis of hepatocytes by upregulating the pro-apoptotic factor Bax, while suppressing the anti-apoptotic factor Bcl-2 (Rashid *et al*., 2013).

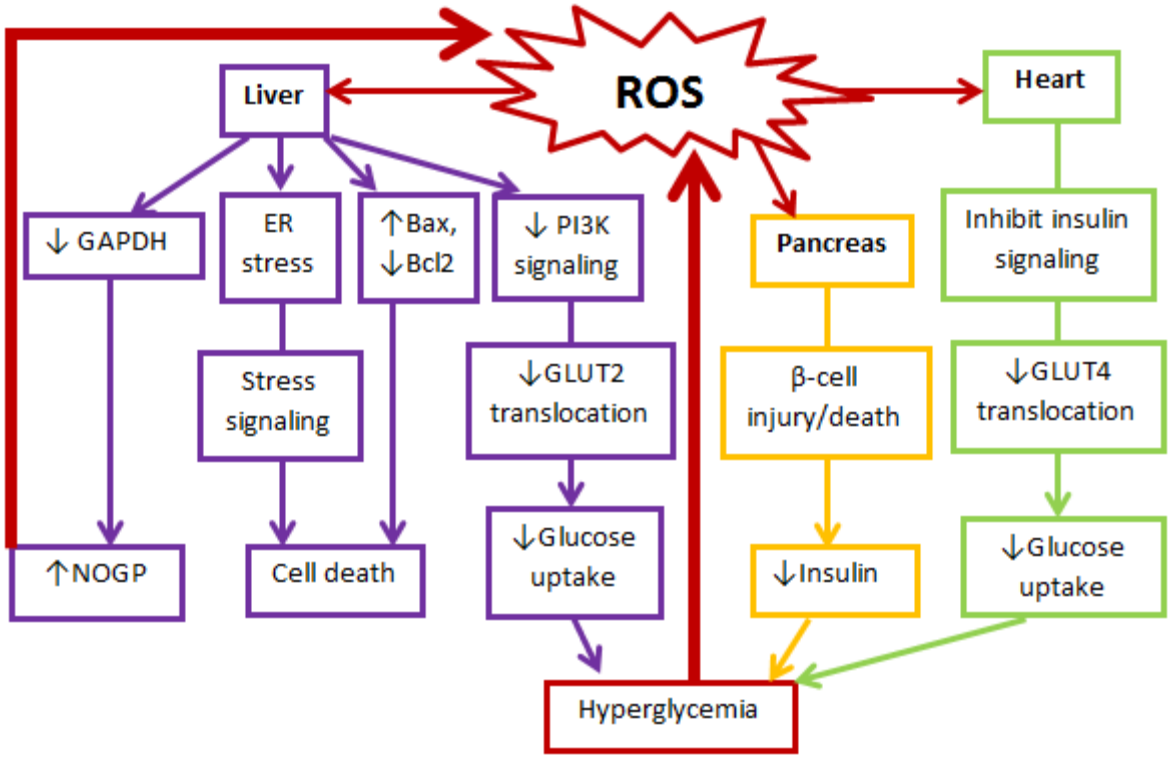

Figure 4.1.2: The role of ROS in cardio-metabolic diseases. ROS may induce damage in various organ systems that contribute to the development and perpetuation of cardio-metabolic conditions.

4.1.2 Non-oxidative glucose metabolism

In section 4.1.1 we explained how ROS can suppress the activity of the glycolytic enzyme GAPDH, which may cause upstream glycolytic intermediates to accumulate and divert into alternative metabolic pathways – the NOGPs. Here glucose enters the polyol pathway, while G-6-P is channeled into the pentose phosphate pathway . F-6-P is diverted into the hexosamine biosynthetic pathway (HBP) where *O*-linked β-*N*-acetyl glucosamine moieties (*O*-GlcNAc) are attached to proteins. Lastly, elevated glyceraldehyde-3-phosphate leads to increase protein kinase C (PKC) activity and the synthesis of advance glycation end products (AGE) (Figure 4.1.3). Besides the role of oxidative stress, we found that SSB consumption reduced the expression of the glycolytic enzyme phosphoglycerate mutase 1 (PGM1 in Figure 4.1.3). Phosphoglycerate mutase 1 catalyzes the 8th reaction in the glycolytic pathway thus its decrease could further increase NOGP activity. In the light of this, we decided to evaluate the activity of the NOGPs in our model.

Research suggests that all but one of the NOGPs play a central role in the mechanisms underlying cardio-metabolic conditions and diabetic complications (reviewed by Poornima *et al*., 2006). Here the pentose phosphate pathway may elicit protective instead of detrimental effects although the precise mechanisms are not yet fully understood. The other four pathways and their role in SSB-induced cardio-metabolic disease will now be discussed.

Figure 4.1.3: Increased NOGP activity. (1) Oxidative damage to DNA leads to the inhibition of glycolytic enzyme, GAPDH while (2) ER stress possibly suppresses the expression of PGM1. Together this may result in (3): the accumulation of upstream glycolytic metabolites which then divert into NOGPs and induce cardio-metabolic complications. Adapted from Benadè (2014).

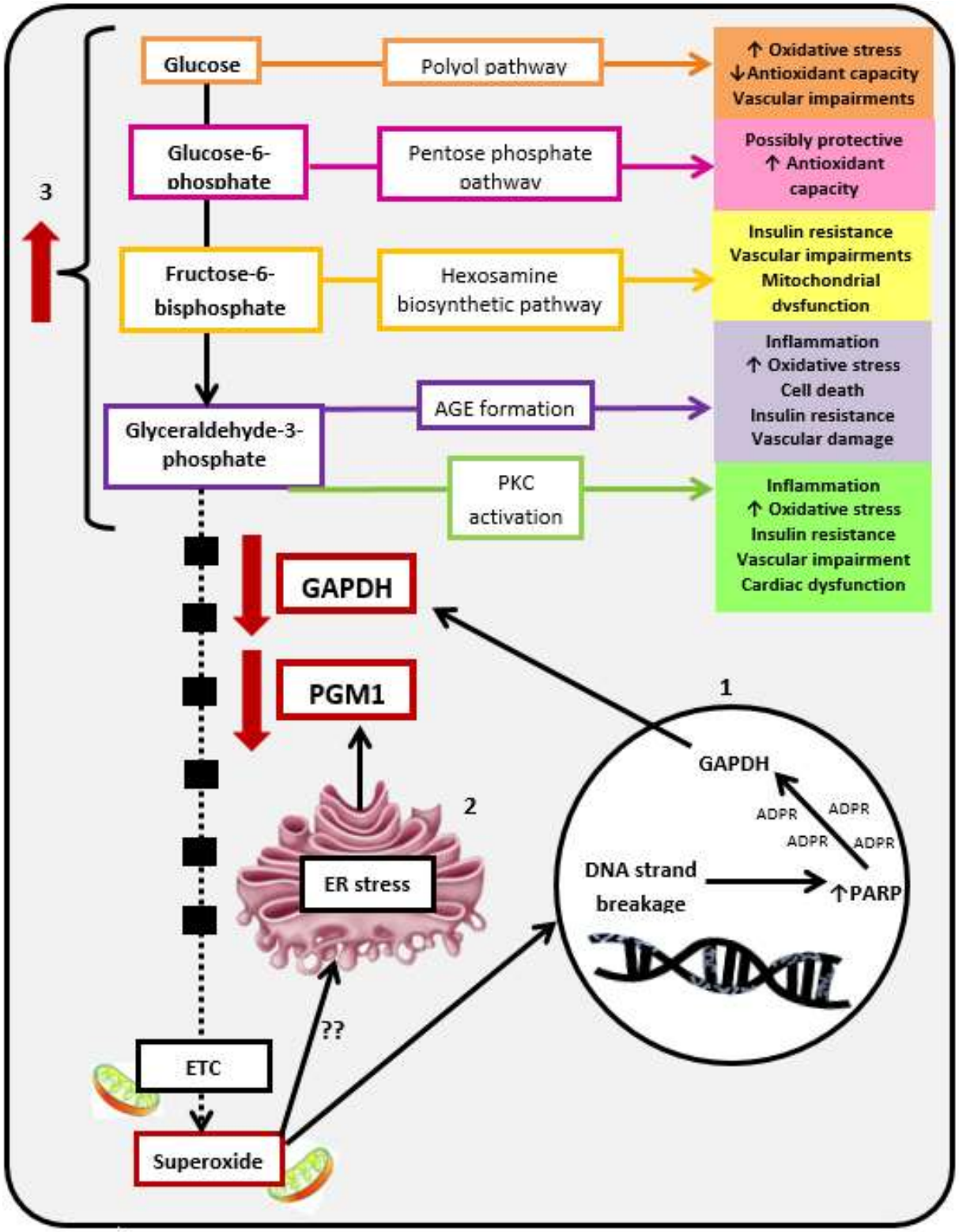

. 4.1.2.1 AGE

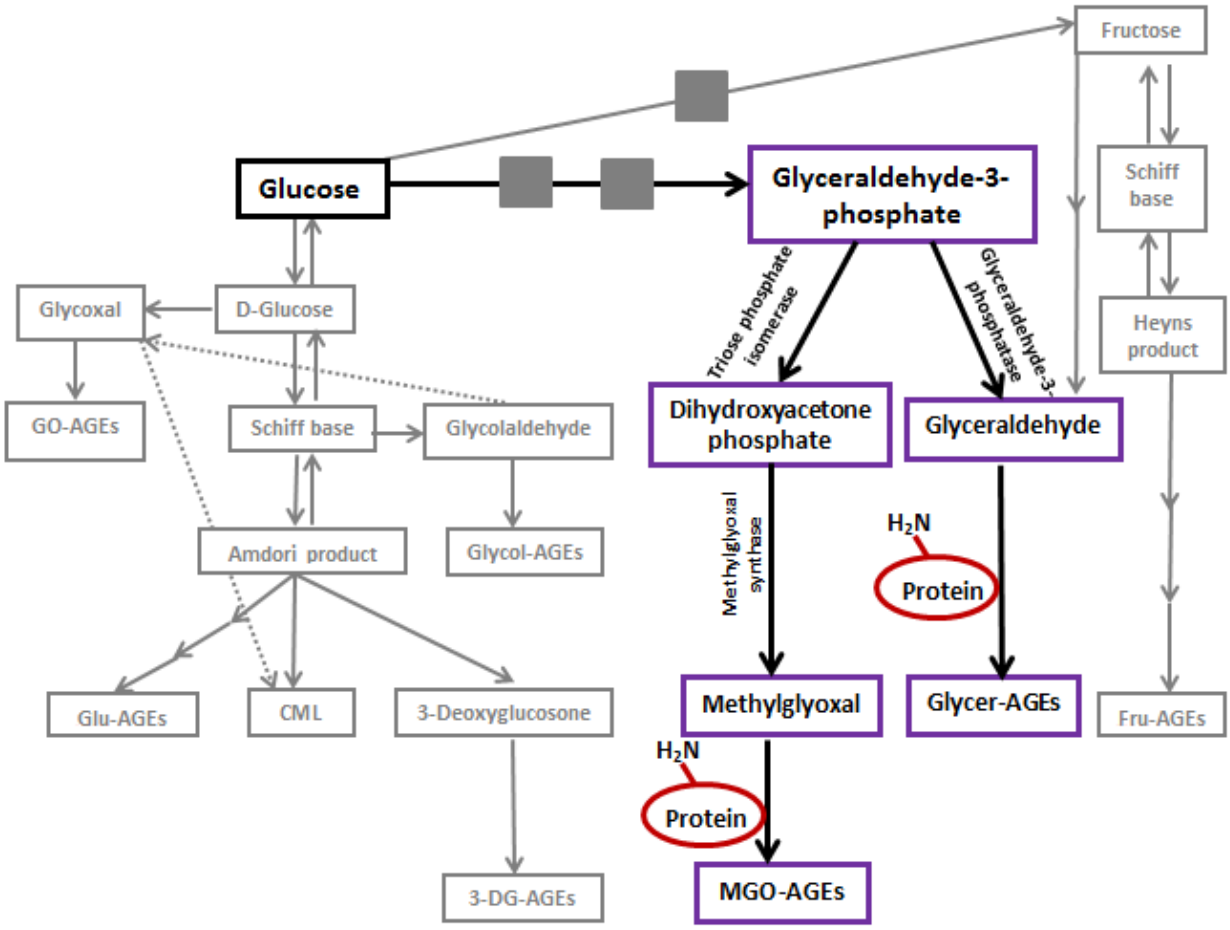

Figure 4.1.4: **AGE formation from glycolytic moieties**. Adapted from Takino (2015).

AGEs are formed when glucose and other glycation agents are attached to proteins, lipids and nucleotides (Bucala *et al*., 1995). This can happen though two possible pathways, both promoted by oxidative stress. The first is marked by the modification of proteins, amine-containing lipids and nucleic acids by reactive triosphosphates like glyceraldehyde-3-phosphate that accumulated under hyperglycemic conditions. The second, the Maillard pathway, relies on the attachment of the carbonyl groups from reducing sugars to the animo acids of targeted proteins. This reaction is reversible and the product is known as a Schiff base. These are then processed to form Amadori/Heyns products and ultimately AGEs after further modification (Refer Figure 4.1.4) (reviewed by Takeuchi & Makita, 2001). Methylglyoxal derivatives produced

form glyceraldehyde-3-phosphate and carboxymethyl-lysine produced form glucose are the most well-known and studied AGEs (Gavin, 2001; Vlassara & Uribarri, 2014).

Hyperglycemia is considered to be a primary endogenous trigger for AGE synthesis. New research, however, suggests that AGEs might also be a cause of hyperglycemia and T2DM and not only a result of it. For example, a clinical trial demonstrated that insulin resistance, inflammation and oxidative stress can be reversed by following a low AGE diet (Uribarri *et al*., 2011). This finding was recently confirmed in an obese cohort during a year-long controlled trial. Participants who consumed a diet low in AGEs had significantly improved insulin sensitivity, together with lowered oxidative stress and inflammation compared to baseline measurements and a control group (Vlassara *et al*., 2016). The link between increased AGE levels and cardio-metabolic perturbations is well studied both *in vitro* and *in vivo* (reviewed by Hueschmann *et al*., 2006; Nowotny, 2015).

AGEs induce damage by modifying signaling proteins and transcription factors (Brownlee, 2005). This is particularly linked to insulin resistance and impaired insulin secretion. For example, Tahara *et al*. (2012) found that increased serum AGE levels correlate with insulin resistance based on HOMA-IR data. However, the exact molecular mechanism behind this is still not clear. Some possible mechanisms include increased expression of TNF-α that inhibits insulin signaling, PKC-mediated pathways, glycation of insulin and increased JNK-mediated IRS-1 inhibition (reviewed in Nowotny *et al*., 2015; Vlassara, 2011). Insulin secretion is diminished by the cytotoxic effect of AGEs on pancreatic β-cells (Lim *et al*., 2008). Methylglyoxal, in particular, is responsible for dysregulated apoptosis as it alters the expression of Bcl2, Bax and caspase (Tajes *et al*., 2014)

AGEs also accumulate within the extracellular matrix. This can lead to tissue stiffness that has significant effects on cardiovascular health e.g. it can cause stiffening of the heart valves (reviewed by Essop, 2016). Changes in the extracellular matrix also alter signaling between the matrix and the cell, leading to cellular dysfunction (reviewed by Brownlee, 2005). Lastly, the interaction between AGEs and receptors for AGEs (RAGE) can also be detrimental (Neeper *et al*., 1992). Under physiological conditions, AGEs normally bind to AGE-receptor1 (AGE-R1) that leads to degradation of AGEs. AGE-peptides can then be excreted through urine, thereby protecting the organism against oxidative stress. However, when there is an excessive amount of AGEs present, AGE-R1 receptors become depleted. Consequently AGEs bind to RAGEs instead (Vlassara & Uribarri, 2014). AGE-RAGE interactions trigger signaling cascades that

may lead to NF-κB-induced inflammation (Balakumar *et al.*, 2010). This interaction is also associated with downstream generation of ROS. Although the expression of AGE-R1 and RAGEs is usually regulated by AGE and ROS levels, the expression of RAGEs remain relatively high in diabetics, while the expression of protective AGE-R1 receptors are suppressed. This is possibly the result of chronic oxidative stress (Vlassara & Uribarri, 2014).

4.1.2.2 PKC

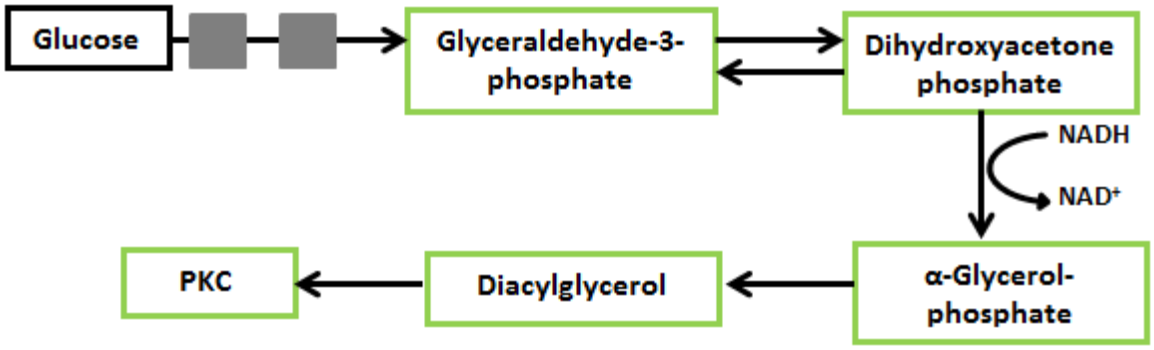

Figure 4.1.5: PKC activation in response to high glucose availability. Adapted from Joseph, 2014.

PKC refer to a cluster of proteins with more than 11 isoforms. PKC alters cell signaling and gene regulation by modifying transcription- and co-factors through the addition of a phosphate group, thereby either enhancing or suppressing its activity (Newton, 1995). PKC isoforms are divided into three groups (i.e. conventional, novel and atypical) based on the combination of co-factors required for activation. When glyceraldehyde-3-phosphate accumulates it can be used to produce diacylglycerol that serves as a co-factor for the activation of conventional (α, βI, βII and γ) and novel PKC isoforms (δ, ε, η and θ) (Shiba *et al*., 1993) (Figure 4.1.5).

Dysregulated PKC activity is linked to pathophysiology in a range of organ systems. For example, PKCβ activity robustly correlates with cardio-metabolic diseases (Geraldes & King, 2010). This isoform is expressed in various organs such as the liver, skeletal muscle and the kidney with exceptionally high levels found in adipose tissue and the brain. The expression of PKCβ is increased by the consumption of large amounts of fatty foods. ROS mediates the activation of PKCβ independent of the presence of Ca^{2+} and phospholipids (reviewed by Mehta,

2014). As PKCβ is particularly implicated in the context of a Westernized diet and cardio-metabolic conditions – it will be the focus of this section.

Animal models are often used to investigate the link between PKCβ and cardio-metabolic conditions e.g. PKCβ knockout mice are lean and characterized by significantly lower levels of body fat compared to wild-type mice. Moreover, such mice were also protected against insulin resistance and hepatic steatosis despite consuming a high fat diet for 12 weeks (Huang *et al*., 2009). In another animal model it was observed that PKCβ is associated with the inhibition of IRS-1 serine residue (Hennige *et al*., 2010). Additionally, this study found that PKCβ also inhibits the expression of genes involved in lipid metabolism (e.g. PGC-1-α, acyl-CoA oxidase and hormone-sensitive lipase) and is linked to intrahepatic lipid deposition (Hennige *et al*., 2010). It can also trigger inflammation via JNK and NF-κB (Butcher & Galkina, 2013), aggravate oxidative stress (H_2O_2 production) and induce mitochondrial damage by triggering the opening of mitochondrial permeability transition pore (Pinton *et al*., 2007). In the heart PKCβ (together with PKCδ) modulates various factors involved in cardiovascular health e.g. nitric oxide synthase, endothelin-1 and sarco/endoplasmic reticulum Ca^{2+}-ATPase (reviewed by

Brownlee, 2005; Giacco & Brownlee, 2010). Inappropriate regulation of such factors can lead to restricted blood flow and impaired relaxation of the cardiac muscle. A recent *in vitro* study performed in our laboratory also showed that PKCβ elcited an inhibitory effect on myocardial insulin-dependent glucose uptake (Joseph *et al*., 2014). Moreover, others showed that the protective properties of exercise in the context of cardio-metabolic diseases are possibly due to the inhibition of PKCβ expression in both murine liver and skeletal muscle (Rao, 2013). To conclude, PKCβ clearly plays a pivotal role in the onset and perpetuation of cardio-metabolic diseases and its value as therapeutic target should not be disregarded.

4.1.2.3 HBP

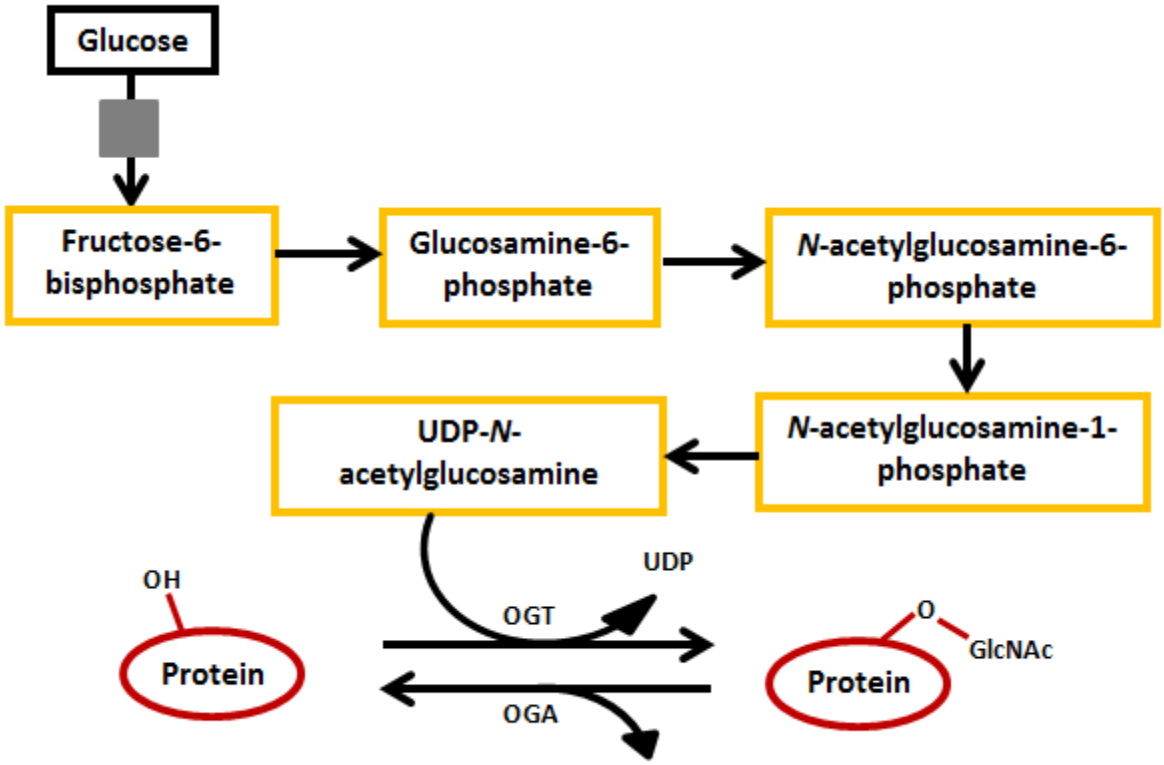

Figure 4.1.6 Protein *O*-GlcNAcylation via the HBP. Adapted from Joseph, 2014.

The HBP is a nutrient-sensing pathway responsible for the regulation of a range of cellular processes (Hanover *et al*., 2010). After G-6-P is converted to F-6-P early in glucose metabolism, F-6-P then has two possible fates – it can continue in the glycolytic pathway or be channel into the HBP (Brownlee, 2001). In healthy individuals only ~2-5% of intracellular glucose will enter the HBP where glutamine:fructose-6-phosphate-amidotransferase is the rate-limiting enzyme that regulates HBP flux (Schleischer & Weigert, 2000). If F-6-P enters the HBP, glutamine acts as amino donor to convert F-6-P to glucosamine-6-phosphate (GlcN-6-P) (refer Figure 4.1.6). GlcN-6-P follows a series of enzymatic reactions to finally produce uridine 5'-diphospho *N*-acetyl glucosamine (Kornfeld, 1967). *O*-GlcNAcylation takes place when the *N*-acetyl glucosamine moiety binds to the hydroxyl group of the threonine or serine residues of proteins (this happens in a similar fashion as protein phosphorylation) to form *O*-GlcNAc products. It is a dynamic process regulated by *O*-GlcNAc transferase that catalyzes the attachment of the *O*-GlcNAc moiety, and *O*-GlcNAcase that removes *O*-GlcNAc residues from

the target protein (Torres & Hart, 1984). *O*-GlcNAcylation plays a major role in a range of cellular processes such as transcription and signaling (Lefebvre *et al*., 2010).

O-GlcNAcylation regulates various cellular processes by modifying transcription factors and RNA polymerase II (reviewed by Hart, 2014). Under physiological conditions protein *O*-GlcNAcylation has beneficial results, however, the level of *O*-GlcNAcylation change rapidly and become maladaptive in response to stress (Lefebvre *et al*., 2010). Hyperglycemia is associated with an inappropriate increase in HBP flux that leads to pathological changes in the expression of various proteins. Transcription factors, signaling molecules and enzymes are targeted in particular and many are linked to cardio-metabolic diseases (Vaidyanathan & Wells, 2014). For example, a mouse model revealed that overexpression of *O*-GlcNAc transferase in the liver is associated with insulin resistance and a perturbed lipid profile (Yang *et al*., 2008). This is likely due to the deactivation through *O*-GlcNAcylation of various signaling molecules of the insulin signaling pathway including Akt1/2, IRS-1/2, the catalytic subunit of PI3K and the β-subunit of the insulin receptor. This may provide some insight into the link between the HBP and hepatic insulin resistance (reviewed by Lefebvre *et al*., 2010; Zhang *et al*, 2014). *O*-GlcNAc modification also plays a crucial role in hepatic metabolism as it regulates the expression of important gluconeogenesic genes (PEPCK and G-6-Pase) via transcription factor FoxO1 (Housley *et al*., 2008). Here FoxO1 *O*-GlcNAcylation corresponds with elevated FoxO1 activity, perhaps due to enhanced DNA binding capacity or increased co-factor affinity (Kuo *et al*., 2008). Anthonisen *et al*. (2010) established a link between *O*-GlcNAc modification and increased expression of lipogenic enzymes. Hepatic energy production is also compromised since *O*-GlcNAcylation of mitochondrial proteins alters membrane potential and other mitochondrial parameters (Banerjee *et al*., 2015).

Besides its effects on hepatic metabolism and insulin sensitivity, *O*-GlcNAcylation is also associated with various other cardio-metabolic perturbations. For example, there is robust evidence from animal and cell culture studies that *O*-GlcNAc modification also induce peripheral insulin resistance (skeletal muscle and adipose tissue) (reviewed by Vaidyanathan & Wells, 2014). Moreover, insulin synthesis and secretion are also altered by the *O*-GlcNAcylation of two pancreatic transcription factors: pancreas homeobox protein 1 and neurogenic differentiation factor 1 (Andrali *et al*., 2007; Gao *et al*., 2003). In the cardiovascular system *O*-GlcNAcylation is associated with vascular occlusions and cardiomyocyte dysfunction (reviewed by Giacco & Brownlee, 2010). Greater *O*-GlcNAcylation is also linked to low grade inflammation through upregulation of the NFκB pathway, although it can exert anti-inflammatory properties in specific

contexts (Baudoin & Issad, 2015). Together, there is a growing collection of literature associating *O*-GlcNAc modification to the pathological patterns in gene expression observed in T2DM and other cardio-metabolic diseases. However, more research is necessary to fully understand the effects of *O*-GlcNAcylation on energy homeostasis and health in general.

4.1.2.4 Polyol pathway

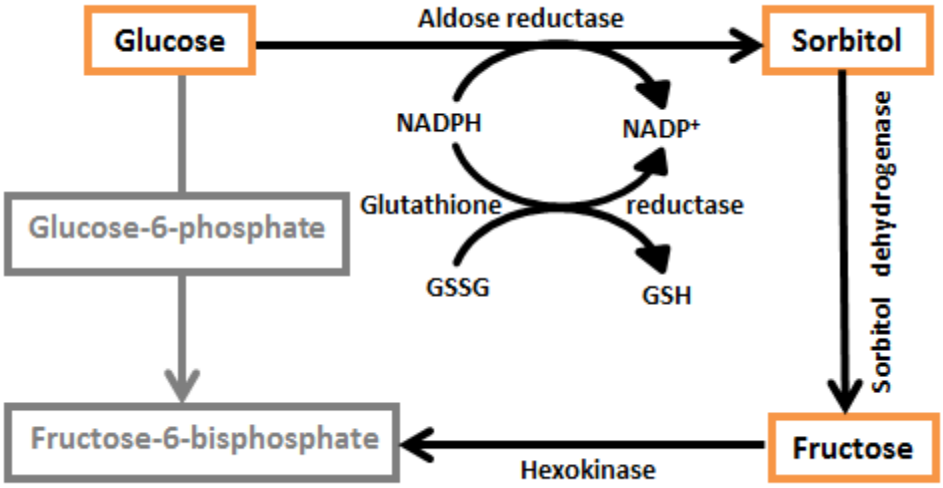

Figure 4.1.7: Two-phased polyol pathway. Adapted from Joseph, 2014.

The polyol pathway refers to the endogenous conversion of glucose to fructose in a two-step process (depicted in Figure 4.1.7). The first rate-limiting step in this pathway is catalyzed by aldose reductase (AR) and yields sorbitol that is in turn converted to fructose by sorbitol dehydrogenase (Giacco & Brownlee, 2010). The polyol pathway plays an important role in reducing toxic aldehydes in the cell to inactive alcohols. Under physiological conditions only ~3% of glucose enters this pathway, but under hyperglycemic conditions this can increase to > 30%. Such a high flux has detrimental consequences (reviewed by Tang *et al*., 2012).

Early studies show that a polyol flux exacerbates oxidative stress via three possible mechanisms. Firstly, AR requires NADPH as a cofactor to convert excess glucose to sorbitol. This leads to the depletion of intracellular NADPH and subsequently decrease the ability of the cell to regenerate an important antioxidant, i.e. reduced glutathione (Cheng & Gonzalez, 1986). The polyol pathway is also associated with increased ROS production. When sorbitol dehydrogenase converts sorbitol into fructose, NAD^+ is concomitantly converted to NADH that

serves as a co-factor for NOX. This allows increased NOX activity and therefore ROS production (Morre *et al*., 2000). Lastly, fructose can be converted to the powerful glycating agents fructose-3-phosphate and 3-deoxyglucosone, thereby increasing the synthesis of AGEs that worsens oxidative stress (Hamada *et al*.,1996).

More recently preclinical studies established an association between elevated polyol flux and cardio-metabolic diseases. For example, Lanaspa *et al*. (2013) observed that intrahepatic fructose production (via the polyol pathway) leads to the development of MetS and intrahepatic lipid deposition. Increased activity of the polyol pathway is also evident in a diabetic mouse model (MRK mice) (Gallagher *et al*., 2016) where such mice displayed a 2.5× increase in sorbitol levels in skeletal muscle together with a 1.7× decrease in reduced glutathione compared to wild-type mice. Increased polyol pathway activity is also robustly linked to diabetic complications (reviewed by Grewal *et al*., 2016). Another study found that genetically modified mice overexpressing human AR experienced cardiac dysfunction when aged (Son, 2012). They further showed that the overexpression of AR leads to worse outcomes after ischemia and reperfusion. Here they measured infarct area, percentage fractional shortening and the expression of acyl-CoA oxidase, pyruvate dehydrogenase kinase 4 and PPAR-α mRNA (genes involved in glucose and FA oxidation). Others found that AR expression influenced caspase-dependent apoptosis (Zhang *et al*., 2014). Moreover, excess sorbitol that is not converted to fructose can lead to osmotic stress and subsequent cell damage since cell membranes are impermeable to sorbitol (Behl *et al*., 2016). Together these data show that the polyol pathway (particularly AR activity) is an important factor in the onset of cardio-metabolism diseasesand that the clinical usage of AR inhibitors may offer therapeutic potential in this regard.

4.1.3 Meta-inflammation

Meta-inflammation (MI) refers to a low-grade inflammatory response that is triggered by metabolic damage associated molecular patterns and is implicated in the development of cardio-metabolic diseases (refer Figure 4.1.8) (Kitamura *et al*., 2013). MI is different from classic inflammation in various ways, e.g. the latter is generally an acute, local response while MI is systemic and chronic. MI leads to the infiltration of macrophages and cytotoxic T-lymphocytes into insulin-dependent tissues specifically, but does not cause structural and functional damage to the infiltrated tissue as with the classic response. Another hallmark of MI is a high level of circulating pro-inflammatory cytokines like TNF-α, ROS and IL-6 (reviewed by León-Pedroza, 2015). The ER overload response (discussed in section 3.4) might be a

possible cause or consequence of MI as similar signaling pathways are involved. In the light of that, this section will provide a brief overview of MI.

Early experimental work indicated an association between metabolic conditions and inflammation. For example, the pro-inflammatory cytokine TNF-α is overexpressed in an obese rodent model as well as in an obese clinical cohort (Hotamisligil, 2006). A possible explanation may be that systemic MI sprouts from inflammation triggered in visceral adipose tissue (Murano *et al*., 2008). As visceral fat increases due to unhealthy dietary choices, some adipocytes may become more distally located from the nearest blood vessel as a result of adipose hypertrophy and hyperplasia. This can lead to a hypoxic state that will result in adipocyte necrosis if prolonged. An inflammatory response is initiated as phagocytes infiltrate such tissues in order to remove necrotic cells. Immune cells infiltrating such tissues are also a source of pro-inflammatory cytokines - thus there is a continuous signal for further tissue infiltration. Moreover, adipocyte hypertrophy and hyperplasia are associated with ROS generation that can, in turn, lead to an elevation in TNF-α and leptin levels (Murano *et al*., 2008).

Perturbations in metabolic homeostasis e.g. hyperglycemia can induce a chronic low-grade inflammatory response by releasing metabolic damage associated molecular patterns that bind to toll-like receptors on membranes of immune cells (Lemaitre, 2008). For example, AGEs can bind to the toll-like receptor 4 on macrophages to initiate a pro-inflammatory signaling cascade. Here the translocation of NF-κB to the nucleus is central to this response as it promotes the transcription of pro-inflammatory factors. Such immune cells ultimately migrate to insulin-dependent tissues, thereby spreading the inflammatory state (reviewed by León-Pedroza, 2015). Besides AGEs, other NOGPs like PKC and the HBP can also play a role in MI onset and perpetuation (Baudoin & Issad, 2015; Butcher & Galkina, 2013)

MI contributes to the onset and progression of T2DM through several mechanisms. TNF-α interferes with the insulin signaling pathway by inhibiting the activity of IRS, Akt or GLUT2/4 via various intracellular pathways such as JNK and NF-κB (refer to the ER overload response in section 3.4) to cause insulin resistance (Hotamisligil *et al*., 1993; Uysal *et al*., 1997). Obese mice that lack TNF-α (whole body knock-out) are protected from developing insulin resistance (Uysal *et al*., 1997). MI also plays a role in β-cell injury as T2DM worsens. Here the islets of Langerhans become inflamed thus inducing insulitis – a condition that can cause an excessive release of pro-inflammatory factors such as TNF-α, IL-6, IL-8 and macrophage chemo-attractive

protein. Besides T2DM, MI is also associated with hypertension and atherosclerosis (reviewed by León-Pedroza, 2015, Schwartz & Reaven, 2006).

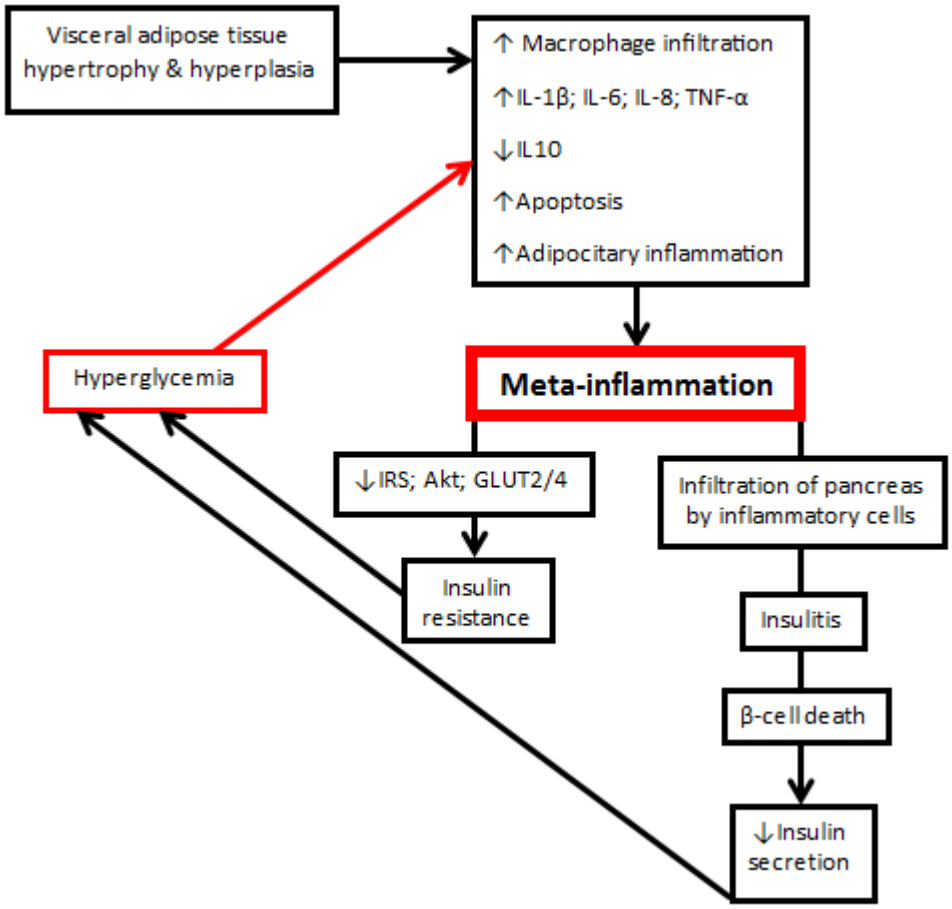

Figure 4.1.8: The onset and perpetuation of meta-inflammation and its role in cardio-metabolic diseases. Adapted from León-Pedroza, 2015.

4.2 Materials and Methods

4.2.1 Oxidative stress analyses

Oxidative stress is one of the possible causes of ER stress (refer to section 3.4). We investigated various markers of oxidative stress in the hope to corroborate that oxidative stress is the underlying mechanism driving ER stress in this model as it seem the most probable in the context of SSB consumption. All oxidative stress analyses were performed in collaboration with

Dr. Dirk Bester at the Oxidative Stress Research Unit, Cape Peninsula University of Technology.

4.2.1.1 Glutathione redox analysis

This protocol was adapted from Asensi *et al*. (1999). In brief a tissue homogenizer (ProScientific Pro200 homogenizer, Oxford, CT) was used to homogenize liver samples (~200 µg) on ice in 2mL Buffer A (50 mM $NaPO_4$, 1 mM EDTA, pH 7.5). For GSSG analysis an additional 10 µL 1-methyl-2-vinyl-pyridinium trifluoromethane sulfonate (30 mM in 0.1 M hydrochloric acid) was added to every 1 mL Buffer A. Thus reduced (GSH) and oxidized (GSSG) samples were prepared separately. Samples were centrifuged (Boeco M240, Boeco, Hamburg, Germany) at 15, 000 × g for 5 min and the supernatants were diluted (10–40×) and used for analysis. A standard curve was prepared using GSH (3 µM) and GSSG (1.5 µM)] stock solutions and Buffer A. All other reagents were also made up in Buffer A. 50 µL of each standard and sample (each in triplicate) were added to the microtiter plate. Next, a multi-pipette (Multichannel Research, Eppendorf, Hamburg, Germany) was used to add 50 µL 0.3 mM 5,5'Dithiobis-(2-nitrobenzoic acid) to each well followed by 50 µL glutathione reductases (0.02U/µL). The plate was incubated for 5 min at room temperature after which 50 µL NADPH (1mM) was added to each well. The absorbance was measured directly afterwards using a Multiskan spectrum platereader (Thermo Electron corporation, Waltham, MA) that was programmed to obtain a reading every 30 sec for a total period of 5 min.

For systemic glutathione redox analysis, EDTA whole blood (BD, Franklin Lakes, New Jersey). was used. Here 5% metaphosphoric acid was added to the samples in a 1:4 ratio whereafter samples were vortexed for 20 sec (DragonLab Mx-S, Dragon Laboratory Instruments, Beijing, China) and centrifuged at 10, 000 × g for 10 min. The supernatant was further diluted with Buffer A and 50 µL was loaded as the sample in the microtiter plate.

4.2.1.2 Oxygen radical absorbance capacity (ORAC)

Liver samples were homogenized in Buffer A as described above. Thereafter it was centrifuged at 12, 000 × g for 10 min (Boeco M240, Boeco, Hamburg, Germany). The supernatant was collected and deproteinized by centrifuging 50 µL of 0.25 M perchloric acid (PCA) and 50 µL supernatant together at 14, 000 × g for 15 min. The resultant supernatants were diluted (2-4×) and 12 µL were added to a black 96-well plate. Of note, all samples should be loaded in triplicate and the first two and last columns of the plate should not be used. A trolox stock

solution (500 µM) is used for a standard series with final concentrations 0, 83, 167, 250, 333 and 417 µM. 12 µL of the standard series was added to the appropriate wells. Next, 138 µL of fluorescein (working solution) was added to each well using a multi-pipette (Multichannel Research, Eppendorf, Hamburg, Germany). The last step was to add 50 µL (25 mg/mL) 2,2'-Azobis (2-methylpropionamidine) dihydrchloride to each well after which the plate was read on a Fluoroskan ascentfluorometer (Thermo Electron Corporation, Waltham, MA) - readings were taken every min for 2 hr.

Blood samples was collected in EDTA vacutainers (Guangzhou Improve Medical Instruments, Guangzhou, China) and centrifuged (Spectrafuge™ 16M, Labnet, Edison NJ) at 1, 300 × g for 30 min to collect the plasma. The plasma (50 µL) was subsequently treated with 50 µL 0.5 M PCA, thereafter the same steps as in the case of tissues were followed. This protocol was adapted from Prior *et al*., (2003) and Cao & Prior (1998).

4.2.1.3 Thiobarbituric acid reactive substances (TBARS)

Liver samples were homogenized in Buffer A as in previous experiments. The supernatant (50 µL) was vortexed (DragonLab Mx-S, Dragon Laboratory Instruments, Beijing, China) together with 6.25 µL butylated hydroxytoluene (4mM in ethanol) and 50 µL ortho-phosporic acid (0.2M). TBA reagent (6.25 µL; 0.11M in 0.1M NaOH) was added and the samples were vortexed again for 10 sec. The samples were placed in a heating bath for 45 minutes at 90°C followed by 2 min on ice and 5 min at room temperature. N-Butanol (500 µL) and saturated NaCl (50 µL) were added to each sample before another 10 sec bout of vortex. Samples were centrifuged (Boeco M240, Boeco, Hamburg, Germany) at 13, 700 × g for 2 min and 300 µL of the top phase were added to the wells. The plate was read at A532-A572. Systemic TBARS were measured by using 50 µL plasma instead of 50 µL homogenate supernatant.

4.2.1.4 Conjugated dienes (CDs)

Liver samples (~100 µg) were homogenized in 2 mL methanol and 1 mL chloroform was added to the lysates. Lysates were vortexed briefly (DragonLab Mx-S, Dragon Laboratory Instruments, Beijing, China) before it was centrifuged (Eppendorf 5810R, Eppendorf, Hamburg, Germany) at 3, 000 × g for 1 min to allow for separation. Of note, for samples that did not separate 100 µL saturated NaCl was added and the samples were re-centrifuged. The bottom layer of the samples were pipetted into fresh microtubes and left open overnight at 4°C to dry out. On the second day 700 µL cyclohexane was added to each of the microtubes which were then

vortexed. Subsequently, 200 µL of sample was added to a 96-well plate that was read in a plate reader (Multiskan spectrum, Thermo Electron corporation, Waltham, MA) . Cyclohexane was used as a blank and all samples were assayed in triplicate.

Plasma assays were done in a similar fashion; however here the initial phase of sample preparation entailed 100 µL plasma in 405 µL methanol and chloroform in a 2:1 ratio.

4.2.2 NOGP analyses

4.2.2.1 AGE

To determine the level of AGEs in the liver samples the OxiSelect™ AGE Competitive ELISA kit (Cell Biolabs, San Diego CA) was used and executed according to the protocol provided. The kit determines the quantity of the AGE proteins in the samples by comparing it to an AGE-bovine serum albumin (BSA) standard curve. A 96-well plate was incubated overnight at 4°C with an AGE conjugate coating. On the second day the plate was blocked for an hour at room temperature before 50 µL the sample/standard are added to the wells. Each sample/standard was assayed in duplicate. The samples were incubated in the wells for 10 min on a belly dancer (Stovall Life Science, Greensboro, NC) and then anti-AGE antibody was added to each well. After incubation (1 hr at room temperature), the contents of the wells were removed and 100 µL diluted secondary antibody-HRP was added to each well. Of note, the wells were washed with a wash buffer between steps. After a final incubation step, the substrate solution was added and time was allowed for color development before (~10 min) the reaction was terminated with the stop solution. A microplate reader (El 800 KC Junior Universal Microplate reader, Bio-Tek Instruments, Winooski VT) was used to read the absorbance at 450 nm.

4.2.2.2 PKCβII and O-GlcNAc

PKCβII and *O*-GlcNAc expression were determined using standard Western blotting techniques as described before (Joseph *et al*., 2014; Mapanga *et al*., 2012). Here the first step was protein extraction, i.e. liver samples (~100 µg) were placed in 2 mL microtubes with 1 mL radio immune precipitation buffer (RIPA buffer) and homogenized (Polytron PT2100, Kinematica, Luzern, Switserland) in 15 sec bouts until all of the tissue was disrupted. RIPA buffer contained protease inhibitors (pepstatin [10 µg/ml], leupeptin [1 µg/ml], apoprotein [1 µg/ml] and phenylmethylsulfonyl fluoride [1 mM]), phosphatase inhibitors (activated Na_3VO_4 [1 mM], NaF [1mM]) and a trypsin inhibitor (benzamidine [1 µg/ml]). The *O*-GlcNAc extractions also

contained Pugnac (1 μM) to prevent the removal of *O*-GlcNAc modifications. The samples were kept on ice throughout the entire procedure. The homogenates were centrifuged (Spectrafuge™ 16M, Labnet, Edison NJ) at 14, 000 × g for 10 min (4°C) and the supernatants (lysate) were collected and stored at -80°C.

Next the protein concentration was determined using the Direct Detect® Infrared Spectrometer (Merck KGaA, Darmstadt, Germany) with RIPA buffer as a blank. Here 2 μL lysate is added to the wells on cards (provided) that slot into the machine. After a drying cycle the amide bonds in protein chains are measured to determine protein concentration. Samples were prepared by diluting the determined amount of lysate in RIPA and Laemmli sample buffers. Thereafter the samples were boiled for 5 min at 95°C and vortexed briefly (Scientific industries, Bohemia NY). Finally the samples were centrifuged at 14, 000 × g for 10 sec (Spectrafuge™ 24D, Labnet, Edison NJ) and stored at -20^{o}C for future use.

The samples were separated by gel electrophoresis at 100 V (~90 min). Here polyacrylamide gels were cast in accordance with the protocol recommended by the Tris-glycine extended Stain-Free™ FastCast™ Acrylamide Kit, 10% #161-0183 (BIO-RAD, Hercules CA). The Transfer Blot (Trans-Blot® Turbo™, transfer system, BIO-RAD, Hercules CA) was used to transfer gels unto polyvinylidine fluoride membranes (BIO-RRAD pre-defined 7 min, mixed molecular weight protocol). Membranes were soaked in methanol for 30 sec and left to dry completely. For *O*-GlcNAc membranes were blocked in 5% BSA prepared in Tris-buffered saline and Tween 20 (TBS-T) for 20 min and then incubated overnight in primary *O*-GlcNAc antibody (CTD110.6, Santa Cruz Biotechnology, Santa Cruz CA) diluted in TBS-T (1:500) at 4°C. On the second day, it was incubated for an hour in secondary anti-mouse HRP-linked antibody (Cell Signaling Technology®, Danvers MA) (also diluted in TBS-T [1:2000]) at room temperature. For PKCβII, membranes were blocked for an hour in 5% fat free milk and probed with a primary PKCβII antibody (Abcam, Cambridge MA) prepared in 5% BSA (1:1000) followed by incubation in secondary HRP-conjugated anti-rabbit antibody (Cell Signaling Technology®, Danvers MA) (1:4000 in TBS-T). After every step, the membranes were washed for 3 × 5 minutes in TBS-T. Finally, 600 μL ECL (BIO-RAD, Hercules CA) was squirted over the membrane to allow imaging of protein bands. All Western blots were imaged with Image Lab™ Software version 4.0 (BIO-RAD, Hercules CA) and total protein was used for normalization.

4.2.2.3 Polyol Pathway

D-sorbitol is an intermediate of the polyol pathway and can be used as a marker for activation of this pathway; hence a colorimetric D-sorbitol assay kit (Abcam, Global Biotech Company, San Francisco CA) was used. Here a sorbitol standard was serially diluted to generate a standard curve. The standard and the samples (50 µL) - prepared in accordance with the kit's instruction manual - were then added (in duplicate) to a 96-well plate. A reaction mixture containing assay buffer, enzyme mix, developer and a probe was prepared and 50 µL was added to each well. After an incubation period of 60 min at 37°C the absorbance was measured at 560 nm on a microplate reader (El 800 KC Junior Universal Microplate reader, Bio-Tek Instruments, Winooski VT).

4.2.3 Inflammation and stress signaling

TNF-α and IκB were selected as markers for inflammation and stress signaling as it would indicate whether the ER overload response has been initiated in this model. Western blotting techniques as described in the previous sections were used to measure the expression of both markers. Both sets of membranes were blocked in 5% BSA before overnight incubation with the respective primary antibody. The specific antibodies used were anti-TNF-α (Abcam, Cambridge MA) and IκB-α antibody (Cell Signaling Technology®, Danvers MA) diluted 1:1000 in TBS-T, both paired with secondary HRP-conjugated anti-rabbit antibody (Cell Signaling Technology®, Danvers MA) (1:4000 in TBS-T). For a detailed protocol refer to Appendix C.

4.2.4 Histology

Based on the proteomic data we were interested to see whether SSB consumption led to the deposition of lipid droplets in the liver. Unfortunately, we could not use standard staining techniques for lipid detection such as Oill-Red-O or SudanIV due to the lack of frozen tissues. Instead we hoped to identify lipid droplets on Hematoxylin and Eosin (H & E) stained sections based on morphological characteristics. These data will be combined with previously collected data to gain a better understanding of SSB induced perturbations in lipid metabolism. An H & E stain Iso allows the detection of other structural changes. ER stress has also been linked to tissue fibrosis (Lenna & Trojanowska, 2012; Tanjore *et al*., 2013). In the light of this a Masson's Trichrome stain was performed.

All histological staining techniques were performed by Mr. Reggie Williams (Technical Supervisor, Department of Anatomical Pathology, Faculty of Medicine and Health Sciences, Stellenbosch University) The liver samples were fixed in formalin and embedded (Leica EG1160 embedding center, Wetzlar, Germany) in paraffin before transverse sectioning (Leica RM2125 RTS microtome, Wetzlar, Germany). The tissue slides were stained with H & E and Masson's Trichrome stains (refer below) to allow for qualitative evaluation of hepatic histology. A Nikon microscope (Nikon Eclipes E400, Tokyo Japan) was used at 10× and 40× magnification to examine the slides and images were created with NIS Elements (Imaging software version 4.10, Tokyo Japan).

4.2.4.1 H & E

Slides were de-paraffinized (two changes of xylene, 5 min each) and hydrated (two changes of 100% alcohol, 5 min each). Thereafter the slides were placed in 95% alcohol (2 min) and 70% alcohol (2 min) before being briefly rinsed in distilled water (dH_2O). Slides were stained in Mayer hematoxylin (Science World, Vancouver, BC) solution (8 min) and washed in warm tap water for 10 min. Next the slides were rinsed in dH_2O and 95% alcohol, 10 dips each. Eosin-phloxine B solution (Science World, Vancouver, BC) was used to counterstain the slides for 30 sec before dehydration steps were followed (95% and two changes of 100 % alcohol, 5 min each). Slides were cleared in two changes of xylene (5 min each) and mounted with a xylene-based mounting medium (Science World, Vancouver, BC) (Avwioro, 2011).

4.2.4.2 Masson's Trichome

Slides were de-paraffinized and hydrated with dH_2O (as described above) before rinsed (in dH_2O) and stained with hematoxylin for 5 min. Running tap water was used to wash the slides until it turned dark blue (~3 min) whereafter it was rinsed in dH_2O. Slides were stained in filtered with Fuschsin Ponceau Orange G stock solution (Sigma-Aldrich, St. Louis, MO) for ~15 min and rinsed with acetic acid water. This was followed by a 5 min mordant step in 5% phosphotungstic acid before staining in light green solution (Kimix Chemicals, Cape Town, South Africa) for ~20 min. Slides were placed in acetic acid water for 5 min. Finally slides were dehydrated with alcohol, cleared in xylene and mounted in DPX mountant (Science World, Vancouver, BC).

4.2.5 Statistical analysis

Statistica 13.0 (StatSoft Inc., Dell Software, Tulsa, OK) was used for statistical analyses. The differences between the experimental groups of normally distributed data were evaluated with one-way ANOVAs and non-parametric data was tested with Kruskal-Wallis ANOVA and median tests. A p-value < 0.05 was considered to be significant. Outliers and extremes were detected using box plots with an outlier coefficient of 2.2 and Levene's tests were used to test for homogeneity of variances. All the data are presented on Graphpad Prism 5.01 (Graphpad Software Inc., San Diego CA) as mean ± SD.

4.3 Results

4.3.1 Oxidative stress

ROS production (especially mitochondrial-derived) can be induced by energy-imbalance and hyperglycemia. The rise in ROS levels can lead to oxidative stress and subsequent molecular damage. A combination of assays that measured antioxidant defense systems and markers for ROS-induced damage were used to determine both systemic and hepatic oxidative states.

4.3.1.1 Glutathione redox analysis

Reduced glutathione is an important scavenger of ROS molecules and its ratio to oxidized glutathione is an indicator of the oxidative state of the sample. A decrease in this ratio would be a sign of increased oxidative stress.

No significant changes were found in liver samples at three months (Figure 4.3.1). However, at six months the SSB group exhibited an increase compared to the Control group ($P < 0.05$). This increase is also found in relation to the Cal-control group, although it is not statistically significant. No significant changes were detected for plasma samples between any of the groups at three or six months.

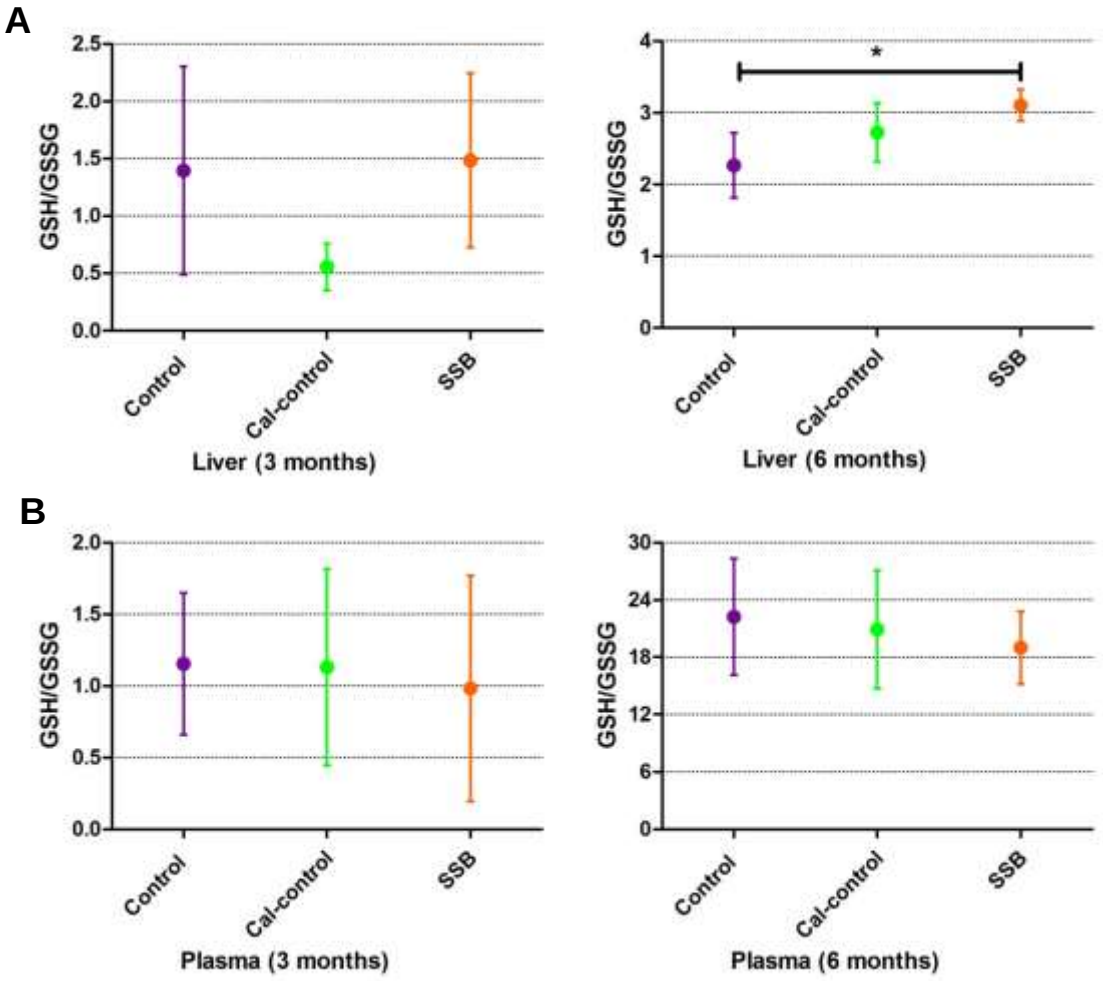

Figure 4.3.1: Oxidative state evaluated by reduced to oxidized glutathione in liver (A) and plasma (B) samples. N ≥ 5 for all groups (liver and plasma). Data are displayed as mean ± SD and significance is shown as * P < 0.05.

4.3.1.2 ORAC

This experiment measured the capacity of the tissue or system (blood samples) to absorb ROS as a defense mechanism against ROS-induced tissue damage. This is achieved by determining the rate of oxidative breakdown of fluorescein (fluorescent molecule). The SSB treatment did not alter the absorbance capacity of the SSB group compared to any of the controls in the liver or plasma at either of the time points (Figure 4.3.2).

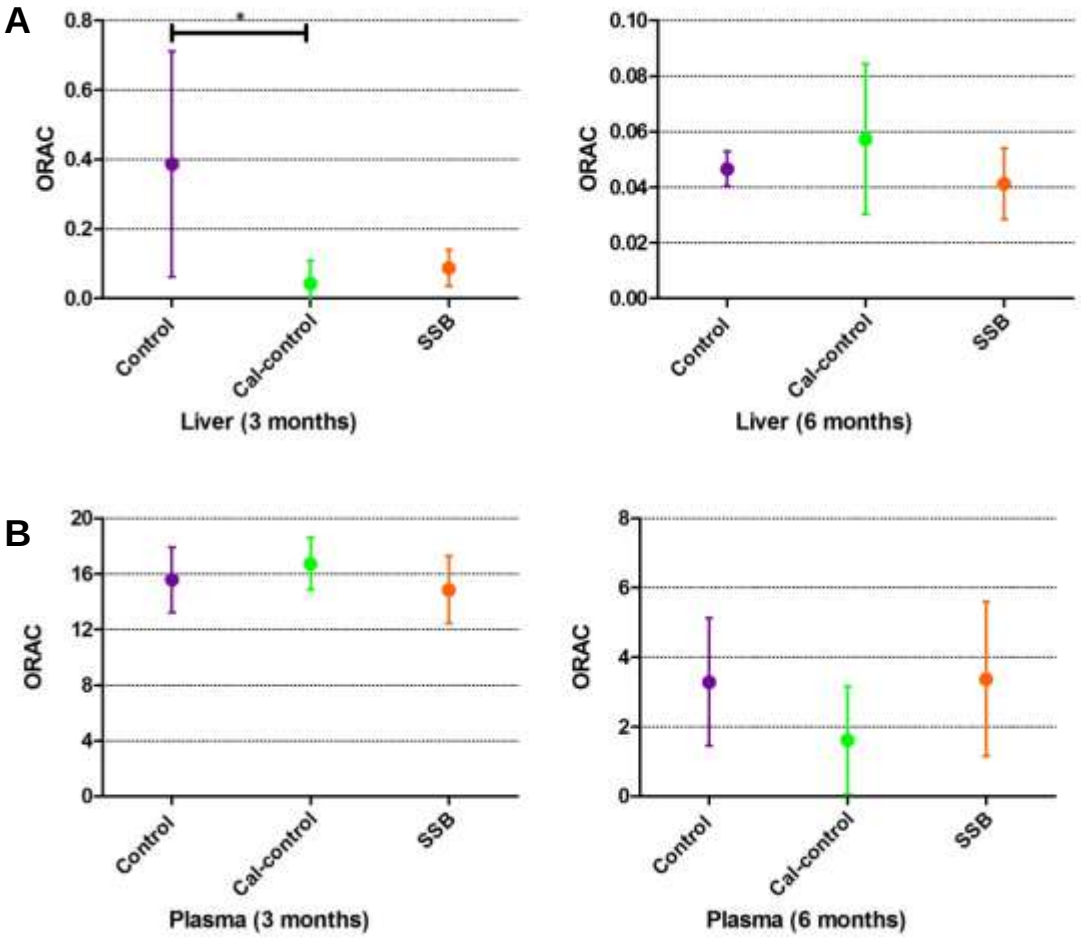

Figure 4.3.2: Tissue-specific (A) and systemic (B) ORAC. N ≥ 5 for all groups. Data are displayed as mean ± SD and significance is shown as * P < 0.05.

4.3.1.3 TBARS

Malondialdehyde (MDA), a product of lipid peroxidation, was measured by using a TBARS assay. SSB consumption did not induce any significant changes in MDA levels in the liver samples at three or six months (Figure 4.3.3). However, plasma samples showed a different trend:after three months MDA levels in both the SSB and Control group were increased compared to the Cal-control group ($P < 0.05$ and $P < 0.005$, respectively) but by six months this change was no longer detected. MDA is only a good marker if a substantial amount of lipid peroxidation has occurred. For this reason we also measured CD levels that will allow the detection of early phases of lipid peroxidation.

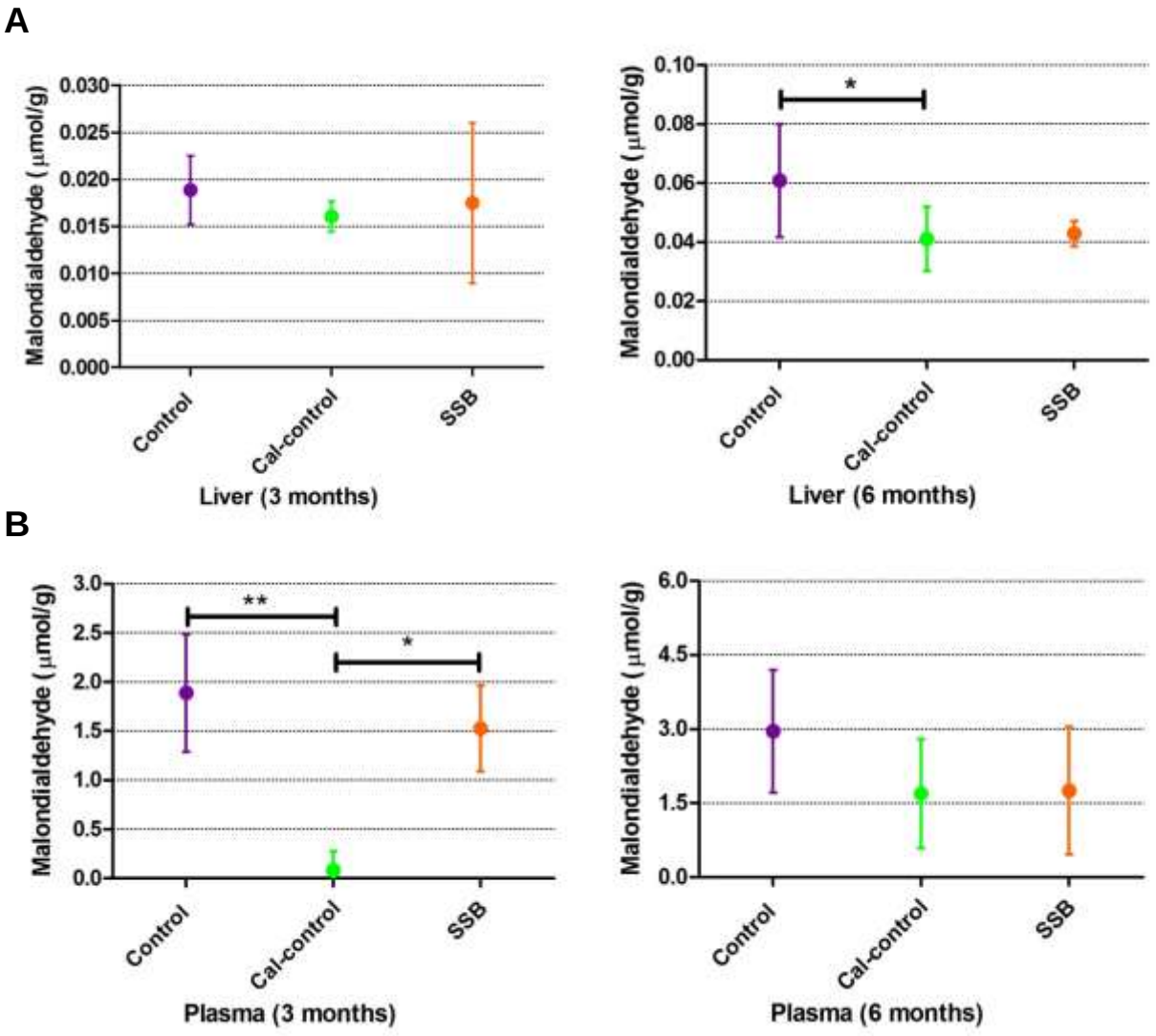

Figure 4.3.3: MDA levels as an indicator of lipid peroxidation. N ≥ 5 for all groups. Data are displayed as mean ± SD and significance is shown as * $P < 0.05$, **$P < 0.005$.

4.3.1.4 CDs

CDs serve as an early marker for lipid peroxidation. No changes were detected in the liver or blood samples at either of the time points, indicating that there was no ROS-induced lipid damage in our model (Figure 4.3.4).

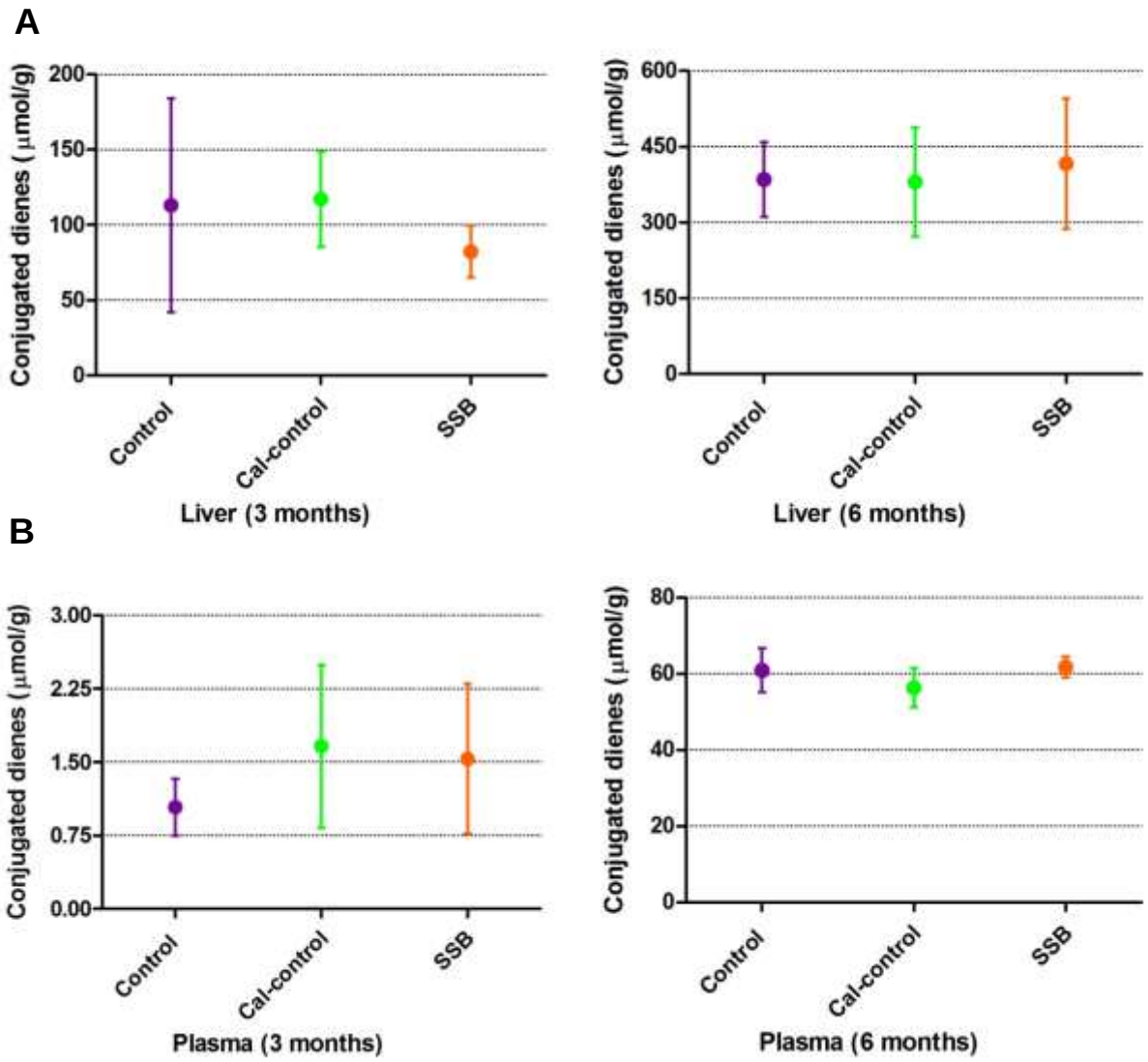

Figure 4.3.4: Early lipid peroxidation evaluated by changes in CD levels. CD levels were measured in (A) the liver and (B) the plasma. N ≥ 5 for all the groups. Data are displayed as mean ± SD.

4.3.2 NOGP analyses

Based on the proteomic analysis and established literature we suspected that moderate SSB intake may suppress glycolysis. This would cause glycolytic intermediates to shunt into the NOPGs that are linked to insulin resistance, exacerbated oxidative stress, inflammation and diabetic complications. NOGPs are the umbrella term that generally refers to the polyol pathway, the HBP, PKC activation and AGE formation. We expected to observe a significant increase in these pathways.

4.3.2.1 AGE

A commercial enzyme-linked immunosorbent assay kit was used to detect and measure AGE protein adducts in order to determine the effect of SSB consumption on AGE formation. Here an increase was observed in the SSB group compared to the Cal-control ($P < 0.05$) at three months (but not the Control group) and no changes were seen at the six-month time point (Figure 4.3.5).

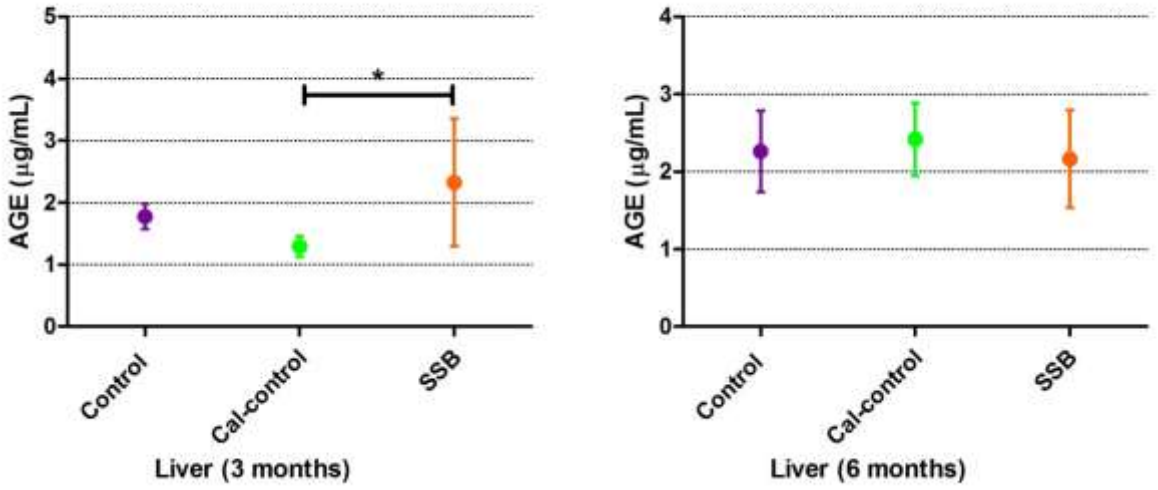

Figure 4.3.5: Quantification of AGE in liver samples. N ≥ 5 for all groups. Data are displayed as mean ± SD and significance is shown as * $P < 0.05$.

4.3.2.2 PKCβII and O-GlcNAc

Western blotting techniques were used to evaluate the relative protein expression of PKCβII, an isoform implicated in cardio-metabolic perturbations (Figure 4.3.6 A on the following page). At three months there were no significant differences between the SSB group and either of the control groups. At six months there was an increase in hepatic PKCβII expression in the SSB group compared to the Cal-control group ($P < 0.005$), but not the Control group. The degree of *O*-GlcNAcylated proteins was also determined as it is indicative of HPB activity. However, no significant differences were observed between any of the groups after three or six months (Figure 4.3.6 B).

4.3.2.3 Polyol pathway

D-sorbitol levels are indicative of polyol pathway activity and were therefore assessed by using a commercially-available kit. The results did not show any significant changes between the respective groups at three or six months (Figure 4.3.7).

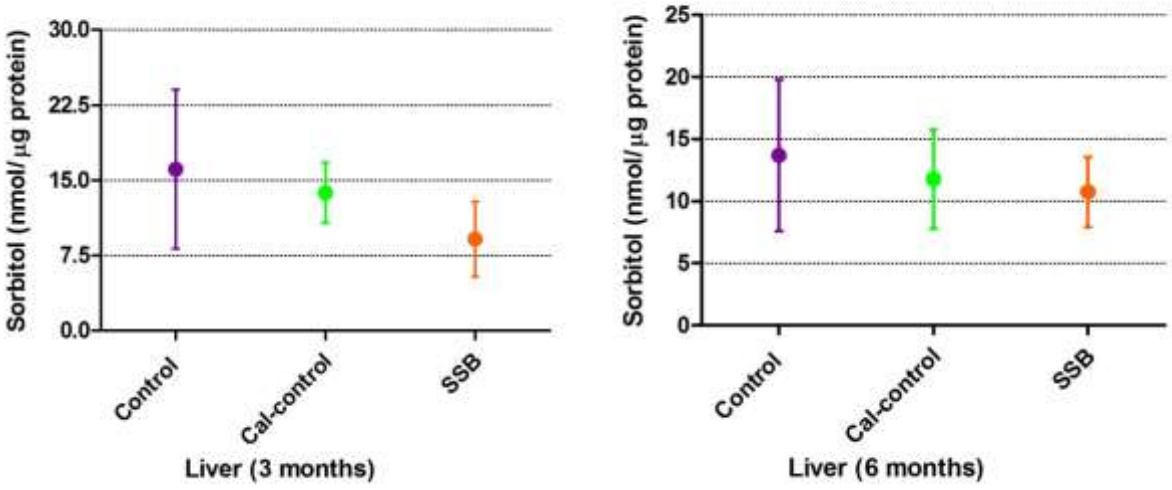

Figure 4.3.7: Measurement of D-sorbitol as a marker for polyol pathway activation. N ≥ 5 for all groups. Data are displayed as mean ± SD.

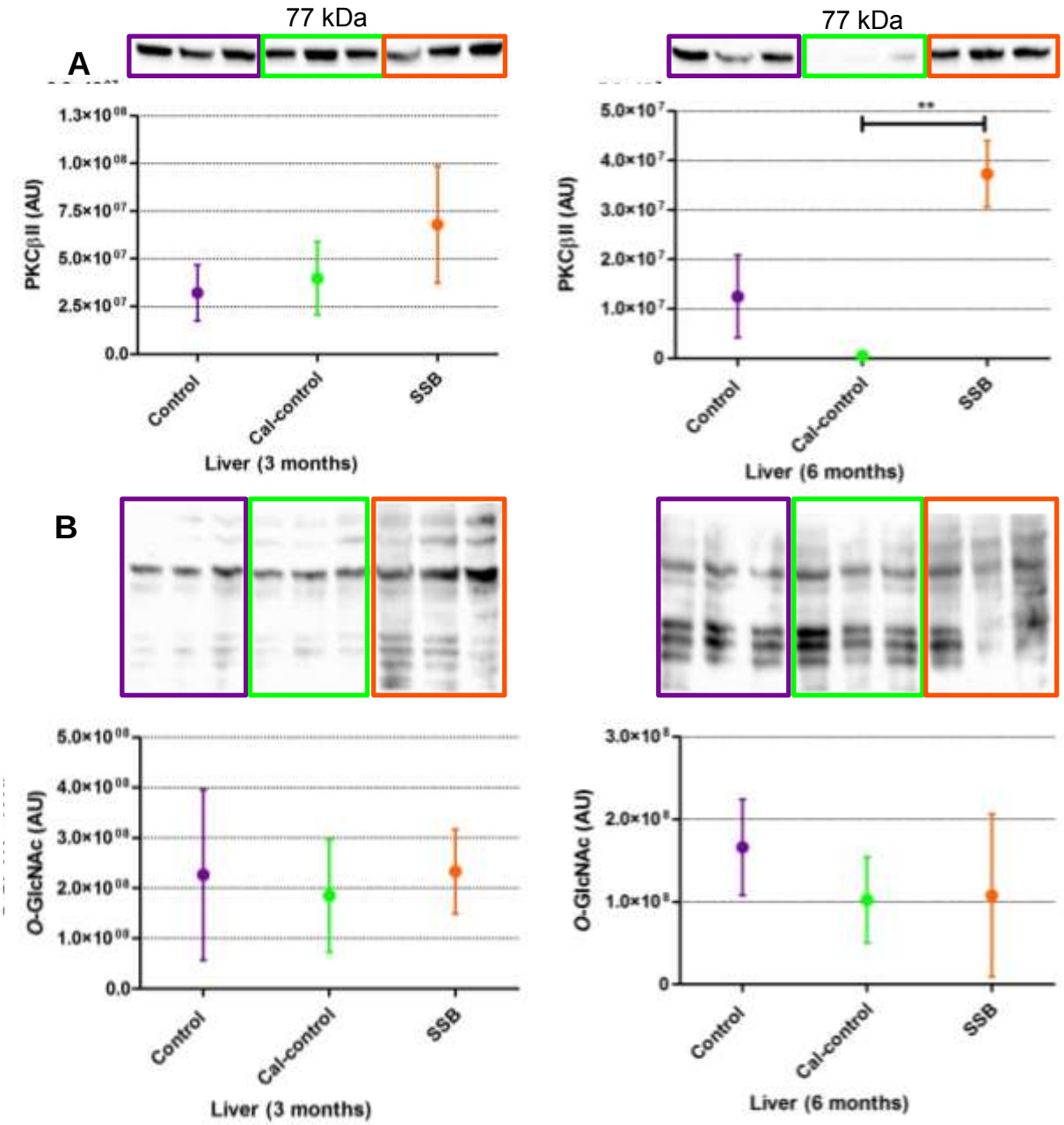

Figure 4.3.6: Evaluation of hepatic PKC expression (A) and *O*-GlcNAcylated proteins (B) N ≥ 5 for all groups. Total protein was used to normalize the data. Data are displayed as mean ± SD and significance is shown as **P < 0.005.

4.3.3 Inflammation

Western blotting techniques were used to evaluate the levels of hepatic TNF-α and IκB following SSB consumption. No changes were observed in TNF-α expression for any of the groups at three or six months. However, this was not the case for the IκB results. Although SSB

treatment did not trigger any significant changes, it is noteworthy that IκB levels in Cal-control samples (three and six months) are almost completely degraded compared to the Control ($P < 0.005$) and SSB ($P < 0.05$) groups, respectively (Figure 4.3.8)

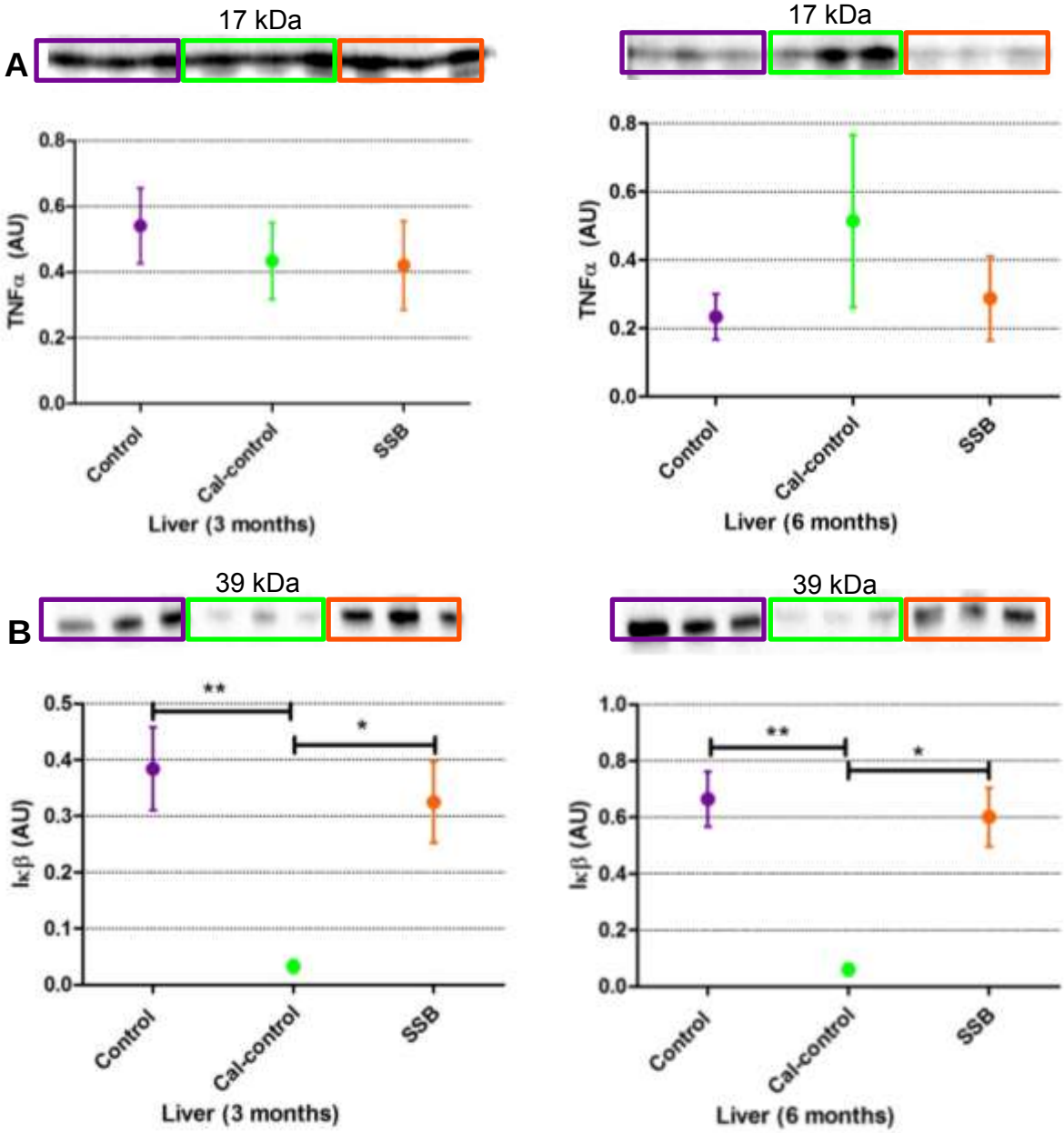

Figure 4.3.8: Assessment of inflammatory markers in livers of SSB-consuming rats. A – TNF-α with n ≥ 5 for all the groups; B - IκB where an n = 6 was employed for all groups. Total protein was used to normalize the data. Data are displayed as mean ± SD and significance is shown as * $P < 0.05$; ** $P < 0.005$.

4.3.4 Histology

4.3.4.1 H & E

H & E is considered the ‘’gold standard’’ histological stain to detect pathology. All basophilic structures in the cell such as cytoplasmic proteins stain pink with eosin, while acidic structures stain blue with hematoxylin. These include structures like the nuclei and ribosomes that contain large amounts of nucleic acids. In the figures (4.3.9 and 4.3.10) hepatic acini were identified by the presence of the portal tract (the cluster of the hepatic portal vein, hepatic artery and bile duct). The hepatocytes closest to the portal tract (zone 1) receives the most oxygenated blood and is the first to be exposed to the metabolites and absorbed from the gastrointestinal system into the portal track. These cells are thus primarily responsible for oxidative metabolic processes like oxidative phosphorylation and fatty acid β-oxidation. A low magnification (10×) was used to detect overall architectural changes in the liver although no significant changes were observed at any time point. We used a higher magnification (40×) to examine hepatocyte ultrastructure. Although some exhibited larger nuclei and other cells were binucleated, this reflects normal features of hepatocytes. The slightly granulated appearance of the cytoplasm is due to the presence of ribosomes (free and in the rough ER). Upon higher magnification the SSB and Cal-control hepatocytes (6 months) displayed intracellular unstained areas. This could possibly be washed out glycogen stores; however, the regular shape suggests that it is more likely accumulating lipid droplets. This was not observed in the Control group and thus likely represents a caloric-induced effect (analyses were guided by a Histology expert [Dr. C. Chase] and .Wheater’s Functional Histology, 2006).

4.3.4.2 Masson’s trichrome

A Masson’s trichrome stain is used to detect connective tissue and collagen. Here the collagen stains green, the nuclei black, the cytoplasm red and erythrocytes yellow to orange. The portal tract is surrounded by a framework of connective tissue. For our samples we did not detect abnormal amounts of collagen in any of the groups at three or six months (Figure 4.3.11 and 4.3.12). Although our model did not manifest any hepatic fibrosis it is arguable that the time period of the model was too short and that the SSB treatment could still cause fibrosis in the long-term.

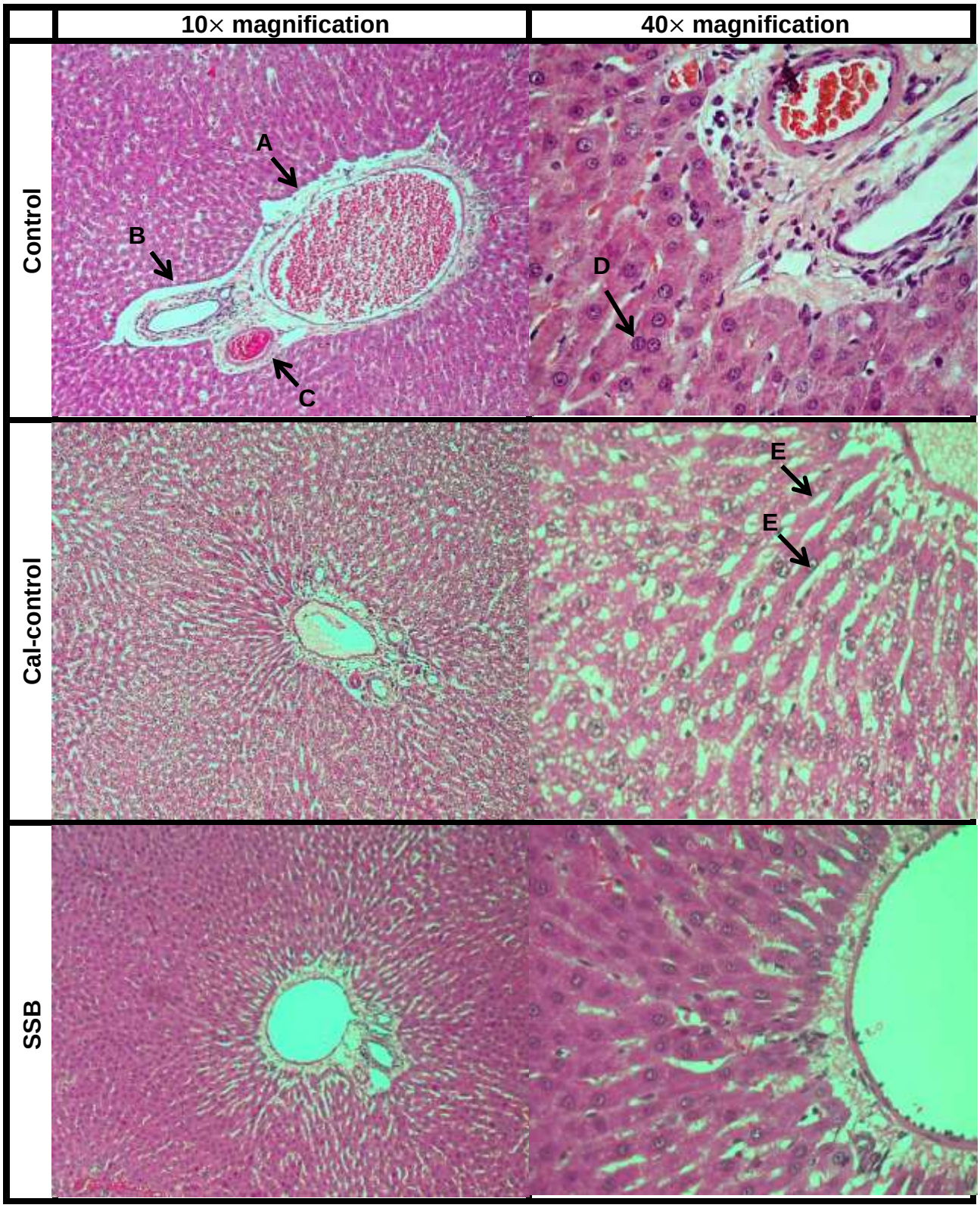

Figure 4.3.9: H&E stain of three-month liver samples. The hepatic portal tract is visible in each of the 10x magnification images. A - terminal portal venule, B – bile duct, C – hepatic artery, D – binucleated hepatocyte, E – Sinusoids. N = 3 for all groups.

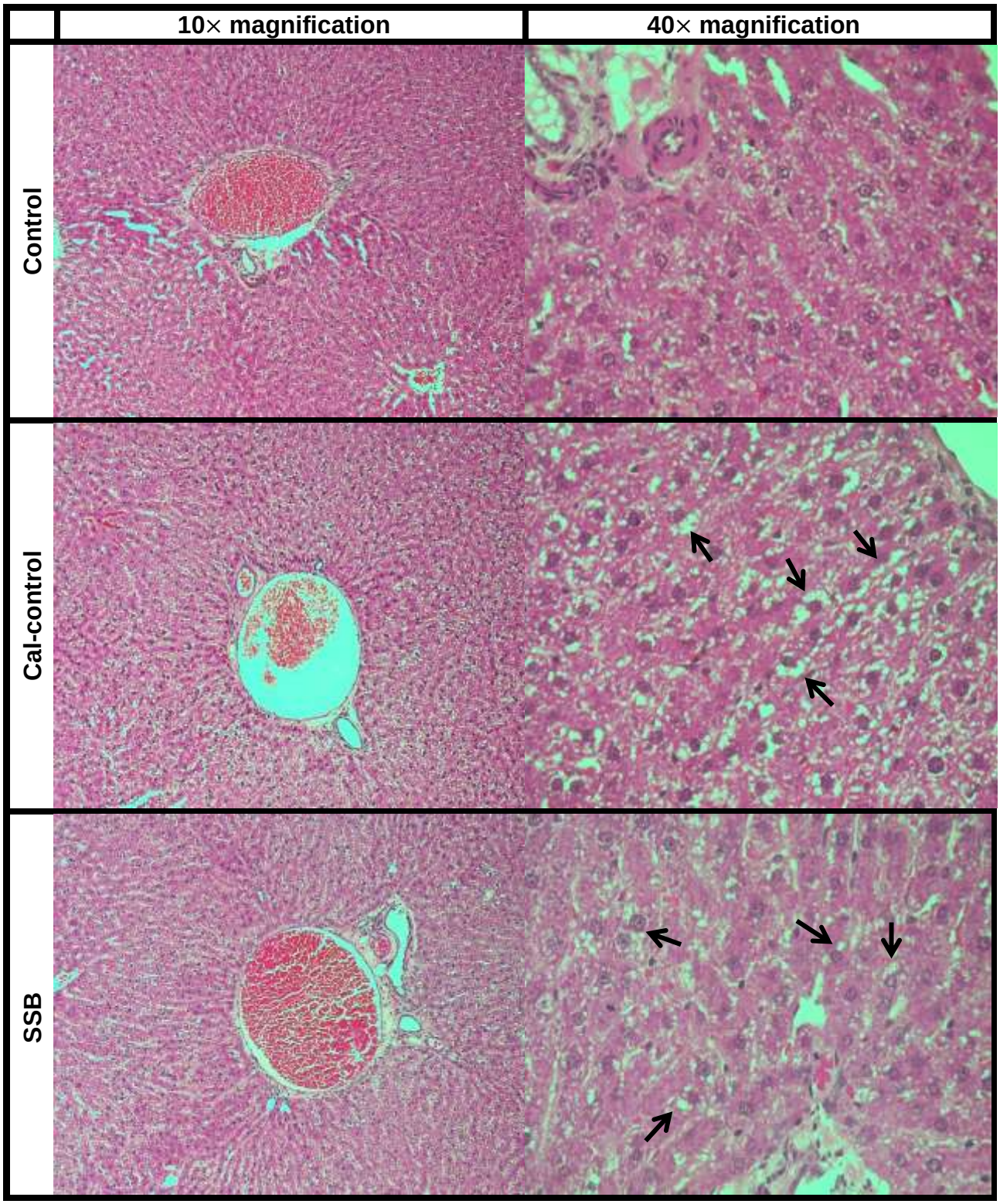

Figure 4.3.10: H&E stain of six-month liver samples. Arrows point to unstained areas in hepatocytes – putative lipid droplets. N = 3 per treatment group.

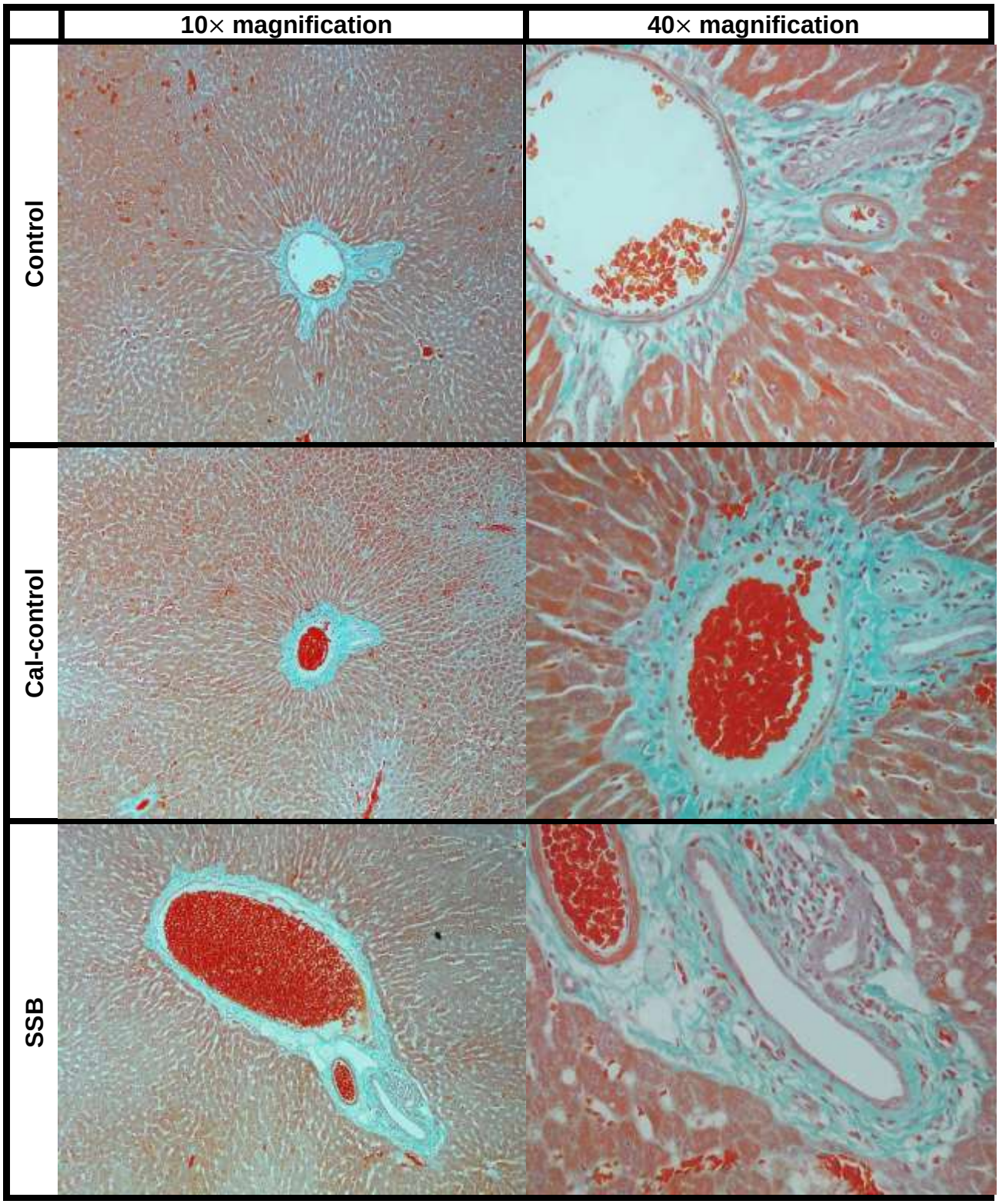

Figure 4.3.11: Masson's trichrome stain of three-month liver samples. The collagenous network surrounding the portal tract is clearly visible. No inappropriate fibrosis is observed in any of the samples. N = 3 for all groups.

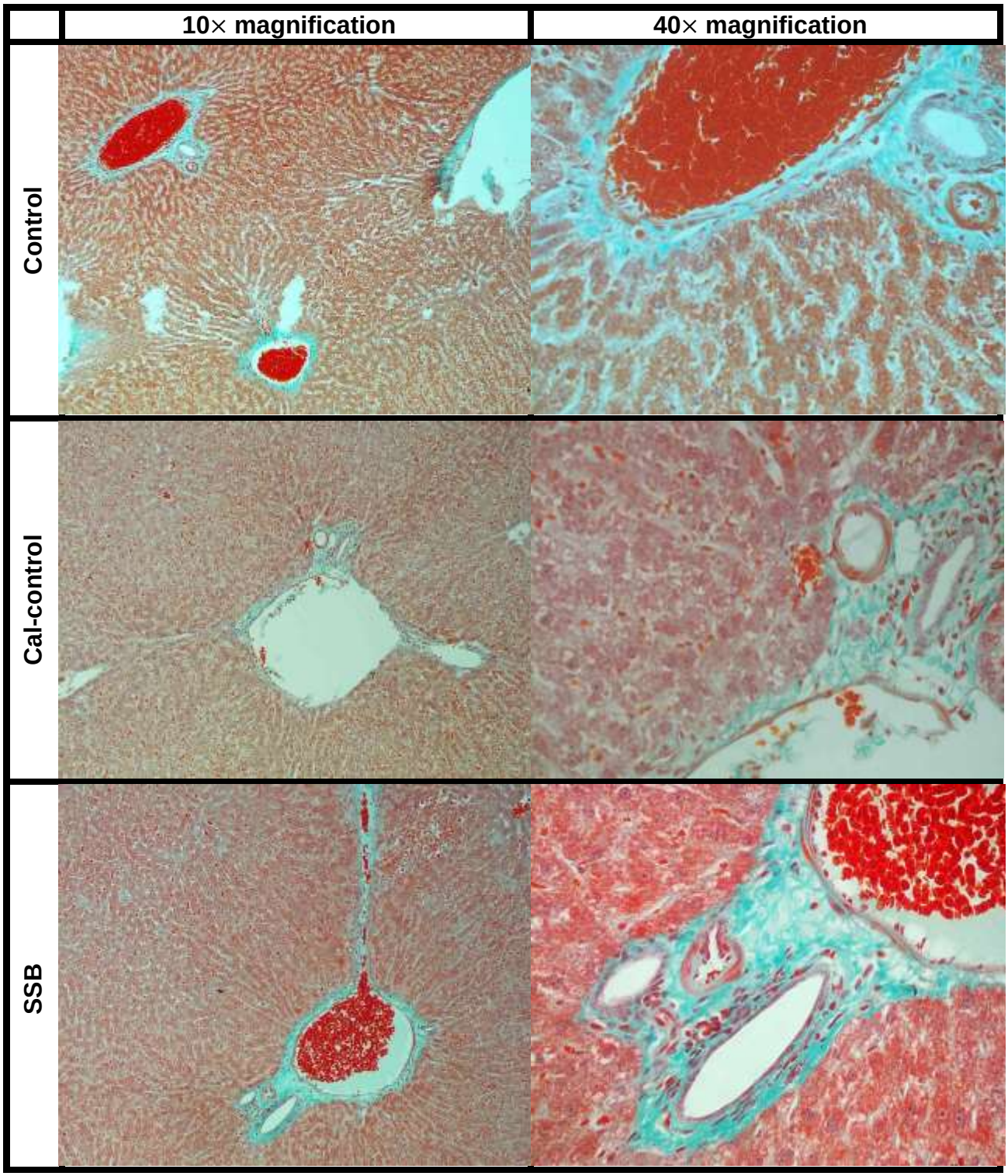

Figure 4.3.12: Masson's trichrome stain of six-month liver samples. At six months there is still no signs of liver fibrosis in any of the groups (n = 3).

4.4 Discussion

We evaluated systemic and hepatic oxidative stress markers to determine whether it could be one of the underlying causes of ER stress in our model. Here four different tests were considered and on the whole SSB intake did not increase either systemic or hepatic oxidative stress. Lozano *et al*. (2016) found similar results after rats consumed 25% fructose water for eight months. In this instance *in situ* ROS production was detected with fluorescent dihydroethidine dye in liver sections, while lipid peroxidation was measured with a TBARS kit in tissue homogenates while systemic oxidative stress was determined using a total antioxidant capacity and TBARS assays. However, some interesting trends emerged when considering the experiments separately. ORAC measurements are indicative of the capacity of the antioxidants to protect the cell against ROS molecules. At three months the hepatic ORAC reading for both the Cal-control and SSB groups are decreased (although only Cal-control versus control in significant) (refer Figure 4.3.2). This suggests that excessive calorie intake, regardless of source, can weaken the antioxidant defense system. At six months the decline in antioxidant capacity has been remedied, possibly by the increased hepatic GSH/GSSG ratio in the Cal-control and SSB group (SSB versus control significant) (Figure 4.3.1). It is important to keep in mind that the ORAC assay is very specific for ROS molecules and does not detect reactive nitrogen specifies. It is therefore possible that these data do not necessarily reflect the complete redox state. Yet, it is reassuring that a similar biphasic pattern was observed in the analysis of kidney samples isolated at the same time points from the same experimental model (Marinus *et al*., 2016). Here our laboratory showed that the SSB group exhibited a reduced antioxidant capacity at three months, but that this was rectified and enhanced by six months, signifying a compensatory effect. However, the overall consequences of oxidative stress were more severe in the kidney and manifested in lipid peroxidation. Another finding worth noting is that the Cal-control group displayed significantly decreased plasma MDA levels at three months compared to the other groups (Figure 4.3.3). This is an unexpected finding since previous work linked a high fat diet to increased lipid oxidation (Lozano *et al*., 2016). We are unclear regarding the significance of our finding and further studies are required to confirm whether this is indeed the case. Based on these data there are no convincing evidence that oxidative stress underlies SSB-induced ER stress. We recommend that future studies investigate cellular and ER calcium handling as putative targets of dysregulation and speculate that it may be a probable cause of SSB-induced ER stress.

Next we investigated the NOGPs. Elevated NOGP activity is not only strongly linked to cardio-metabolic complications, but could indicate that moderate SSB consumption suppressed the glycolytic pathway. We hypothesized that enhanced sugar consumption would induce a collective increase in hepatic NOGP activity, but we observed varying results. PKCβII expression is markedly increased at three and six months (yet not statistically) in the SSB group compared to the other groups (Figure 4.3.6). In support, we also observed elevated PKCβII expression in heart tissues of our model (Driescher, 2014). PKCβII is a downstream target of mitochondrial ROS and NOX-signaling (Joseph, 2014) and although we could not measure mitochondrial ROS, preliminary data show that SSB consumption could increase NOX activity in the liver (six months) (Benadè, 2014) and kidney (Marinus *et al*., 2016). Another study conducted on cardiomyocytes of diabetic animals argue that PKC is indeed the key modulator of hyperglycemia-induced perturbations (Davidoff, 2004), thus possibly explaining why we observed the most conclusive effect in PKCβII expression.

The SSB group also displayed a slight increase in hepatic AGE levels at three months, but this tapered down by six months (Figure 4.3.5). This finding corresponds (in part) to the pattern observed in the heart tissue, although in this instance the decrease observed at six months was more severe. The activity of the HPB remained unaltered (Figure 4.3.6). It was a surprising finding since previous work from our group and others provide robust evidence that the HBP is involved in hyperglycemia/insulin resistance-induced damage (Fricovsky *et al*., 2012; Na *et al*., 2013; Rajamani *et al*., 2011). However, all these studies focused on the heart; therefore it is possible that the HBP does not play such a prominent role in the context of the liver. Finally, polyol pathway activity was similar between all groups at three and six months (Figure 3.2.7). Of note, Lanaspa *et al*. (2013) found that the polyol pathway was upregulated in rats consuming glucose-sweetened beverages and that this directly translated to hepatic lipid accumulation. Although the polyol pathway activity was seemingly unaltered in our model we detected lipid droplets in the six month samples (histological analysis). Based on this finding, we speculate that the polyol pathway is activated in a punctuate fashion, but went undetected due to the limited time points used in this study. Since we detected minimal significant changes in the NOGPs, we conclude that moderate SSB consumption does not have a marked inhibitory effect on the glycolytic pathway.

We used histological staining techniques (H & E and Masson's Trichrome) to assess lipid deposition, fibrosis and overall structural quality of the liver samples (Figure 4.3.9-4.3.12). In agreement with Figlewicz *et al*., (2009) and Lozano *et al*. (2016) there was no structural damage

in any of the samples. At six months, however, the H & E stains revealed an increase in intracellular lipid droplets in the SSB and Cal-control group. This is in agreement with others who also observed a moderate increase in hepatic lipid stores of fructose- and sucrose-consuming rats (Jürgens *et al*., 2005). This is further supported by our earlier experimental work where the results from a commercial triglyceride kit revealed that hepatic triglyceride levels were significantly higher at six months in SSB-consuming rats compared to water-consuming rats (Benadè, 2014). Together these data corroborate the proteomic data indicating that SSB consumption promotes hepatic lipid storage. This effect seems to be time dependent, since we detected no differences at three months, thus prolonged SSB consumption may induce significant lipid accumulation in the liver. We did not detect signs of fibrosis (Masson's Trichrome slides) after three or six months, despite the fact that ER stress is been linked to fibrosis in the literature.

Finally we hoped to determine whether the moderate SSB consumption triggered stress pathways associated with ER stress (known as the ER overload response) since there was insufficient support for this response in the proteomic data. Here we determined the expression levels of TNF-α and IκB as the former is considered a master regulator of inflammation while IκB is directly linked to NF-κB activity. IκB bind to NF-κB in the cytosol to prevent its translocation to the nucleus. In this manner increased IκB levels will attenuate NF-κB activation. By contrast, lower IκB levels (by degradation process) are linked to NF-κB activation. In our model moderate SSB consumption did not alter hepatic TNF-α and IκB expression, although IκB levels were significantly reduced in the Cal-control group at three and six months (Figure 4.3.8). This is likely a fat-specific response and hence not directly relevant to this study. Additionally, circulating CRP levels were below the detectable range in blood samples. Together this suggests that frequent but moderate SSB (and high sugar) intake do not initiate the ER overload response. This finding is in agreement with earlier pre-clinical studies (Figlewicz *et al*., 2009; Lozano *et al*., 2016). By contrast, some of our preliminary data showed an SSB-induced increase in hepatic JNK activity after six months. Therefore, more research is required to fully elucidate whether the ER overload response is triggered and how its downstream effects will manifest in response to moderate SSB consumption.

4.5 References

Aerberli, I., Gerber, P.A., Hochuli, M., Kohler, S., Haile, S.R., Gouni-Berthold, I., … Bernies, K. (2011). Low to moderate sugar-sweetened beverage consumption impairs glucose and lipid metabolism and promotes inflammation in healthy young men: a randomized controlled trial. *Am J Clin Nutr*, *94*, 479–485.

Andrali, S., Qian, Q., & Ozcan, S. (2007). Glucose mediates the translocation of NeuroD1 by O-linked glycosylation. *J Biol Chem*, *282*, 15589–15596.

Anthonisen, E., Berven, L., Holm, S., Nygård, M., Nebb, H., & Grønning-Wang, L. (2010). Nuclear receptor liver X receptor is O-GlcNAc-modified in response to glucose. *J Biol Chem*, *285*, 1607–1615.

Aouacheri, O., Saka, S., Krim, M., Messaadia, A., & Maidi, I. (2015). The investigation of the oxidative stress-related parameters in type 2 diabetes mellitus. *Canadian Journal of Diabetes*, *39*(1), 44–49.

Araki, E., & Nishikawa, T. (2010). Oxidative stress: A cause and therapeutic target of diabetic complications. *J Diabetes Investig*, *1*(3), 90–97.

Avwioro, G. (2011). Histochemical uses of haematoxylin—a review. *J Pharm Clin Sci*, *1*, 24–34.

Balakumar, P., Rohilla, A., Krishan, P., Solairaj, P., & Thangathirupathi, A. (2010). The multifaceted therapeutic potential of benfotamine. *Pharmacol Res*, *61*, 482–488.

Banerjee, P., Ma, J., & Hart, G. (2015). Diabetes-associated dysregulation of O-GlcNAcylation in rat cardiac mitochondria. *PNAS*, *112*(19), 6050–6055.

Baudion, L., & Issad, T. (2015). O-GlcNAcylation and inflammation: a vast territory to explore. *Front Endocrinol*, *5*(235), 1–8

Behl, T., Kaur, I., & Kotwani, A. (2016). Implication of oxidative stress in progression of diabetic retinopathy. *Surv Ophthalmol*, *61*, 187–196.

Benadè, J. (2014). *Cardio-metabolic complications induced by long-term sugar-sweetened beverage consumption*. Stellenbosch University, Stellenbosch, South Africa.

Bocci, V., Zanardi, I., Huijberts, M., & Travagali, V. (2011). Diabetes and chronic oxidative stress. A perspective based on the possible usefulness of ozone therapy. *Diabetes Metab Syndr*, *5*, (45–49), 2011.

Brownlee, M. (2001). Biochemistry and molecular cell biology of diabetic complications. *Nature*, *414*, 813–820.

Brownlee, M. (2005). The Pathobiology of Diabetic Complications: A Unifying Mechanism. *Diabetes*, *54*, 1615–1626.

Bucala, R., Mitchell, R., Arnold, K., Innerarity, T., Vlassara, H., & Cerami, A. (1995). Identification of the major site of apolipoprotein B modification by advanced glycosylation end products blocking uptake by the low-density lipoprotein receptor. *J Biol Chem*, *270*, 10828–10832.

Butcher, M., & Galkina, E. (2013). Old Suspect—New Evidence. The Role of PKCβ in Diabetes Mellitus–Accelerated Atherosclerosis. *Arterioscler Thromb Vasc Biol*, *33*, 1737–1738.

Cao, G., & Prior, R. (1998). Measurement of oxygen radical absorbance capacity in biological samples. *Methods Enzymol*, *299*, 50–62.

Ceriello, A., & Testa, R. (2009). Antioxidant Anti-Inflammatory Treatment in Type 2 Diabetes. *Diabetes Care*, *32*(Suppl 2), S232–S236.

Chandramohan, R., & Pari, L. (2014). Protective effect of umbelliferone on high-fructose diet-induced insulin resistance and oxidative stress in rats. *Biomed Aging Pathol*, *4*(1), 23–28.

Cheng, H., & Gonzalez, R. (1986). The effect of high glucose and oxidative stress on lens metabolism, aldose reductase, and senile cataractogenesis. *Metab Clin Exp*, *35*(4 Suppl 1), 10–14.

Choi, S., Benzie, I., Ma, S., Strain, J., & Hannigan, B. (2008). Acute hyperglycemia and oxidative stress: Direct cause and effect? *Free Radic Biol Med*, *44*, 1217–1231.

Davidoff, A., Davidson, M., Carmody, M., Davis, M., & Ren, J. (2004). Diabetic cardiomyocyte dysfunction and myocyte insulin resistance: role of glucose-induced PKC activity. *Mol Cell Biol*, *262*, 155–63.

Driescher, N. (2014). *Establishing a rodent model of long-term consumption of sugar-sweetened beverages*. Stellenbosch University, Stellenbosch.

Du, X., Matsumura, T., Edelstein, D., Rossetti, L., Zsengeller, Z., Szabo, C., & Brownlee, M. (2003). Inhibition of GAPDH activity by poly(ADP-ribose) polymerase activates three major pathways of hyperglycemic damage in endothelial cells. *J Clin Invest*, *112*, 1049–1057

Essop, M. (2016). AGEing heart valves: a bittersweet stiffening process? *J Clin Pathol*, *69*(9), 1–4.

Figlewicz, D., Ioannou, G., Bennett Jay, J., Kittleson, S., Savard, C., & Roth, C. (2009). Effect of moderate intake of sweeteners on metabolic health in the rat. *Physiol Behav*, *98*, 618–624.

Fricovsky, E., Suarez, J., Ihm, S., Scott, B., Suarez-Ramirez, J., Banerjee, I., … Dillmann, W. (2012). Excess protein O-GlcNAcylation and the progression of diabetic cardiomyopathy. *Am J Physiol Regul Integr Comp Physiol*, *303*(7), R689–R699.

Gallagher, E., LeRoith, D., Stasinopoulos, M., Zelenko, Z., & Shiloach, J. (2016). Polyol accumulation in muscle and liver in a mouse model of type 2 diabetes. *J Diabetes Complications*, *30*(6), 999–1007.

Gao, Y., Miyazaki, J., & Hart, G. (2003). The transcription factor PDX-1 is post-translationally modified by O-linked N-acetylglucosamine and this modification is correlated with its DNA binding activity and insulin secretion in β-cells. *Arch Biochem Biophys*, *415*, 155–163

Gavin, J. (2001). Pathophysiologic mechanisms of postprandial hyperglycemia. *Am J Cardiol*, *88 (Suppl)*, 4H–8H.

Geraldes, P., & King, G. (2010). Activation of protein kinase C isoforms and its impact on diabetic complications. *Circ Res*, *106*, 1319–1331.

Giacco, F., & Brownlee, M. (2010). Oxidative stress and diabetic complications. *Circ Res*, *107*(9), 1059–1070.

Grewal, A., Bhardwaj, S., Pandita, D., Lather, V., & Sekhon, B. (2016). Updates on Aldose Reductase Inhibitors for Management of Diabetic Complications and Non-diabetic Diseases. *Mini Rev Med Chem*, *16*(2), 120–163.

Hamada, Y., Araki, N., Horiuchi, S., & Hotta, N. (1996). Role of polyol pathway in nonenzymatic glycation. *Nephrol Dial Transplant*, *11*(Suppl 5), 95–98.

Hanover, J., Krause, M., & Love, D. (2010). The hexosamine signaling pathway: O-GlcNAc cycling in feast or famine. *Biochimica et Biophysica Acta*, *1800*(2), 80–114.

Hart, G. (2014). Three decades of research on O-GlcNAcylation – a major nutrient sensor that regulates signaling, transcription and cellular metabolism. *Front Endocrinol*, *5*(183), 1–4.

Hennige, A., Heni, M., Machann, J., Staiger, H., Sartorius, T., Hoene, M., … Häring, H. (2010). Enforced expression of protein kinase C in skeletal muscle causes physical inactivity, fatty liver and insulin resistance in the brain. *J Cell Mol Med*, *14*, 903–913.

Hotamisligil, G. (2006). Inflammation and metabolic disorders. *Nature*, *444*, 860–867.

Hotamisligil, G., Shargill, N., & Spiegelman, B. (1993). Adipose expression of tumor necrosis factor-alpha: direct role in obesity-linked insulin resistance. *Science*, *259*(5091), 87–91.

Housley, M., Rodgers, J., Udeshi, N., Kelly, T., Shabanowitz, J., Hunt, D., … Hart, G. (2008). O-GlcNAc regulates FoxO activation in response to glucose. *J Biol Chem*, *283*(24), 16283–16292.

Huang, W., Bansode, R., Mehta, M., & Metha, K. (2009). Loss of Protein Kinase Cβ Function Protects Mice Against Diet Induced Obesity and Development of Hepatic Steatosis and Insulin Resistance. *Hepatology*, *49*(5), 1525–1536.

Hueschmann, A., Regensteiner, J., Vlassara, H., & Reusch, J. (2006). Diabetes and Advanced Glycoxidation End Products. *Diabetes Care*, *29*(6), 1420–1432

Johnson, R., Perez-Pozo, S., Sautin, Y., Manitius, J., Sanchez-Lozada, L., Feig, D., … Nakagawa, T. (2009). Hypothesis: Could Excessive Fructose Intake and Uric Acid Cause Type 2 Diabetes? *Endocr Rev*, *30*(1), 96–116.

Joseph, D. (2014). *Hyperglycemia and a "series of unfortunate events" – the impact of oxidative stress and glucose metabolic dysfunction on insulin resistance* (Unpublished PhD thesis). Stellenbosch University, Stellenbosch.

Joseph, D., Kimar, C., Symington, B., Milne, R., & Essop, M. (2014). The detrimental effects of acute hyperglycemia on myocardial glucose uptake. *Life Sci*, *105*(1–2), 31–42.

Kitamura, H., Kimura, S., Shimamoto, Y., Okabe, J., Ito, M., Miyamoto, T., … Miyoshi, I. (2013). Ubiquitin-specific protease 2-69 in macrophages potentially modulates metainflammation. *FASEB J*, *27*(12), 4940–4953.

Kornfeld, R. (1967). Studies on l-glutamine d-fructose 6-phosphate amidotransferase: I. Feedback inhibition by uridine diphosphate-N-acetylglucosamine. *J Biol Chem*, *242*, 3135–3141.

Kuo, M., Zilberfarb, V., Gangneux, N., Christeff, N., & Issad, T. (2008). O-GlcNAc modification of FoxO1 increases its transcriptional activity: A role in the glucotoxicity phenomenon? *Biochimie*, *90*, 679–685.

Lanaspa, M., Ishimoto, T., Li, N., Cicerchi, C., Orlicky, D., Ruzicky, P., … Johnson, R. (2013). Endogenous fructose production and metabolism in the liver contributes to the development of metabolic syndrome. *Nat Commun*, *4*(2434), 1–16.

Lazo-de-la-Vega-Monroy, M., & Fernández-Mejía, C. (2013). Oxidative Stress in Diabetes Mellitus and the Role Of Vitamins with Antioxidant Actions. In *Oxidative stress and chronic degenerative diseases - A role for antioxidants* (pp. 209–232). Intech.

Lefebvre, T., Dehennaut, V., Guinez, C., Olivier, S., Drougat, L., Mir, A., … Michalski, J. (2010). Dysregulation of the nutrient/stress sensor O-GlcNAcylation is involved in the etiology of cardiovascular disorders, type-2 diabetes and Alzheimer's disease. *Biochimica et Biophysica Acta*, *1800*, 67–79.

Lemaitre, L. (2008). Toll-like receptors – taking an evolutionary approach. *Nat Rev Genetics*, *9*(3), 165–178.

Lenna, S., & Trojanowska, M. (2012). The role of endoplasmic reticulum stress and the unfolded protein response in fibrosis. *Curr Opin Rheumatol*, *24*(6).

León-Pedroza, J., González-Tapia, L., Del Olmo-Gil, E., Castellanos-Rodríguez, D., Escobedo, G., & González-Chávaz, A. (2015). Low-grade systemic inflammation and the development of metabolic diseases: From the molecular evidence to the clinical practice. *Cirugia Y Cirujanos*, *83*(6), 543–551.

Lim, M., Park, L., Shin, G., Hong, H., Kang, I., & Park, Y. (2008). Induction of apoptosis of Beta cells of the pancreas by advanced glycation end-products, important mediators of chronic complications of diabetes mellitus. *Ann N Y Acad Sci*, *1150*, 311–315.

Lozano, I., Van der Werf, R., Bietiger, W., Seyfritz, E., Peronet, C., Pinget, M., … Dal, S. (2016). High-fructose and high-fat diet-induced disorders in rats: impact on diabetes risk, hepatic and vascular complications. *Nutr Metab*, *13*(15). https://doi.org/10.1186/s12986-016-0074-1

Mapanga, R., Rajamani, U., Dlamini, N., Zungu-Edmondson, M., Kelly-Laubscher, R., Shafiullah, M., & Essop, M. (2012). Oleanolic acid: a novel cardioprotective agent that blunts hyperglycemia-induced contractile dysfunction. *PLoS ONE*, *7*(10), e47322.

Marinus, F., Bester, D., Driescher, N., & Essop, M. (2016). *Long-term sugar-sweetened beverage consumption triggers increase oxidative stress in the rat kidney*. Poster presented at the PSSA, Cape Town, South Africa.

Matsuda, M., & Shimomura, I. (2013). Increased oxidative stress in obesity: Implications for metabolic syndrome, diabetes, hypertension, dyslipidemia, atherosclerosis, and cancer. *Obes Res Clin Pract*, *7*, e330–e341.

Mehta, K. (2014). Emerging role of protein kinase C in energy homeostasis: A brief overview. *World J Diabetes*, *15*(5), 3.

Morre, D., Lenaz, G., & Morre, D. (2000). Surface oxidase and oxidative stress propagation in aging. *J Exp Biol*, *203*, 1513–1521.

Murano, I., Barbatelli, V., Parisani, V., Latini, C., Muzzonigro, G., Castellucci, M., & Cinti, S. (2008). Dead adipocytes, detected as crown-like structures, are prevalent in visceral fat depots of genetically obese mice. *J Lipid Res*, *49*(7), 1562–1568.

Na, J., Musselman, L., Pendse, J., Baranski, T., Bodmer, R., Ocorr, K., & Cagan, R. (2013). A Drosophila model of high sugar diet-induced cardiomyopathy. *PLoS Genet*, *9*(1), e1003175.

Neeper, M., Schmidt, A., Brett, J., Yan, S., Wang, F., Pan, Y., … Shaw, A. (1992). Cloning and expression of a cell surface receptor for advanced glycosylation end products of proteins. *J Biol Chem*, *267*(21), 14998–15004

Newton, A. (1995). Protein kinase C: structure, function, and regulation. *J Biol Chem*, *270*, 28495–28498.

Nowotny, K., Jung, T., Höhn, A., Weber, D., & Grune, T. (2015). Advanced Glycation End Products and Oxidative Stress in Type 2 Diabetes Mellitus. *Biomolecules*, *5*, 194–222.

Panigrahy, S., Bhatt, R., & Kumar, A. (2016). Reactive oxygen species: sources, consequences and targeted therapy in type 2 diabetes. *J Drug Target*, 1029–2330 (Online).

Poornima, I.G., Parikh, P., & Shannon, R.P. (2006). Diabetic cardiomyopathy: the search for a unifying hypothesis, *Circ Res*, *98*, 596–605.

Prior, R., Hoang, H., Gu, L., Wu, X., Bacchiocca, M., Howard, L., … Jacob, R. (2003). Assays for hydrophilic and lipophilic antioxidant capacity (ORACfl) of plasma and other biological and food samples. *J Agric Food Chem*, *51*, 3273–3279.

Rajamani, U., Joseph, D., Roux, S., & Essop, M. (2011). The hexosamine biosynthetic pathway can mediate myocardial apoptosis in a rat model of diet-induced insulin resistance. *Acta Physiol (Oxf)*, *202*(2), 151–157.

Rao, X., Zhong, J., Xu, X., Jordan, B., Maurya, S., Braunstein, Z., … Sun, Q. (2013). Exercise protects against diet-induced insulin resistance through downregulation of protein kinase Cβ in mice. *PLoS ONE*, *8*(12), e81364.

Rashid, K., Sinha, K., & Sil, P. (2013). An update on oxidative stress-mediated organ pathophysiology. *Food Chem Toxicol*, *62*, 584–600.

Rolo, A., & Palmeira, C. (2006). Diabetes and mitochondrial function: role of hyperglycemia and oxidative stress. *Toxicol Appl Pharmacol*, *212*, 167–179.

Schleischer, E., & Weigert, C. (2000). Role of the hexosamine biosynthetic pathway in diabetic nephropathy. *Kidney Int Suppl*, *58*(77), S13-18.

Schwartz, E., & Reaven, P. (2006). Molecular and Signaling Mechanisms of Atherosclerosis in Insulin Resistance. *Endocrinol Metab Clin N Am*, *35*, 525–549.

Senft, D., & Ronai, Z. (2015). UPR, autophagy, and mitochondria crosstalk underlies the ER stress response. *Trends in Biochemical Sciences*, *40*(3), 141–148.

Shen, G.X. (2010). Oxidative stress and diabetic cardiovascular disorders: roles of mitochondria and NADPH oxidase. *Can J Physiol Pharmacol*, *88*, 241–248.

Shiba, T., Inoguchi, T., Sportsman, J., Heath, F., Bursell, S., & King, G. (1993). Correlation of diacylglycerol level and protein kinase C activity in rat retina to retinal circulation. *Am J Physiol*, *265*, E783–E793.

Son, N., Ananthakrishnan, R., Yu, S., Khan, R., Jiang, H., Ji, R., … Ramasamy, R. (2012). Cardiomyocyte Aldose Reductase Causes Heart Failure and Impairs Recovery from Ischemia. *PLoS ONE*, *7*(9), e46549.

Styskal, J.L., Van Remmen, H., Richardson, A., & Salmon, A.B. (2012). Oxidative stress and diabetes: What can we learn about insulin resistance from antioxidant mutant mouse models? *Free Radic Biol Med*, *52*, 46–58.

Tahara, N., Yamagishi, S., Matsui, T., Takeuchi, M., Nitta, Y., Kodama, N., … Imaizumi, T. (2012). Serum levels of advanced glycation end products (AGEs) are independent correlates of insulin resistance in nondiabetic subjects. *Cardiovasc. Ther.*, *30*, 42–48.

Tajes, M., Eraso-Pichot, A., Rubic-Moscardo, F., Guivernau, B., Bosch-Morato, M., Valls-Comamala, V., & Munoz, F. (2014). Methylglyoxal reduces mitochondrial potential and activates Bax and caspase-3 in neurons: Implications for Alzheimer's disease. *Neurosci Lett*, *580*, 78–82.

Takeuchi, M., & Makita, Z. (2001). Alternative routes for the formation of immunochemically distinct advanced glycation end-products in vivo. *Curr Mol Med*, *1*, 305–315.

Takino, J., Nagamine, K., Hori, t, Sakasai-Sakai, A., & Takeuchi, M. (2015). Contribution of the toxic advanced glycation end-products-receptor axis in nonalcoholic steatohepatitis-related hepatocellular carcinoma. *World J Hepatol*, *7*(23), 2459–2469.

Tang, W., Martin, K., & Hwa, J. (2012). Aldose reductase, oxidative stress, and diabetic mellitus. *Front Pharmacol*, *3*(87), 1–8.

Tangvarasittichai, S. (2015). Oxidative stress, insulin resistance, dyslipidemia and type 2 diabetes mellitus. *World J Diabetes*, *6*(3), 456–480. Torres, C., & Hart, G. (1984). Topography and polypeptide distribution of terminal N-acetylglucosamine residues on the surfaces of intact lymphocytes. Evidence for O-linked GlcNAc. *J Biol Chem*, *259*, 3308–3317.

Tanjore, H., Lawson, W., & Blackwell, T. (2013). Endoplasmic reticulum stress as a pro-fibrotic stimulus. *Biochim Biophys Acta*, *1832*(7), 940–947.

Uribarri, J., Cai, W., Ramdas, M., Goodman, S., Pyzik, R., Chen, X., … Vlassara, H. (2011). Restriction of advanced glycation end products improves insulin resistance in human type 2 diabetes: potential role of AGER1 and SIRT1. *Diabetes Care*, *34*, 1610–1616.

Uysal, K., Wiesbrock, S., Marino, M., & Hotamisligil, G. (1997). Protection from obesity induced insulin resistance in mice lacking TNF-α function. *Nature*, *389*, 610–614.

Vaidyanathan, K., & Wells, L. (2014). Multiple tissue-specific roles for the O-GlcNAc post-translational modification in the induction of and complications arising from type II diabetes. *J Biol Chem*, *289*(50), 34466–34471.

Vlassara, H. (2011). AGEs as a preventable cause of diabetes and its complications. *Diabetol Chron*, *24*(3), 155–160.

Vlassara, H., & Uribarri, J. (2014). Advanced Glycation End Products (AGE) and Diabetes: Cause, Effect, or Both? *Curr Diab Rep*, *14*(1), 453.

Vlassara, H., Cai, W., Tripp, E., Pyzik, R., Yee, K., Goldberg, L., … Uribarri, J. (2016). Oral AGE restriction ameliorates insulin resistance in obese individuals with the metabolic syndrome: a randomised controlled trial. *Diabetologia*, *59*, 2181–2192.

Yang, X., Ongusaha, P., Miles, P., Havstad, J., Zhang, F., So, W., … Evans, R. (2008). Phosphoinositide signalling links O-GlcNAc transferase to insulin resistance. *Nature*, *451*(7181), 964–969.

Young B, Lowe, J., Stevens, A., & Heath, J. (2006). *Wheater's Functional Histology. A text and colour atlas* (5th ed.). Churchill Livingston: Elsevier

Zhang, C., Huang, C., Tian, Y., & Li, X. (2014). Polyol pathway exacerbated ischemia/reperfusion-induced injury in steatotic liver. *Oxid Med Cell Longev*. https://doi.org/10.1155/2014/963629

Zhang, K., Ruonan, Y., & Yang, X. (2014). O-GlcNAc: a bittersweet switch in liver. *Front Endocrinol*, *5*(221), 1–7.

Chapter 5: Concluding remarks

Cardio-metabolic diseases such as T2DM and CVD cause ~19 million deaths annually (WHO factsheet #355, 2015). The prevalence of cardio-metabolic diseases is increasing rapidly especially in low- and middle-income countries, e.g. the amount of obese children in Africa has doubled over the past 25 years (WHO Fact sheet #311, 2016) while the IDF predicts that Africa will suffer a 93% increase in the incidence of T2DM between 2014 and 2035 (IDF Diabetes Atlas, 2014). In South Africa the statistics are just as condemning: currently ~15% of all adult males and ≥ 30% of females are obese (BMI ≥ 30 kg/m^2), ~27.5% suffer from hypertension, ~35% display elevated cholesterol levels and ~12.5% exhibit fasting blood glucose levels associated with diabetes. Researchers rightfully refer to cardio-metabolic diseases as a global pandemic (Grundy, 2007; Lewis & Hennekens, 2016; Skrha, 2014). In parallel, there has been a global increase in sugar consumption (Lustig *et al*., 2012). In the US the average sugar consumption is ≥ 36 teaspoons/capita/day (conversion 100 calories = 6 teaspoons). The average South African consumes 12-18 teaspoons of sugar per day (converted from Lustig *et al*., 2012). Although this seems moderate compared to the US, it is still more than double the amount recommended by the WHO (≤ 6 teaspoons per day). A significant portion of excess sugar intake is derived from SSBs (US Department of Agriculture & US Department of Health and Human Services, 2010) and SSB consumption continues to increase globally (Basu *et al*., 2013).

Despite the large volume of epidemiological data supporting the link between SSB consumption and the onset of cardio-metabolic diseases, there are currently insufficient clinical data to confirm causality (Stanhope, 2015). As a result, the health effects of frequent SSB intake remains disputed. Moreover, the available clinical studies produced inconsistent results in several of the parameters that were measured (refer to section 1.2.3.4) – thus hindering the deduction of coherent, plausible pathophysiological mechanisms. In the light of this, the CMRG established a unique rat model for long-term moderate SSB consumption which allows for in-depth molecular and functional analyses. Unlike most other animal models that simply diluted SSB/sugar into the rodents' drinking water, we administered SSB by gavaging. Moreover, we supplied the *actual* SSB (in moderate amounts) unlike the majority of studies that used fructose, glucose or sucrose in excessive amounts. This allowed us to improve on some drawbacks of previous studies, i.e. not being able to regulate how much each rat consumed, controlling for inappropriately high sugar dosages compared to overall caloric intake, and by evaluating the

effects of an actual SSB. By using a relatively low dosage we aimed to generate data that will be far more applicable to the majority of the population and also to detect the earliest perturbations underlying ultimate onset of disease – before the onset of significant functional changes.

Hindsight is always 20/20. Despite our attempts to improve on previous study protocols, the current study is not without its own limitations. We recommend that future studies conduct expression proteomics on samples from more than one time point as this will aid in the interpretation of ambiguous results. The mitochondrial bioenergetics data were particularly difficult to interpret and in this respect high-resolution mitochondrial respirometry should provide valuable insight. Furthermore, we recommend that post-translational protein modifications should also be taken into consideration instead of focusing solely on hepatic protein expression levels. We further recommend that various markers of ER stress should be evaluated to corroborate the link between moderate SSB intake and ER stress. Lastly, we recommend that the SSB intervention should be assessed over a longer time period in order to even better understand the consequences of long-term SSB intake.

This study generated two main findings:

- Moderate long-term SSB intake induced minimal changes in systemic markers of cardio-metabolic complications together with no significant body weight alterations and functional changes in the liver;
- SSB consumption did, however, induce hepatic ER stress as an early metabolic perturbation – this effect is driven mainly through increased caloric intake rather than the SSB *per se*.

What is the verdict? Is it safe to consume SSBs on a regular basis? Findings from the current study support a firm ‘’no’’ as a response to this question. Due to the caloric make-up of SSBs, it almost inevitably leads to excessive calorie intake with downstream intracellular effects. Here our data revealed that even moderate SSB consumption triggers hepatic ER stress and subsequent intracellular responses despite minimal phenotypic and functional changes. Of concern, the SSB-induced shift in the hepatic protein expression profile resembles the signature found in insulin resistant/diabetic models. Thus a key, broader public message derived from this thesis is that SSB consumption contributes to the onset of cardio-metabolic diseases without the manifestation of any early phenotypic/functional “warning signs”. We propose that

focusing on easily identifiable and measurable markers of ER stress may provide a novel biomarker to detect risk at a much earlier stage in this context.

Don't drink Jive* – stay alive! (*or any other SSB)

5.1 References

IDF Diabetes Atlas: the global burden. International Diabetes Federation [online]. Available: http://www.idf.org/diabetesatlas/5e/the-global-burdan. (2015).

US Department of Agriculture, & US Department of Health and Human Services. (2010). Dietary Guidelines for Americans. Retrieved from http://www.health.gov/dietaryguidelines/dga2010/DietaryGuidelines2010.pdf

Basu, S., McKee, M., Galea, G., & Stuckler, D. (2013). Relationship of soft drink consumption to global overweight, obesity, and diabetes: A cross-national analysis of 75 countries. *Am J Public Health*, *103*, 2071–2077.

Grundy, S. (2008). Metabolic syndrome pandemic. *Arterioscler Thromb Vasc Biol*, *28*(4), 629–636.

Lewis, S., & Hennekens, C. (2016). Regular Physical Activity: A “Magic Bullet” for the Pandemics of Obesity and Cardiovascular Disease. *Cardiology*, *134*(3), 360–363.

Lustig, R., Schmidt, L., & Brindis, C. (2012). The toxic truth about sugar. *Am J Clin Nutr*, *95*, 283–289.

Skrha, J. (2014). Diabetes mellitus--a global pandemic. Keynote lecture presented at the Wonca conference in Prague in June 2013. *Eur J Gen Pract*, *20*(1), 65–68.

Stanhope, K. (2015). Sugar consumption, metabolic disease and obesity: The state of the controversy. *Crit Rev Clin Lab Sci*, *Early online*, 1–16. https://doi.org/10.3109/10408363.2015.1084990

World Health Organization. (2015). Noncommunicable diseases Fact Sheet 355. Retrieved from http://www.who.int/mediacentre/factsheets/fs355/en/

World Health Organization. (2016). Obesity and overweight Fact Sheet 311. Retrieved from http://www.who.int/mediacentre/factsheets/fs311/en/

Appendix A

UNIVERSITEIT·STELLENBOSCH·UNIVERSITY
jou kennisvennoot • your knowledge partner

Protocol Approval

Date: 03-Jun-2013

PI Name: DRIESCHER, Natasha

Protocol #: SU-ACUM13-00012

Title: The role of post-prandial hyperglycaemia in the onset of cardio-metabolic diseases

Dear Natasha DRIESCHER, the Response to Modifications, was reviewed on 28-May-2013 by the Research Ethics Committee: Animal Care and Use via committee review procedures and was approved. Please note that this clearance is only valid for a period of twelve months. Ethics clearance of protocols spanning more than one year must be renewed annually through submission of a progress report, up to a maximum of three years.

Applicants are reminded that they are expected to comply with accepted standards for the use of animals in research and teaching as reflected in the South African National Standards 10386: 2008. The SANS 10386: 2008 document is available on the Division for Research Developments website www.sun.ac.za/research.

Please remember to use your protocol number, SU-ACUM13-00012 on any documents or correspondence with the REC: ACU concerning your research protocol.

Please note that the REC: ACU has the prerogative and authority to ask further questions, seek additional information, require further modifications or monitor the conduct of your research.

We wish you the best as you conduct your research.

If you have any questions or need further help, please contact the REC: ACU secretariat at WABEUKES@SUN.AC.ZA or .

Sincerely,

Winston Beukes

REC: ACU Secretariat

Research Ethics Committee: Animal Care and Use

Appendix B: Proteomics

Sample preparation

Liver tissue (100 µg) was placed in 0.5 mL extraction buffer (triethylammonium bicarbonate [TEAB, Sigma; 100 mM], Urea [8 M], Tween20 [0.5%], NaCl [100 mM], EDTA [2 mM] and triscarboxyethyl phosphine (TCEP, Fluka; 5-10 mM]) and homogenized (Polytron PT2100, Kinematica, Luzern, Switserland) for 3 × 15 sec bursts. Thereafter the samples were centrifuged (Spectrafuge™ 24D, Labnet, Edison NJ) for 10 min at 12000 x g and 400 µL supernatant was collected into fresh microtubes. Acetone cooled to -20°C (1.6 mL) was added to each sample. The content was mixed and the tubes were left overnight at -20°C. On the second day the samples were centrifuged (Spectrafuge™ 24D, Labnet, Edison NJ) once more (12000 xg for 10 min) and the pellets were collected and sent to the Central Analytical Facility (Faculty of Medicine and Health Sciences, Stellenbosch University) where the rest of the experimental work was completed under supervision of Dr. Mare Vlok (Laboratory Manager).

The supplied pellets were dissolved in 100 mM TEAB containing 4 M guanindine-hydrochloride (Sigma-Aldrich, St. Louis, MO) and 1% octylglucopyranoside by sonication for 5 min. The protein suspension was centrifuged at 12 000 × g for 10 min (Spectrafuge™ 24D, Labnet, Edison NJ). The supernatant was removed and the proteins were precipitated once more with 5 volumes acetone cooled to -20°C (overnight). The next day proteins were pelleted by centrifugation (Spectrafuge™ 24D, Labnet, Edison NJ) 12 000 × g for 10 minutes before being dissolved in 100 mM TEAB containing 4M guanindine-hydrochloride. Proteins concentration was determined spectrophotometrically at 280 nm using a NanoDrop spectrophotometer (Thermo Scientific, Waltham, MA).

In-solution digest

All reagents used were analytical grade or equivalent. Samples were reduced by adding 50 mM TCEP; Fluka in 100 mM TEAB (final concentration 5mM TCEP) for 30 min at room temperature. Following reduction, cysteine residues were modified to methylthio-cysteine using 200 mM methane methylthiosulphonate (MMTS; Sigma-Aldrich, St. Louis, MO) in 100 mM TEAB (final concentration 20 mM) for 30 min. After modification the samples were diluted to 98 µL with 100 mM TEAB. Proteins were digested by adding 5 µL trypsin solution (1µg/ µL) (Promega Corporation, Fitchburg, WI) followed by an 18 hr incubation at 37°C. The samples were dried

down and resuspended in 100 µL 2% acetonitrile (Sigma-Aldrich [Fluka], St. Louis, MO): water and 0.1% formic acid (FA; Sigma-Aldrich, St. Louis, MO).

Desalting

Residual digest reagents were removed using an in-house manufactured C 18 stage tip (Empore Octadecyl C 18 extraction discs; Sigma-Aldrich (Supelco), St. Louis, MO. The 20 µL sample was loaded onto the stage tip after activating the C 18 membrane with 30 µL methanol (Sigma-Aldrich, St. Louis, MO) and equilibration with 30 µL 2% acetonitrile:water; 0.05% TFA. The bound sample was washed with 30 µL 2% acetonitrile: water, 0.1% formic acid before elution with 30 µL 50% acetonitrile: water; 0.1% formic acid. The eluate was evaporated to dry and dried peptides were dissolved in 20 µL 2% acetonitrile:water; 0.1% FA for liquid chromatography and mass spectrometry analysis.

Liquid chromatography

Dionex nano-RSLC Liquid chromatography was performed on a Thermo Scientific Ultimate 3000 RSLC equipped with a 0.5 cm × 300 µm C_{18} trap column and a 35 cm × 75 µm in-house manufactured C18 column (Luna C18, 3.6 µm; Phenomenex, Torrance, CA) analytical column. The solvent system used was loaded: 2% acetonitrile:water; 0.1% FA; Solvent A: 2% acetonitrile:water; 0.1% FA and Solvent B: 100% acetonitrile:water. The samples were loaded onto the trap column using loading solvent at a flow rate of 15 µL/min from a temperature controlled autosampler set at 7^{o}C. Loading was performed for 5 min before the sample was eluted onto the analytical column. Flow rate was set to 500 nL/min and the gradient generated as follows: 2.0% -10%B over 5 min; 5% -25% B from 5 -50 min using Chromeleon non-linear gradient 6, 25%-45% from 50-65 min, using Chromeleon non-linear gradient 6. Chromatography was performed at 50°C and the outflow delivered to the mass spectrometer through a stainless steel nano-bore emitter.

Mass spectrometry

Mass spectrometry was performed using a Thermo Scientific Fusion mass spectrometer equipped with a Nanospray Flex ionization source (Thermo Scientific, Waltham, MA). The sample was introduced through a stainless steel emitter. Data were collected in positive mode with spray voltage set to 2 kV and ion transfer capillary to 275°C. Spectra were internally calibrated using polysiloxane ions at m/z = 445.12003 and 371.10024. MS1 scans were performed using the orbitrap detector set at 120 000 resolution over the scan range 350-1650

with AGC target at 3 E5 and maximum injection time of 40 minutes. Data was acquired in profile mode. MS2 acquisitions were performed using monoisotopic precursor selection for ion with charges +2-+6 with error tolerance set to +/- 0.02 ppm. Precursor ions were excluded from fragmentation once for a period of 30 seconds. Precursor ions were selected for fragmentation in HCD mode using the quadrupole mass analyzer with HCD energy set to 32.5%. Fragment ions were detected in the orbitrap mass analyzer set to 15 000 resolution. The AGC target was set to 1E4 and the maximum injection time to 45 minutes. The data was acquired in centroid mode.

Data analysis

The raw files generated by the mass spectrometer were imported into the Proteome Discoverer v1.4 (Thermo Scientific, Waltham, MA) and processed using the SequestHT algorithm here included in Proteome Discoverer. Data analysis was structured to allow for methylthio as a fixed modification as well as NQ deamidation (NQ), oxidation (M). Precursor tolerance was set to 10 ppm and fragment ion tolerance to 0.02 Da. The database used was the Rattus rattus database obtained from Uniprot Knowledge Base (The UniProt Consortium, 2014). The raw files generated were also converted to Mascot generic format (mgf) and the files interrogated using the Myrimatch algorithm through SearchGUI. Search parameters were set as for Sequest HT search. The results files were important into Scaffold 1.4.4 and identified peptides validated using the X!Tandem search algorithm included in ScaffoldQ+ (Proteome Software, Portland, OR). Peptide and protein validation were done using the Peptide and Protein Proph*et al*gorithms. Protein quantitation was performed by first performing a ANOVA analysis and applying the Hochberg-Benjamini correction (significant when $P < 0.00275$ after correction). The proteins showed to be statically different were marked for fold change calculations. Two replicates, 1-3A Rep1 and 2-3A Rep1 deviated significantly from the other replicates and were excluded from the quantitation analysis.

Appendix C: Western blotting techniques

Protein extraction from tissues

Preparation of RIPA buffer

Base ingredients

- **Tris-HCl** (buffering agent prevents protein denaturation)
- **NaCl** (salt prevents non-specific protein aggregation)
- **NP-40** (non-ionic detergent to extract proteins; 10% stock solution in H_2O) or use **Triton X-100**
- **Na-deoxycholate** (ionic detergent to extract proteins; 10% stock solution in H_2O; protect from light). **Adjust the pH** to 9, then boil, cool, and re-adjust the pH to 9. Repeat this process until the solution becomes colorless

Note: Do not add Na-deoxycholate when preparing lysates for kinase assays. Ionic detergents can denature enzymes, causing loss of activity.

RIPA protease inhibitors

- **Phenylmethylsulfonyl fluoride** (PMSF) (200 mM stock solution in isopropanol; store at room temperature)
- **EDTA** (calcium chelator; 100 mM stock solution in H_2O, pH 7.4)
- **Leupeptin** (store frozen in aliquots, 1 mg/mLin H_2O)
- **Aprotinin** (store frozen in aliquots, 1 mg/mLin H_2O)
- **Pepstatin** (store frozen in aliquots, 1 mg/mLin methanol)

RIPA phosphatase inhibitors

- **Activated Na_3VO_4** (200 mM stock solution in H_2O; see sodium orthovanadate activation protocol).
- **NaF** (200 mM stock solution: store at room temperature)

Note: Do not add phosphatase inhibitors when preparing lysates for phosphatase assays.

RIPA trypsin inhibitors

- **Benzamidine** (200 mM stock solution -dissolve in ddH_2O – store at -20ºC)

Note: When blotting for *O*-GlcNAc, Pugnac should be added to prevent the removal of *O*-GlcNAc modifications. Make 200 µM stock solution

Sodium orthovanadate activation protocol

1. Sodium orthovanadate should be activated for maximal inhibition of protein phosphotyrosyl-phosphatases.
2. Prepare a 200 mM solution of sodium orthovanadate.
3. Adjust the pH to 10 using either 1 N NaOH or 1 N HCl. The starting pH of the sodium orthovanadate solution may vary depending on different lots of the chemical. The solution will become yellow in color at pH 10.
4. Boil the solution until it turns colorless (~ 10 min).
5. Cool to room temperature.
6. Re-adjust the pH to 10 and repeat steps 3 and 4 until the solution remains colorless and the pH stabilizes at 10.
7. Store the activated sodium orthovanadate as aliquots at -20°C.
8. This procedure de-polymerizes the vanadate, converting it into a more potent inhibitor of protein tyrosine phosphatases.

Procedure:
Prepare 100 mLmodified RIPA buffer as follows:

- Add 790 mg Tris base to 75 mLdistilled water (ddH_2O). Then add 900 mg NaCl and stir the solution until all solids are dissolved. Using HCl, adjust the pH to 7.4.
- Add 10 mLof 10% NP-40 to the solution.
- Add 2.5 mLof 10% Na-deoxycholate and stir until solution is clear.

- Add 1 mLof 100 mM EDTA to the solution. Adjust the volume of the solution to 100 mLusing a graduated cylinder.
- Ideally, the remaining protease and phosphatase inhibitors should be added to the solution on the same day for running of the assay. Therefore, it is best to aliquot the buffer in 10 mLaliquots without the protease inhibitors and store at 2-8°C.

- RIPA with inhibitors - on day of use, thaw the required amount of RIPA buffer and add the appropriate volume of protease inhibitors to the buffer.

For 10 mLRIPA add:

10 µL aprotonin; 10 µL of leupeptin; 50 µL of PMSF, Na_3VO_4, and NaF and benzamidine, 100 µL pepstatin and 50 µL Pugnac.

NB: these are the volumes for 10 mLof RIPA, but with the exception of PMSF, the diluted inhibitors are stable in aqueous solution for up to 5 days. Add PMSF last; PMSF have a half-life of 30 minutes in aqueous solution.

The final concentrations in the modified RIPA buffer should be:

Tris-HCl: 50 mM, pH 7.4	Leupeptin: 1 µg/mL
NP-40: 1%	Aprotonin: 1 ug/ml
Na-deoxycholate: 0.25%	Pepstatin: 10 ug/ml
NaCl: 150 mM	Na_3VO_4: 1 mM
EDTA: 1 mM	NaF: 1 mM
PMSF: 1 mM	PUGNAc: 1µM
Benzamidine: 1 µg/mL	

Protein extraction

- Cut tissue samples into small pieces and place into a 2 mLmicrotube.
- Pour RIPA buffer into the microtubes containing the tiny pieces of tissue samples – (aim to make homogenates that are 1:2 w/v tissue: lysis buffer).
- Using a dounce homogenizer (Ultra-Turrax homogenizer, IKA, China), homogenize the tissue until a fine slurry is obtained.
- Transfer the homogenates to fresh pre-chilled 2 mLmicrotubes and keep on ice.
- Once the foam has dissipated (~1 hour) collect the content of the microtube and transfer it into a clean tube.
- Centrifuge (Spectrafuge™ 24D, Labnet, Edison NJ) at 17 226 × g. for 15 min at 4ºC.
- Transfer the supernatants (protein lysates) to clean pre-chilled microtubes.
- Perform Direct Detect® protein determination and then freeze samples at -80ºC.

Direct Detect® protein determination

- Apply 2 µL of sample solution (position 2-4) and sample buffer blank (position 1) on the card.
- Select the appropriate calibration curve on the machine
- Insert the card vertically into the slot in the top of the sampling accessory.
- The card notch should face towards the center of the instrument (align arrows on card and instrument).
- Instrument dries samples, then measures each spot.
- Acquire spectra.
- Statistical data displayed for all 3 samples.
- User can select which data points to exclude, if any.
- User has option to print a report of current data, or export as a .CSV file.
- Compare results to internal Amino Acid Analysis verified BSA standard or create your own standard curve.

- Enter data into appropriate excel template to determine loading amounts for Western blots.

Sample preparation

Laemmli's loading buffer

ddH_20	3.8 mL
0.5 M Tris-HCl, pH 6.8	1.0 mL
Glycerol	0.8 mL
10% (w/v) SDS	1.6 mL
0.05% (w/v) Bromophenol blue	0.4 mL

Materials:

0.5 mL microtubes

Sharp tweezers or a syringe needle

β-mercaptoethanol

Ice

Heating block set to 95^{o}C (or beaker of water on hot plate)

Vortex (Scientific industries, Bohemia NY)

Microtube centrifuge (Spectrafuge™ 24D, Labnet, Edison NJ)

Method

- Make a working solution of Laemmli's sample buffer – 850 µL Laemmli's stock buffer solution together with 150 µL β-mercaptoethanol (work in fume hood). Vortex (Scientific industries, Bohemia NY) thoroughly.
- Calculate the appropriate volume of each sample to give equal loading protein amounts (e.g.: 50 µg protein/sample) and calculate the number of sample sets needed.

- Label microtubes for each sample.
- Add the appropriate amount of working solution of Laemmli's and RIPA buffer, as calculated, to each appropriate tube (work in fume hood).
- Add the appropriate volume of each protein sample to respective microtubes.
- Close samples and punch small hole in lid with tweezers or syringe needle.
- Heat samples on heating block for 5 minutes.
- Centrifuge (Spectrafuge 24D Labnet, Edison NJ) each tube at 17, 226 × g (briefly for ~10 sec) and place on ice immediately.
- Samples can now either be stored at -20°C for future use or directly loaded onto gels.
-

Western blotting

Gels

Polyacrylamide gel electrophoresis (PAGE) gels were casted according to the protocol provided by the Tris-glycine extended (TGX) Stain-Free™ FastCast™ Acrylamide Kit, 10% #161-0183 (BIO-RAD, Hercules CA).

- Add 7.5 µL of protein marker (BIO-RAD, unstained Precision Plus Protein™ standard, Hercules CA) to the first lane on the far left of each precast gel (BIO-RAD, Hercules CA).
- Add the appropriate amount of sample slowly into respective lanes using the gel-loading tips.
- Place the green lid with appropriate leads (black to black: red to red) on top of the tank and connect to the power pack (Power PAC 1000, BIO-RAD, Hercules CA).
- Add running buffer to just below the line indicated on the tank.

Running buffer: 10x SDS (1L)

- 10 g SDS
- 30.3 g Tris-base

- 144.1 g glycine

Dissolve in 800.mL ddH_2O, adjust volume to 2 L. Make 1x running buffer by adding 100 mL 10× running buffer to 900 mL ddH_2O.

- Run at 100V (constant), 400 mA for 85-90 min to allow samples to migrate through gel.
- Switch off power and disconnect electrodes. Remove gel plates from the tank and immediately proceed to the electro-transfer step.
- Image gels to evaluate sample migration as well as visualizing total protein content of each sample (Image Lab™ Software version 4.0, BIO-RAD, Hercules CA).

Transfer using Transfer Turbo and Chemi-Doc:

- Open the transfer pack (Trans-Blot® Turbo™, transfer pack, BIO-RAD, mini format, 0.2 µm PVDF, single application, Hercules CA) and place the blotting paper marked “bottom” on bottom of the Transfer Blot (Trans-Blot® Turbo™, transfer system, BIO-RAD, Hercules CA) cassette on top. Gently roll out any air bubbles.
- Place the gel on top of the membrane with the low molecular weight protein side facing towards the center of the cassette and again gently roll out any trapped air bubbles.
- Then place the blotting paper marked “top” from the transfer pack over the gel and roll out air bubbles (align the blotting paper tabs in the same manner as when it came out of the transfer pack).
- Place lid on top and lock in place.
- Place the cassette in the Transfer Blot (Trans-Blot® Turbo™, transfer system, BIO-RAD, Hercules CA) and set to transfer for 7 min (unless stated otherwise), this will allow the protein to be transferred from the gel onto the membrane.
- Check that protein has transferred and then place in methanol for ~30 sec then leave to dry completely.
- Rinse membrane 3 x 5 min with TBS-T.

10× TBS Buffer:

- 48.4 g Tris
- 160 g NaCl

Dissolve in 1.5 L ddH_2O. Set pH to 7.6 with HCl and adjust volume to 2 L.

1× TBS-T buffer:

- 100 mL 10× TBS buffer
- 900 mL ddH_2O
- 1 mL Tween

- Block for 1 hr in 5% BSA (TNF-α, IκB) or 5% milk (PKCβII) made up in TBS-T. *O*-GlcNAc must be blocked in 5% BSA, but only for 20 min.
- Wash 3 x 5 minutes in TBS-T (unless stated otherwise).
- Place membrane in 50 mL Falcon tube (BD Bioscience, Bedford MA) containing 5 mL of primary antibody

  ***O*-GlcNAc** (CTD110.6, Santa Cruz Biotechnology, Santa Cruz CA); 1:500 dilution; in TBS-T

  PKCβII (Abcam, Cambridge MA);

  anti-TNF-α (Abcam, Cambridge MA),1:1000 dilution; in 5% BSA

  IκB-α (Cell Signaling Technology®, Danvers MA) diluted 1:1000 in TBS-T
- Place on rotator in 4ºC walk-in fridge overnight.

DAY 2:

- Remove membrane from primary antibody (save antibody – freeze at -20ºC).
- Wash 3 x 5 minutes in TBS-T.
- Prepare secondary antibodies by diluting in 5 mL TBS-T in a 50 mL Falcon tube (BD Bioscience, Bedford MA).

PKCβII, IκB-α, TNF-α: Secondary HRP-conjugated anti-rabbit antibody (Cell Signaling Technology®, Danvers MA); 1:4000; in TBS-T

***O*-GlcNAc:** anti-mouse monoclonal secondary antibody (anti-mouse IgG, HRP-linked, Cell Signaling Technology®, Danvers MA); 1:2000; in TBS-T

- Place on roller for 1 hour at room temperature.
- Pour off secondary antibody into tube and freeze for later use.
- Wash membrane 3 x 5 minutes in TBS-T.
- NB: in order to image your stain free blot the imaging steps below must be followed before the addition of the ECL. For this it is necessary that the gel was activated prior to electrophoretic transfer. The images that are taken after the addition of the ECL is known as chemiluminescent blots.
- Take ECL reagents (BIO-RAD, Hercules CA) A & B from fridge and equilibrate to room temperature.
- Prepare ECL substrate in a 1:1 ratio of A:B. Use foil-covered microtubes to prepare solution as ECL is light sensitive.
- Pour off the TBS-T from membrane and add ECL, spreading evenly over the surface of the membrane by gentle tilting. If MW of protein is known, just add ECL to this area to save on the amount of ECL as it is very costly.
- Swirl gently for 2 minutes.
- Place membrane on tray of the ChemiDoc (BIO-RAD, ChemiDoc™, XRS+ system, Hercules CA) taking care to remove any visible bubbles.

Image analysis on Chemi-Doc:

- Select “Image Lab™ Software version 4.0 (BIO-RAD, Hercules CA), quantification analysis” program from desktop on computer.
- The ‘’start’’ page will pop up – can choose an existing protocol or create a new one.
- All protocol settings can be modified by selecting the item on the left under “Protocol Set Up”.
- For self-poured gels: Select “Blot” and then select “Chemi” from drop-down window.

- Next, set the imaging area to 12 x 9 cm (W x L).
- Specify the optimum exposure e.g. “intense bands”.
- Default color is auto selected – you can change this if required.
- Select “Lane and Band Detection”.
- Select either “Low” or “High” for intense or faint bands or use the “custom” slider to set exact sensitivity.
- Select “Analyze MW” then select MW standard used, the appropriate lane and the regression method (linear, semi-log) - if using Bio-Rad marker you can analyze against this (a stain-free marker was used in order to activate and visualize total protein content before the gel was transferred to the membrane). The stain-free gel does not require a loading control as the total protein content is visualized and analysed for normalization. Gels are visualized to calculate total protein content (Image Lab™ Software version 4.0, BIO-RAD, Hercules CA)
- Generate a report: Specific output, then provide a customized name and specify whether to be printed or displayed.
- Save the protocol summary.
- Load the gel into the imager and position it on the stage using the “position gel” option – this will produce a live image of the gel’s position –adjust by opening the top door of Chemi-doc- adjust the zoom settings and position to obtain image exactly as required.
- When gel is correctly positioned, click on “Run Protocol”.
- Once protocol has run, the images and report will be displayed with all selected analyses applied.
- Save the images required to an appropriate folder in ‘’Documents’’.
- Analyze images using: Image Lab™ Software version 4.0 (BIO-RAD, Hercules CA)

Quantitative analysis (Total protein normalization)

- Create a multichannel image with the stain-free blot in “Channel 1” and the chemiluminescent blot in “Channel 2”. The multichannel image option can be found in the “File” tab. Click OK
- Click on the “RGB” icon to deselt the overlay option
- Use the “Lane and Bands” tool to detect the lanes on your stain-free image. The lanes should be wide enough to include the entire band width. Additionally the lanes should all have similar widths and should not touch each other. The disk size should be set to 70 to subtract the background.
- Copy and paste the lanes over to the chemiluminescent blot – adjust the lanes if necessary.
- Choose “Detect Bands” on the “Band” tab to detect all bands on the chemiluminescent blot. Adjust the bands as needed
- Select “Normalization” in the Analysis Tool Box. Select the stain-free gel as the normalization channel. “Total Lane Protein” must be selected.
- Go to the “MW Protein Standard” in the Analysis Tool Box. On the stain-free gel tick the box below the MW standard lane (protein ladder)
- Select “Analysis Table” from the main toolbar and export the required data.